UNIVERSITY OF SALERNO

DEPARTMENT OF PHARMACEUTICAL SCIENCES

PhD course in Pharmaceutical Sciences

IX course NS (XXIII)

2007-2010

"Design, synthesis and biological evaluation of new small molecule modulators of Arginine methyltransferases"

Tutor   **PhD Student**

Prof. Gianluca Sbardella   Ciro Milite

Coordinator

Prof.ssa Nunziatina De Tommasi

I

"

INDEX

ABSTRACT

The methylation of arginine residues is a prevalent post-translational modification, found on both nuclear and cytoplasmic proteins, catalyzed by the protein arginine N-methyltransferase (PRMT) family of enzymes. To date there have been only a few publications describing small-molecule chemical modulators of the PRMTs. In this thesis are report the synthesis of a number of compounds structurally related to arginine methyltransferase inhibitor 1 (**AMI-1**). The structural alterations that we made included: 1) the substitution of the sulfonic groups with the bioisosteric carboxylic groups; 2) the replacement of the ureidic function with a bisamidic and mixed urea-amidic moiety; 3) the introduction of a N-containing basic moiety; 4) the positional isomerization of the amino- hydroxynaphthoic moiety; and 5) bioisosteric substitution of naphthol with indole. The biological activity of these compounds has been assessed against a panel of arginine methyltransferases (fungal RmtA, hPRMT1, hCARM1, hPRMT3, hPRMT6) and lysine methyltransferase (SET7/9 and G9a) using histone and nonhistone proteins as substrates. Molecular modeling studies for a deep binding-mode analysis of test compounds were also performed. The bis-carboxylic acid derivatives **1b** and **7b** emerged as the most effective PRMT inhibitors, both in vitro and in vivo, being comparable or even better than the reference compound (**AMI-1**) and practically inactive against the lysine methyltransferase SET7/9. We also identified **33a** as the first powerful and selective activator of CARM-1.

Moreover an enantioselective α-amination of aryl oxindoles catalyzed by a dimeric quinidine has been developed. This procedure is general, broad in substrate scope, and affords the desired products in good yields with good to excellent enantioselectivities.

CHAPTER 1

INTRODUCTION

1.1 Epigenetics

There are several existing definitions of epigenetics, the most comprehensive and up to date is: "The structural adaptation of chromosomal regions so as to register, signal or perpetuate altered activity states"[1]. This definition is inclusive of chromosomal marks, because transient modifications associated with both DNA repair or cell-cycle phases and stable changes maintained across multiple cell generations qualify. It focuses on chromosomes and genes, implicitly excluding potential three-dimensional architectural templating of membrane systems and prions, except when these impinge on chromosome function. Also included is the exciting possibility that epigenetic processes are buffers of genetic variation, pending an epigenetic (or mutational) change of state that leads an identical combination of genes to produce a different developmental outcome. An implicit feature of this proposed definition is that it portrays epigenetic marks as responsive, not proactive. In other words, epigenetic systems of this kind would not, under normal circumstances, initiate a change of state at a particular locus but would register a change already imposed by other events.

1.2 Histone modifications

The nucleosome is the fundamental unit of chromatin structure in all eukaryotes. It comprises a core of eight histones (two H2A, H2B, H3 and H4 histones) around which 147 base pairs of DNA are wrapped in 1.75 superhelical turns[2]. Given the intimate association between histones and DNA, it is not surprising that histones influence almost every aspect of DNA function. In some cases they are influential just by their presence — for example by hiding or revealing transcription factor binding sites or influencing polymerase progression. In other cases their effects can be more subtle and can

depend on chemical modification of specific histone amino acids. The amino-terminal tails of all eight core histones protrude through the DNA and are exposed on the nucleosome surface, where they are subject to an enormous range of enzyme-catalyzed modifications of specific amino-acid side chains[3], include acetylation of lysines, methylation of lysines and arginines, and phosphorylation of serines and threonines. Histone modifications are functionally linked to a variety of processes that are continuously occurring within the cell — for example, transcriptionally active promoters show an overall increase in acetylation of core histones and a more selective increase in methylation at particular lysines and arginines[3b]. Patterns of histone modification associated with ongoing transcription can change rapidly and cyclically in response to external stimulation. In this context, histone modifications can be considered the endpoints, on chromatin, of cellular signaling pathways and a mechanism through which the genome can respond to environmental stimuli. To allow such responses, it is likely that the modifications themselves are rapidly turning over[4]. Histones can also exert longer-term effects on genomic function, largely by defining and maintaining chromatin structures throughout the cell cycle, or from one cell generation to the next (Figure 1.1).
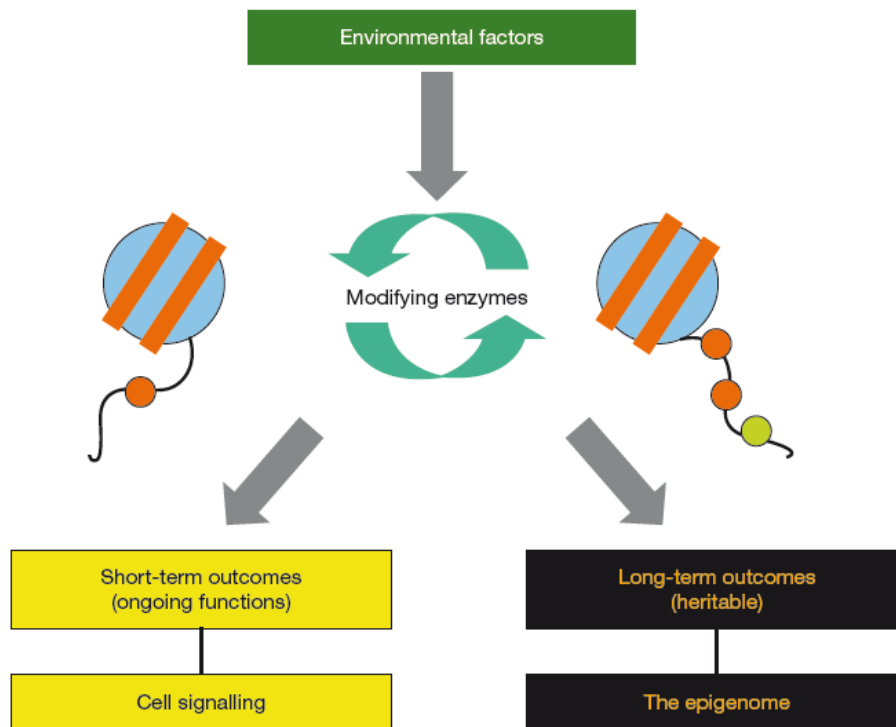
Figure 1.1 *Histone modifications can generate both short-term and long-term outcomes.* Histone tail modifications are put in place by modifying and demodifying enzymes, whose activities can be modulated by environmental and intrinsic signals. Modifications may function in both short-term, ongoing processes (such as transcription, DNA replication and repair) and in more long-term functions (as determinants of chromatin conformation, for example, heterochromatin formation, or as heritable markers that both predict and are necessary for, future changes in transcription). Short-term modifications are transient and show rapidly fluctuating levels. Long-term, heritable modifications need not necessarily be static: in theory they could still show enzyme-catalyzed turnover, but the steady-state level must be relatively consistent.

The identification of the enzymes that directly modify histones has been the focus of intense activity over the last 10 years. Enzymes have been identified for acetylation, phosphorylation ubiquitination, sumoylation, ADP-ribosylation, deimination, and proline isomerization. Most modifications have been found to be dynamic, and enzymes that remove the modification have been identified.

There are two characterized mechanisms for the function of modifications. The first is the disruption of contacts between nucleosomes in order to ''unravel'' chromatin and the second is the recruitment of nonhistone proteins. The second function is the most characterized to date. Thus, depending on the composition of modifications on a given histone, a set of proteins are encouraged to bind or are occluded from chromatin. These proteins carry with them enzymatic activities (e.g., remodeling ATPases) that further modify chromatin. The need to recruit an ordered series of enzymatic activities comes from the fact that the processes regulated by modifications (transcription, replication, repair) have several steps. Each one of these steps may require a distinct type of chromatin-remodeling activity and a different set of modifications to recruit them.

Modifications may affect higher-order chromatin structure by affecting the contact between different histones in adjacent nucleosomes or the interaction of histones with DNA. Of all the known modifications, acetylation has the most potential to unfold chromatin since it neutralizes the basic charge of the lysine.

The abundance of modifications on the histone tail makes ''crosstalk'' between modifications very likely (Figure 1.2)[5]. Mechanistically such communication between modifications may occur at several different levels. Firstly, many different types of modification occur on lysine residues. This will undoubtedly result in some form of antagonism since distinct types of modifications on lysines are mutually exclusive. Secondly, the binding of a protein could be disrupted by an adjacent modification. The best example of this being that of phosphorylation of H3S10 affecting the binding of HP1 to methylated H3K9[6]. Thirdly, the catalytic activity of an enzyme could be compromised by modification of its substrate recognition site; for example, isomerization of H3P38 affects methylation of H3K36 by Set2[7]. Fourthly, an

enzyme could recognize its substrate more effectively in the context of a second modification; the example here is the GCN5 acetyltransferase, which may recognize H3 more effectively when it is phosphorylated at H3S10[8].
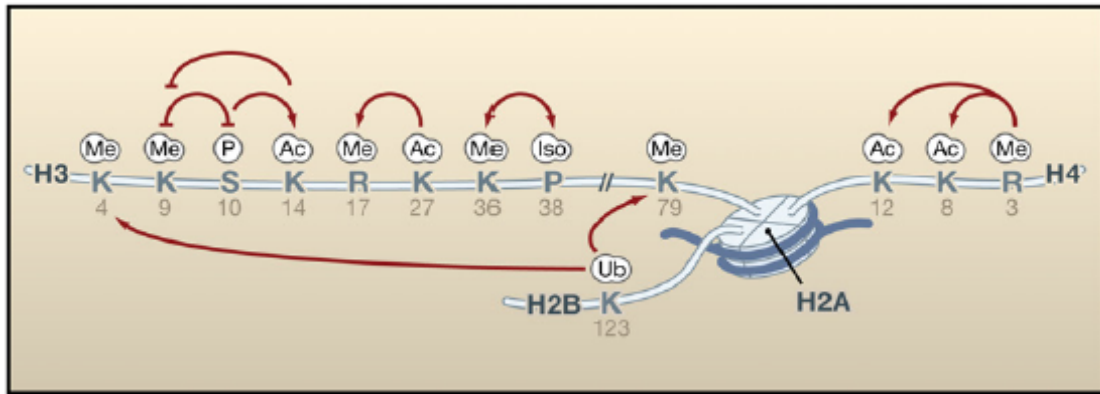
Figure 1.2 *Crosstalk between Histone* The positive influence of one modification over another is shown by an arrow and the negative effect by a dish-line.

1.3 Histone arginine methyltransferases (*PRMTs*)

The methylation of proteins and the enzymes that carry out these reactions increased the dimensions of the regulation of gene transcription by marking genes to be or not to be transcribed[9]. Protein methylation can occur on amino acids such as lysine, arginine, histidine, or proline, and on carboxy groups[10]. Arginine methylation of mainly nuclear proteins is an important posttranslational modification process involved in structural remodeling of chromatin, signal transduction, cellular proliferation, nucleocytoplasmatic shuttling, translation, gene transcription, DNA repair, RNA processing, or mRNA splicing[11]

1.3.1. Biochemical reaction of PRMTs

The PRMT enzymes remove one residue, the methyl group, from the donor molecule *S*-adenosyl- L-methionine (AdoMet) to generate the product *S*-adenosyl- L-homocystein (AdoHcy), and hereby transferring the residue to an acceptor molecule which is the terminal nitrogen atom of the guanidinium side chain of an individual arginine residue in the target protein (Figure 1.3)[12]. As there are three nitrogens in the guanidine group, putatively all of them could be methylated; the two ω-guanidino nitrogen atoms and the internal δ-guanidino nitrogen atom[13]. Indeed, mono- and dimethylation reactions of arginine are found to occur in mammalians: ω-N^G-monomethylarginine (MMA), symmetric ω-N^G,N'^G -dimethylarginine (sDMA), or asymmetric ω-N^G,N^G dimethylarginine (aDMA) (Fig. 3). The third methylated arginine is generated by monomethylation of the internal δ-guanidino nitrogen atom of arginine (δ-N-methyl-L-arginine) and has so far been documented only for yeast proteins[14]. According to their methylation status, the PRMT enzymes were classified into different group types. While the type-I PRMT enzymes catalyze the formation of MMA and aDMA, the type-II PRMT enzymes form MMA and sDMA. The enzymes PRMT1, PRMT3, PRMT4, PRMT6, or PRMT8 belonging to the type-I and PRMT5, PRMT7, or PRMT9 to the type-II enzymes[13b, 15]. Finally, type-III PRMT enzymes catalyze methylation at the δ-guanidino group in yeast[14].

Only very recently have different enzymes been identified which counteract the methylation process by catalyzing a demethylation step and so remove methyl residues from the target proteins (e.g., LSD1, JMJD6). It should be pointed out that JMJD6, a Jumonjidomain-containing protein, is the only arginine specific demethylase so far identified[16].
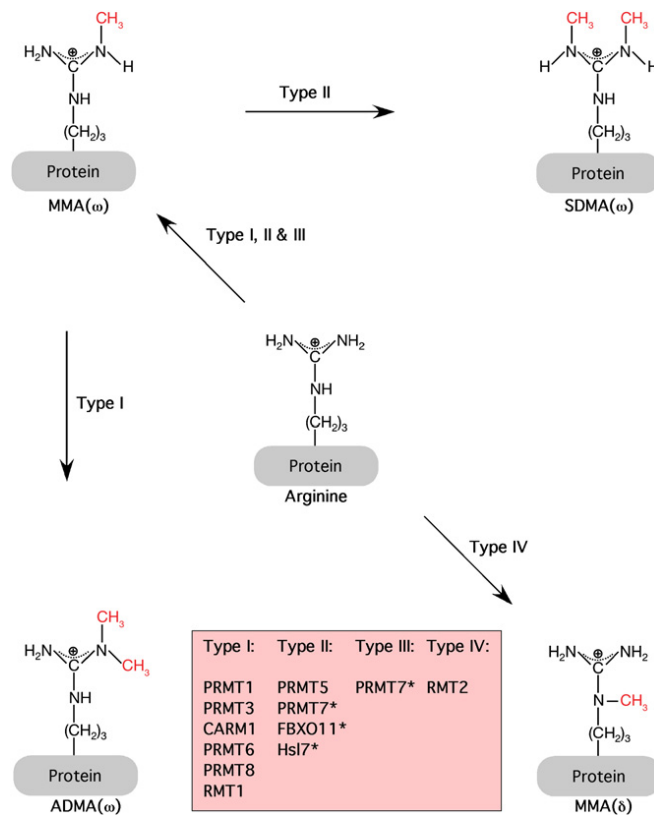
Figure 1.3 *Methylation of the arginine side chain by PRMTs.* Depicted is the amino acid arginine in target proteins. Type-I and type-II enzymes catalyze the formation of MMA by transfer of a methyl group to the x-guanidino group. In addition, transfer of an additional methyl group results in aDMA (type-I enzymes), or sDMA (type-II enzymes). Type-III enzymes transfer the methyl group to the internal d-nitrogen.

1.3.2. PRMTs in mammalian, characterization and biological role

1.3.2.1 PRMT1

PRMT1 was the first protein arginine *N*-methyltransferase in mammalian cells to be cloned and discovered independently from different groups as a protein interacting with the mammalian intermediate early TIS21 protein and the leukemia-associated BTG1 protein, or with the intracellular domain of the IFNα receptor[17]. PRMT1 is the predominant type-I PRMT present in

mammalian cells and tissues is expressed in every cell type investigated[18]. Two important processes mediated by PRMT1 are the methylation of histone H4 to regulate gene transcription and of the elongation factor SPT5 which regulates its interaction with RNA polymeraseII[19]. Furthermore, PRMT1 methylates proteins involved in RNA processing such as poly(A)-binding proteins and proteins in DNA repair and checkpoint control[20]. Besides ribosomal and RNA-binding proteins, a kinase adaptor protein (SAM68) is methylated by PRMT1 indicating a role in cell cycle regulation[21].

1.3.2.2 PRMT3

PRMT3 belongs to the type-I enzyme and is expressed widely in human tissues with subcellular localization in the cytoplasm[13a]. An important feature of PRMT3 is the ZnF domain in the amino-terminal part of the protein Using deletion studies of this motif, it was concluded that this domain confers substrate specificity and appears to be required for the enzyme to bind and methylate target proteins associated with RNA[22]. PRMT3 was able to transfer methyl groups to ribosomal and RNAbinding proteins. Interestingly, the interaction of a tumor suppressor gene important in lung carcinomas (DAL-1/4.1B) with PRMT3 inhibited its ability to methylate cellular substrates and modulated its enzymatic activity negatively. This suggested an important mechanism through which the suppressor gene was able to affect tumor cell growth[23].

1.3.2.3 CARM1 (PRMT4)

PRMT4 belongs to the type-I class of PRMT enzymes and its gene is expressed in all tissues investigated with an increased expression in heart, kidney, and testis[24]. The PRMT4 protein is able to bind directly to the p160 family of coactivators and in doing so amplifying the nuclear receptor mediated transactivation of target genes. Furthermore, PRMT4 can

synergistically enhance the nuclear receptor function and influence gene activation of ER or AR regulated genes[25]. In addition, the coactivator function of PRMT4 relies on its ability to transfer the methyl group to the amino-terminal tail of histone H3 after recruitment to the promoter by nuclear receptors and p160 coactivators. This is believed to link the process of methylation directly with transcriptional function[24]. A positive regulation of cell cycle gene like cyclin E and an involvement in estrogen stimulated breast tumors was described for PRMT4. The methylation of SRC3 by PRMT4 decreased the ER-mediated transactivation suggesting that PRMT4 not only activates transcription but also terminates hormone signaling by disassembly of the coactivator complex[26]. The nuclear localization of PRMT4 propose an involvement in muscle differentiation where PRMT4 plays a fundamental role during skeletal myogenesis by activating specifically myogenic genes[27]. Embryos with a targeted disruption of PRMT4 were small in size, died perinatally and had a defect during T-cell development. In these animals, estrogen-responsive gene expression was aberrant indicating genetic evidence for an important role of PRMT4 in hormone mediated transcriptional regulation[28]. Recently, it was shown that PRMT4 is involved in lipid metabolism by promoting adipocyte differentiation, suggesting an important role in adipose tissue biology[29]. Finally, it was described that PRMT4 was able to cooperate with PRMT1 and be involved in STAT5- and NF-jB-dependent gene expression or in transcriptional activation by the tumor suppressor p53[30].

1.3.2.4 PRMT5

PRMT5 was isolated in a two-hybrid search for proteins interacting with the Janus tyrosine kinase (Jak2), implying a role in cytokine-activated transduction pathways. In human tissues, PRMT5 is widely expressed with some higher level in heart, muscle, and testis[31]. PRMT5 plays a significant role in control and modulation of gene transcription, as the proteins methylated by

PRMT5 are important in the regulation of genes such as IL-2 and cyclin E1. In addition, PRMT5 was able to transfer methyl residues to the tumor suppressor p53 and help to discriminate between the cell cycle response and the apoptotic response. Furthermore, as arginine methylation has the potential to alter the effects of p53 activation, it may therefore provide a suitable drug target for the manipulation of the p53 pathway[32].

1.3.2.5 PRMT6

PRMT6 belongs to the type-I enzyme of PRMTs catalyzing the formation of aDMA (Figure 3). Interestingly, the methylation of selected proteins of the human immunodeficiency virus type-1 (HIV-1) by PRMT6 down-regulated gene expression by acting as a restriction factor for viral replication representing a form of innate cellular immunity[33]. In addition, PRMT6 methylated proteins from the high mobility group A (HMGA1a) family of architectural nuclear factors which were important in chromatin dynamics, placing PRMT6 in the context of chromatin structure organization. Recently, PRMT6 methylation of arginine in histone H3 has also been shown to play an important role in post-translational modification.

1.3.2.6 PRMT8

Expression analysis using Northern analysis revealed a unique tissue-specific expression as PRMT8 transcripts were largely found in human brain. Indeed, by using PRMT8 fusion or mutation constructs, it could be shown that the cellular localization of PRMT8 is not the nucleus or the cytoplasm but its association with the plasma membrane using the unique Myr motif in the protein[34]. In addition, it was shown that the interaction between the methyltransferase PRMT8 and its potential substrate protein is maintained, although the substrate is completely methylated. This suggests that PRMT8

has, besides the methyltransferase activity, another additional functional activity on the plasma membrane.

1.3.2.7 Less known PRMTs: 2,7,9,10,11

PRMT2 transcripts were detected in most human tissues with an increased expression in heart, prostate, ovary, and the neuronal system. Analysis using two-hybrid screening approaches identified PRMT2 as interacting with different nuclear hormone receptors such as the ERa and the androgen receptor (AR). The amplification of ER signaling by PRMT2 strongly depends on the cellular background and differs between neuroblastoma and prostate cells.

It was shown that the PRMT7 protein is localized in both cellular compartments: the nucleus and the cytosol of mammalian cells. PRMT7 was initially characterized in hamster cells as a protein that modulates drug sensitivity to DNA-damaging agents. PRMT7 is unusual among the other family members in that two PRMT core domains are present. For the functionality of the enzyme, both domains are required as each separate domain was unable to function alone. Beside PRMT5, PRMT7 was characterized as a type-II methyltransferase that was able to synthesize sDMA residues in proteins and was able to methylate proteins such as histones, myelin basic protein, fibrillarin, and spliceosomal proteins. PRMT7 is involved in cancer treatment as inhibitor of the enzyme activity sensitizing cancer cells to chemotherapeutics.

PRMT9, also known as F-box only protein 11 (FBXO11), was identified by motif search using part of the sequence of the conserved methyl donor binding domain of PRMTs. Recently, an association between polymorphism in the PRMT9 gene and inflammation of the middle ear was shown, indicating the importance of methylation in disease. Interestingly, besides regulating development, PRMT9 was identified as an adaptor protein to be responsible

for posttranslational modification of the tumor suppressor gene p53 by inhibiting the transcriptional activity without affecting its stability. As PRMT9 is a Nedd8 ligase for p53, a direct relationship between neddylation of the suppressor protein and the methyltransferase activity is unknown.

PRMT10 was predicted by its homology to PRMT7. One human transcript encoding a protein with 845 amino acids is described. No biochemical activity or substrates have been determined but the resemblance to PRMT7 suggested that PRMT10 may also belong to the type-II arginine methyltransferases.

PRMT11 was found by homology search using the sequence of PRMT9. GenBank analysis shows a nitrous oxidase accessory protein (NosD) conserved C-terminal motif that may be important for inorganic ion transport and metabolism. Because of the similarity with PRMT9, it is predicted that PRMT11 also has a methyltransferase activity and may belong to the type-II of PRMT enzymes, but no biochemical data and functional information are known at this time[35].

1.4 Histone methyltransferases inhibitors

Despite extensive research aimed at better understand the role of PRMTs in physiological and pathological pathways, elucidating the structure of these enzymes, and gaining insights into the mechanism of methyl transfer, the search for modulators of histone methyltransferases is still in its infancy, in fact there are only few PRMTs inhibitors (PRMTi) and no one in clinical trials (Scheme 1.1). The development of PRMTi is not only hampered by the lack of crystallographic structural information for enzyme–inhibitor complexes, and only few PRMTs crystal structure are known to date[36].

1.4.1 PRMTi obtained by means of high-throughput and virtual screening

The first inhibitors of protein arginine methyltransferases were discovered in 2004 by using the yeast arginine methyltransferase enzyme Hmt1p and the Npl3 protein as substrate.
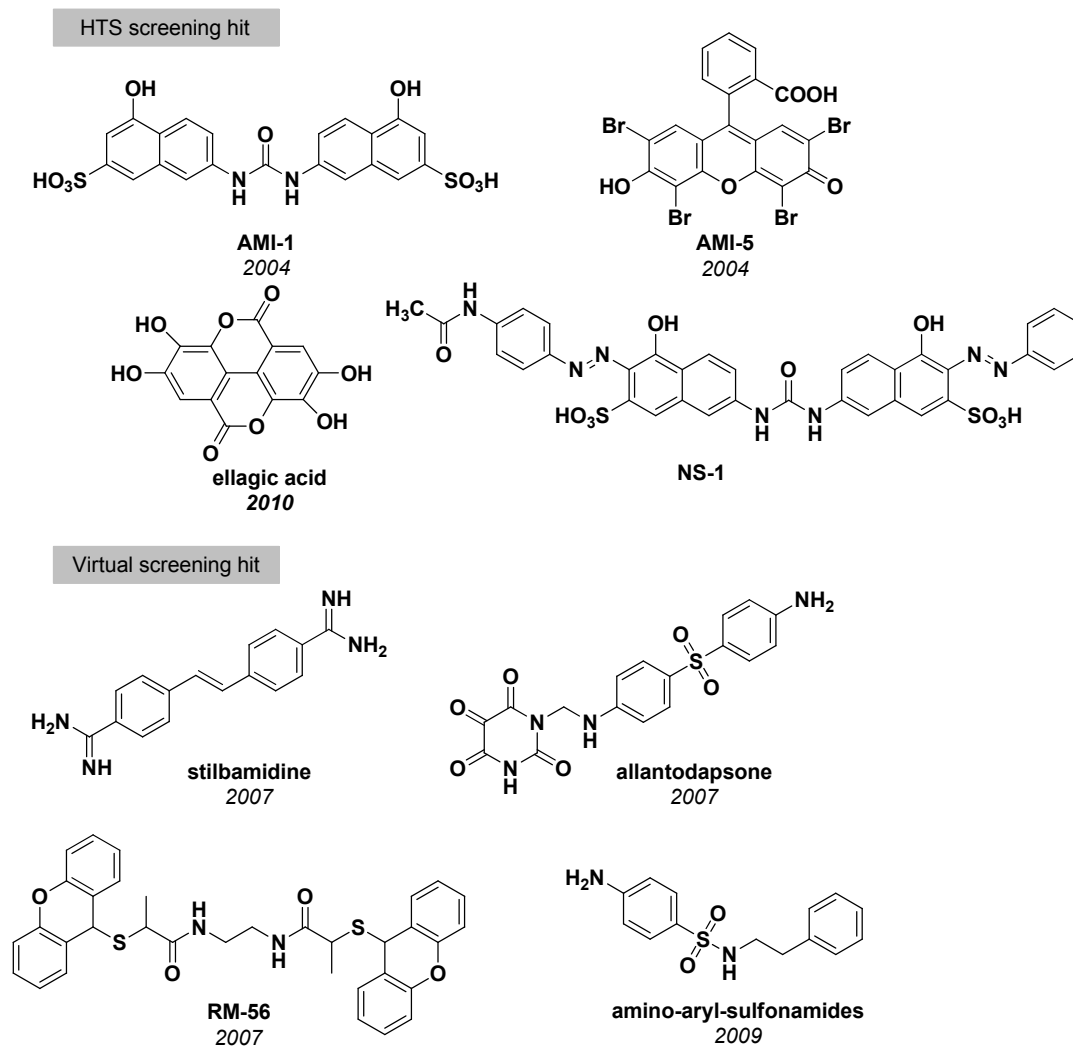
Scheme 1.1 *Inhibitors of PRMTs trough random and virtual screening.*

The screen resulted in the discovery of nine potent compounds that inhibit PRMT1 (in vitro IC_{50} values below 20 μm). After further experiments had been carried out that included PRMT3, 4, and 6, it was shown that all nine

AMIs inhibit all arginine methyltransferases that were tested. Assays against the lysine methyltransferases Suv39H1, Suv39H2, SET7/9, and DOT1 demonstrated that only AMI-1 is able to inhibit arginine methyltransferases selectively[37].

In 2007, the first target-based approach to inhibitors of histone arginine methyltransferase was presented[38]. Spannhoff et al. created a PRMT1 homologue model that served as a template for the virtual screening of a compound library. Only the compounds that showed accordance with the model (competition for the substrate, not for the cosubstrate SAM) and that possessed favorable docking results were tested first against RmtA and then against hPRMT1. When tested on HepG2 cells, two compounds, stilbamidine and allantodapsone (Scheme 1.1), displayed a strong hypomethylating effect. Later, the same group also presented the finding of a new lead structure, RM-65, for the inhibition of RmtA/PRMT1 by means of a fragmentbased virtual screen[39].

Heinke et al.[40] expanded their virtual and biological screening for novel inhibitors. Structure-based virtual screening of the Chembridge database comprising 328 000 molecules was performed and a series of amino-aryl-sulfonamides was also found to be active in the micromolar range.

One of the intriguing yet novel inhibitor is ellagic acid (TBBD) which has been found to be specific to CARM1/PRMT4 activity both in vitro and in vivo. This inhibitor binds to the enzyme–substrate complex based on the substrate sequence and thereby inhibits the enzyme modification on a single site alone[41]. This has not only led to the identification of a novel mechanism of enzyme inhibition but also has provided a tool to monitor the single residue, H3R17 methylation specifically.

By employing a similar approach, a specific inhibitor of PRMT1 (**NS-1**) has been identified wherein the inhibition of enzyme function is brought about by binding to the substrate[42].

1.4.1 PRMTi obtained trough synthetic optimization

In the last four year a few paper showing compound obtained from synthetic optimization has been published (Scheme 1.2).

Curcumin-like scaffolds with bromo- or dibromophenol substructures, obtained from formal simplification of AMI-5, showed an IC_{50} value up to 14 μm against the Aspergillus homologue of PMRT1, RmtA.
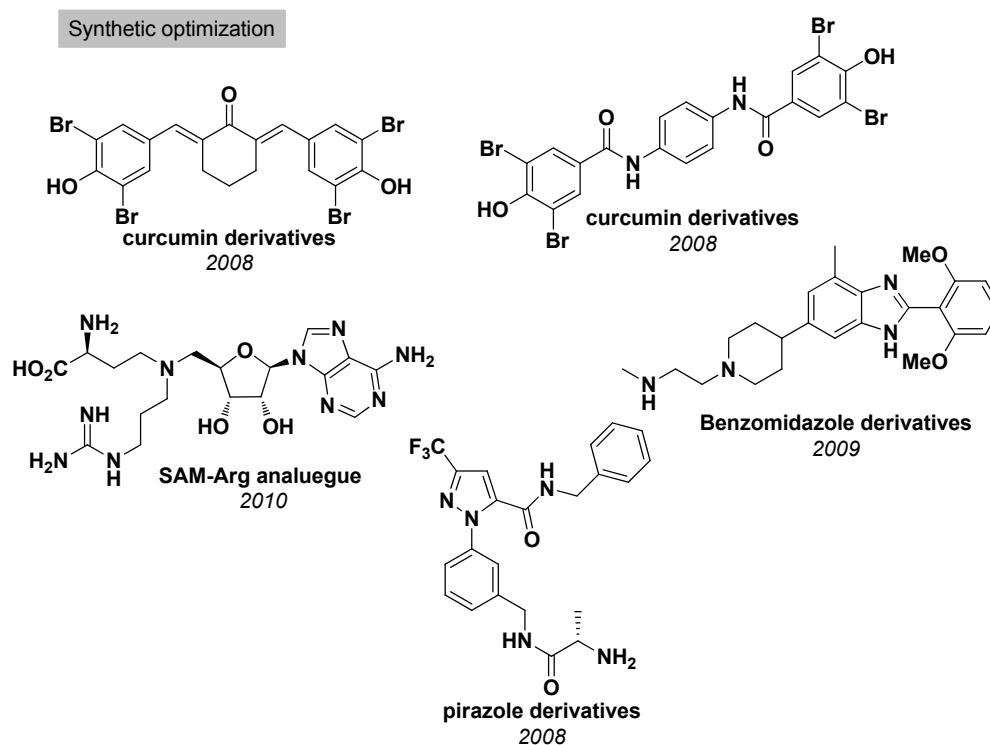
Scheme 1.2. *Inhibitors of PRMTs trough synthetic optimization.*

Compound **7** and compound **8**, the most powerful inhibitors of PRMTs of that series showed not selectivity between PRMTs and HKTMs.

Purandare et al., in 2008, starting from a high throughput screening, identified a pyrazole amide derivative and closely related analogs as 'hits' with modest activity in the CARM1 mediated methylation assay. Subsequent synthetic optimization led to the identification of a potent selective inhibitor of CARM1[43].

Another interesting molecule has been developed in 2009. Starting also in this case from a compound obtained by means of high-throughput screening and using typical medicinal chemistry approach, Wan et al. identified a good inhibitor of CARM-1[44] with benzoimidazole structure.

Finally, in 2010, the first selective bisubstrate inhibitor of PRMT-1 has been reported. This hybrid between SAM and Arg, showed a good inhibitor activity and selectivity[45].

CHAPTER 2

AIM OF THE WORK

2.1 Validating the *Hit*

As already mentioned, the first potent and selective PRMTs inhibitors has been discovered by Bedford and coll. in 2004[37]. Being interested in small molecule modulators of epigenetic targets[46] and, particularly, of histone-modifying enzymes, we focused our attention on AMI structures and noticed that all of them were dyes or dye-like derivatives. Particularly, two scaffolds (**A** and **B**, Scheme 2.1) emerged as privileged ones.
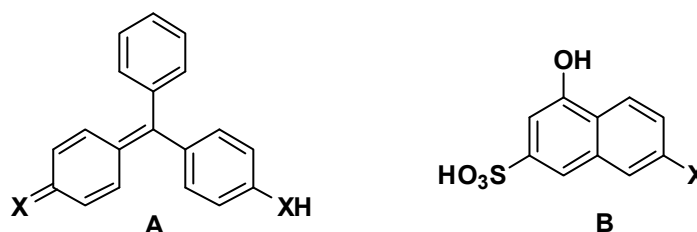
Scheme 2.1. *Privileged scaffold*

The second step was the preparation of a small series of compound containing the two scaffolds shown, that was used for biological and virtual screening assay. All the data obtained allowed us to describe the binding mode of AMI-1 and related compound into the catalytic domain of the PRMT1 fungal homologue RmtA and more interestingly to understand the AMI-1 selectivity (Figure 2.2)[47].
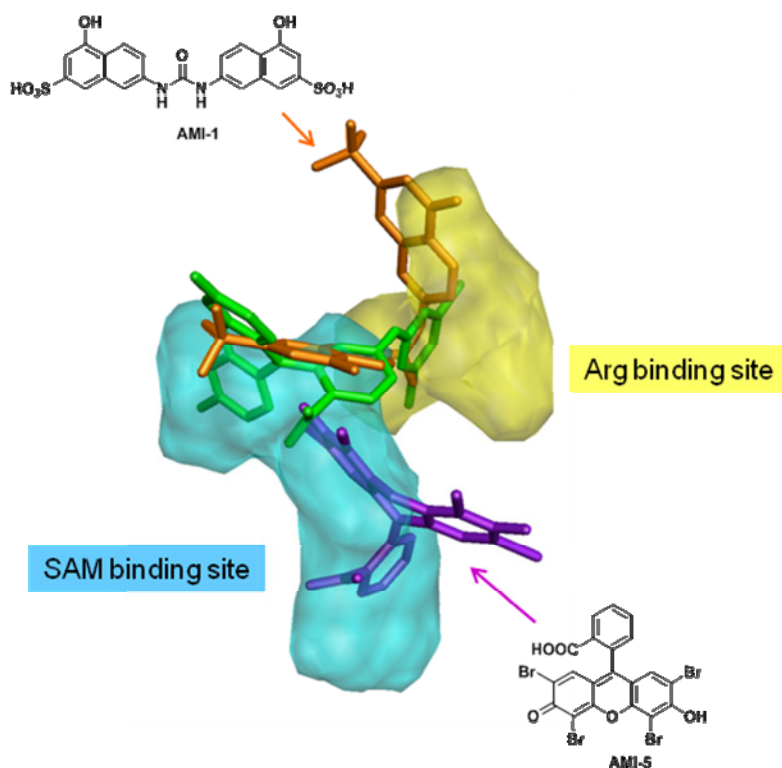
Figure 2.2. *PRMTi binding mode* In yellow and cyan are represented the Arg and SAM sites, respectively.

An hypothesis for AMI-1 selectivity is displayed in Figure 2.2: the compound is docked by the software (Autodock/X-Score) between the Arg and the SAM pocket without fully occupy them. On the other hand, AMI-5 is docked only in the SAM pocket and this data explain its lack of selectivity between methyltransferases.

Moreover, these analyses hinted that two regions in the RmtA catalytic site, the pocket formed by Ile 12, His 13, Met16, and Thr49 (dark gray area in Figure 2.3) and the SAM methioninic portion binding site delimited by Arg 22, Asp44, Gly 46, Cys 47, Ile 51, Leu 52 and Glu112 (light gray area in Figure 2.3), should be taken into account when designing novel inhibitors.
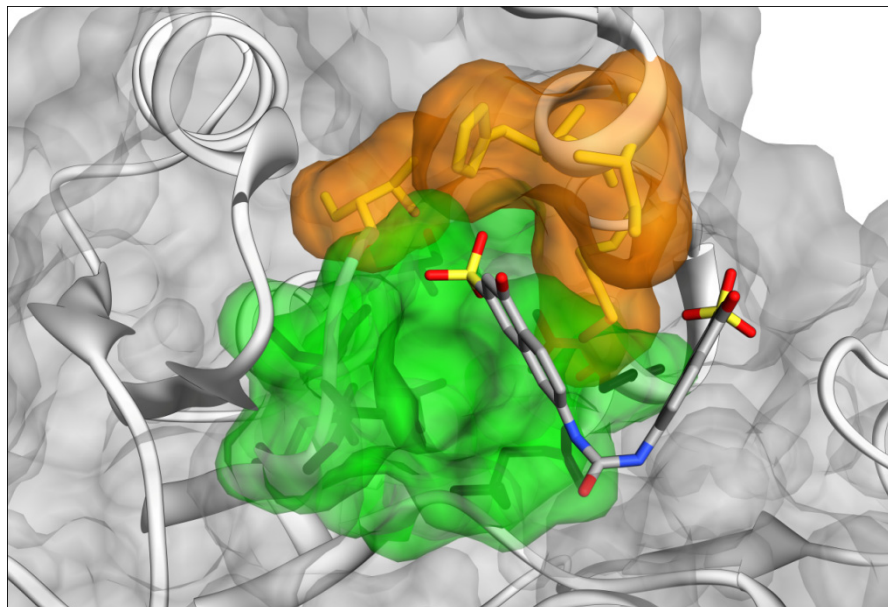
Figure 2.3. *The two additional binding pockets in the RmtA catalytic site that emerged from three-dimensional QSAR studies.* The area highlighted in light gray is delimited by Arg 22, Asp44, Gly 46, Cys 47, Ile 51, Leu 52 and Glu 112, whereas the area depicted in dark gray is formed by Ile 12, His 13, Met16, and Thr 49. The binding mode of AMI-1 (stick representation, carbon atoms in gray) is also shown.

However, before undertaking the exploration of the two aforementioned additional pockets, we realized that AMI-1 should be optimized as it is likely to have low bioavailability and would probably not penetrate the blood–brain barrier due to the bisanionic structure. Moreover, it is related to suramin-type sulfonated ureas, reported to give pleiotropic interactions with many proteins[48].

2.1 Aim of the work

Therefore, we designed a number of derivatives characterized by the substitution of the sulfonic groups with the bioisosteric carboxylic groups, the replacement of the ureidic function with a bisamidic moiety, the introduction of a N-containing basic moiety or the positional isomerization of the

aminohydroxynaphthoic moiety and the subsequence substitution of the naphthalene ring with an indolic one (Figure 2.4).
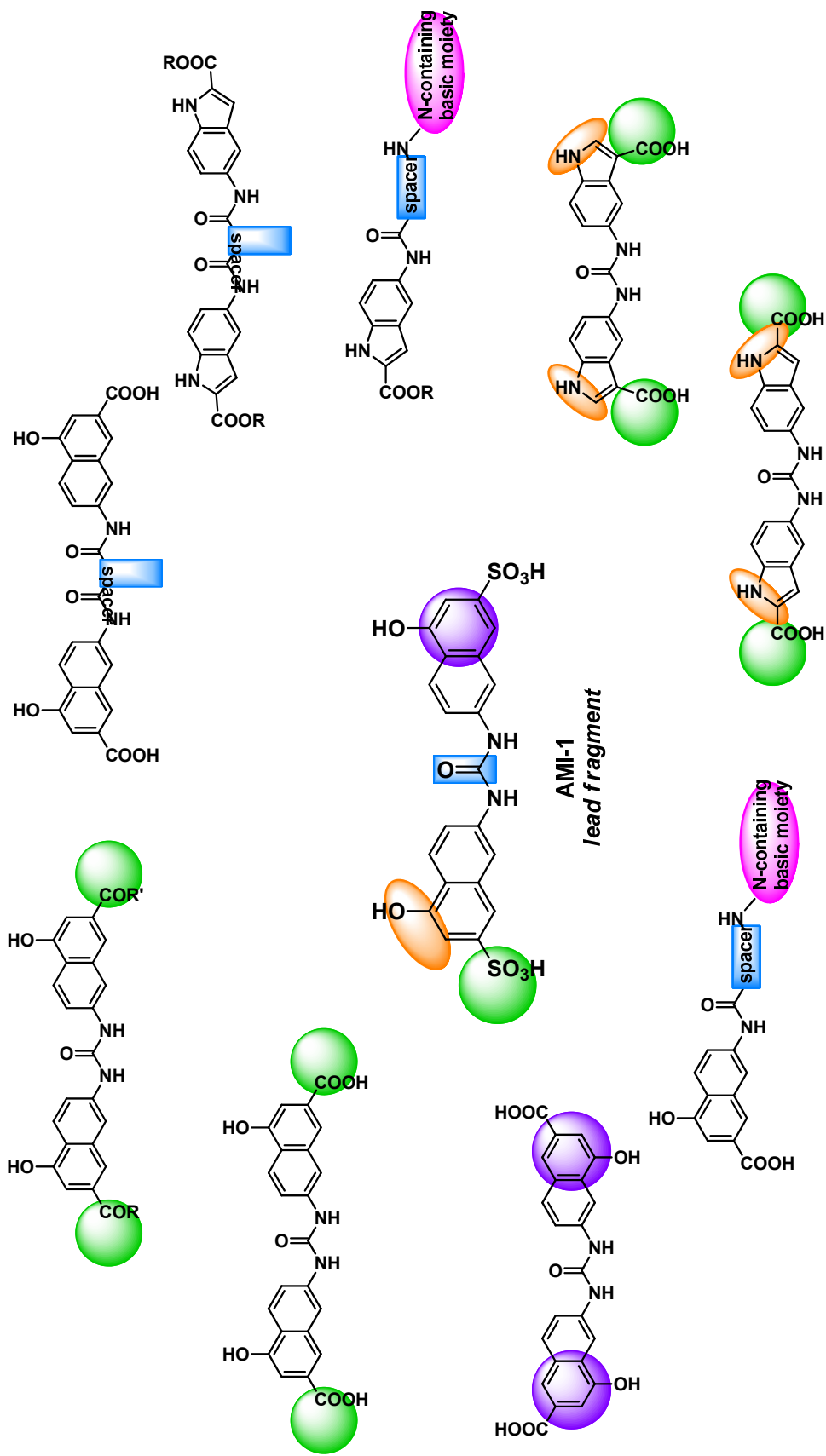
Figure 2.4. Aim of the work

28

CHAPTER 3

CHEMISTRY

3.1 Synthesis of 7-amino-4-hydroxy-2-naphtoic acid (12a)

The key step in the synthesis of derivatives showed previously was the synthesis of the building block, the 7-amino-4-hydroxy-2-naphthoic acids (Scheme 3.1). The synthesis of this building block may seems trivial but it isn't. At that time only failed attempted syntheses of this compound were reported[49].
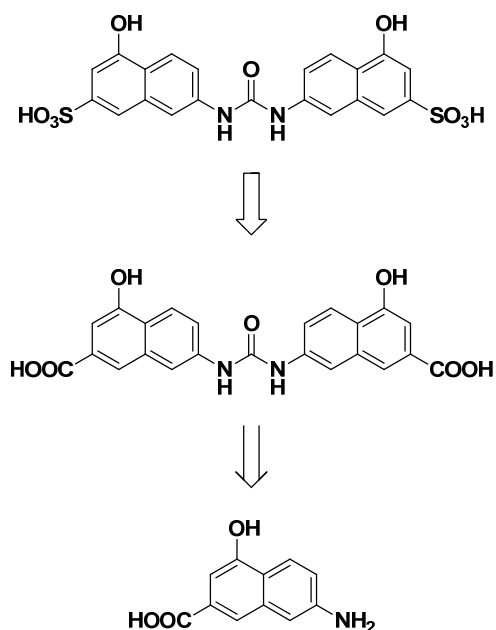
Scheme 3.1. *Retrosynthetic approach to the synthesis of PRMTi.*

So we had to develop a convenient pathway leading to the 7-amino-4-hydroxy-2-naphtoic acid...

We used a Wittig reaction between 3-nitrobenzaldehyde and carboxyphosphorane **10**[50] to regioselectively[51] prepare the (E)-nitrophenylitaconate **11a**[52] which was selectively reduced with zinc dust in

acetic acid to amino derivative **11b** (Scheme 3.2). Ring closure via microwave-assisted Friedel–Crafts acylation was followed by hydrolysis of the crude furnished a mixture of title acids **12a** and **12b** (1:2 ratio, determined by NMR) in a satisfactory 70% overall yield, without intentional purification of the intermediates.
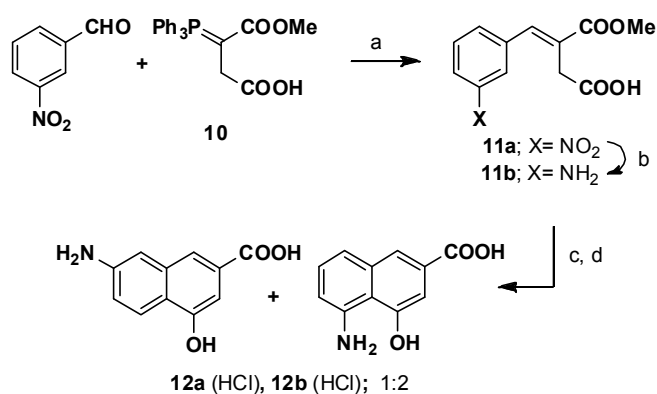
Scheme 3.2. ***Reagents and conditions*:** (a) benzene, rt, 24 h; (b) Zn (6 mol equiv), AcOH, rt, 24 h; (c) AcONa (1.5 mol equiv), Ac2O, MW (300 W, 5 min); (d) HCl 8 N, 5 h.

With the mixture of the two isomeric acids in our hands, we turned our attention to their separation. As a matter of fact, accordingly to what was previously reported for similar derivatives[49] this task revealed to be not easy. After the failure of fractionated crystallization and both conventional and flash chromatography, we were able to separate the mixture only through analytical RP-HPLC (Fig. 3.1). Unfortunately, this result was not reproducible on a preparative scale (preparative RP-HPLC, same conditions).
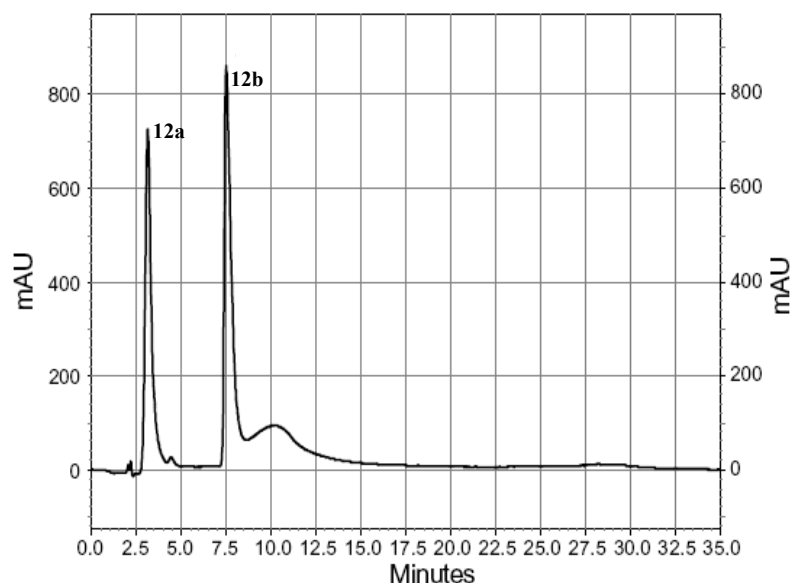
Figure 3.1 *Analytical RP-HPLC separation of isomers 12a and 12b* was performed on C18 column (Vydac 218TP152010) using a gradient of acetonitrile (40–70% acetonitrile in 30 min) in 0.1% aqueous TFA at 1 mL/min.

For this reason we decided to investigate if the expected difference in reactivity resulting from the relative positions of the amino and the hydroxyl group in the two compounds could be exploited for their separation. Actually, the reaction of the mixture of ethyl esters **13a** and **13b** (from **12a** and **12b**, respectively) with CDI in THF at 0 °C for 3 h converted **13b** into the cyclic carbamate **14** (Scheme 3.3), leaving **12a** unreacted (33% and 55% yield, respectively). The two derivatives were easily separated by double extraction and then quantitatively converted into acids[53].
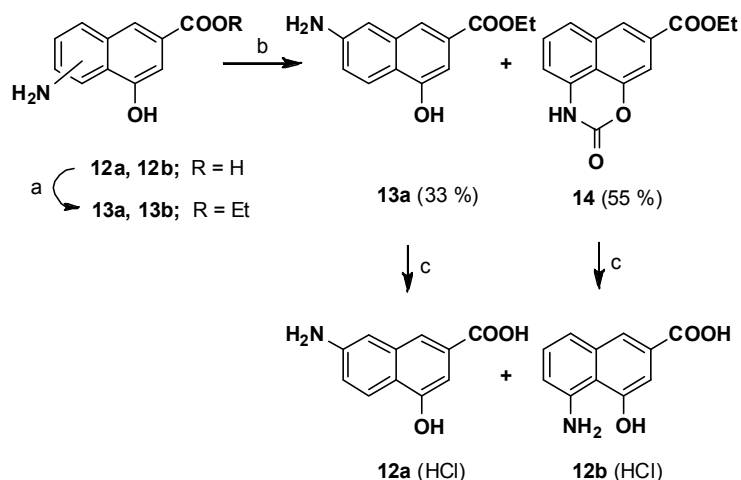
Scheme 3.3. *Reagents and conditions*: (a) EtOH, H_2SO_4, reflux, 24 h; (b) CDI, THF, 0 °C, 3 h; (c) HCl 8 N, 5 h.

This already valid synthetic scheme has been further optimized in our research lab. The different reactivity can be translated also in different chelating ability; **12a** was conveniently obtained by precipitating its 5-amino-isomer **12b** as an insoluble cobalt (II) complex salt (Scheme 3.4).
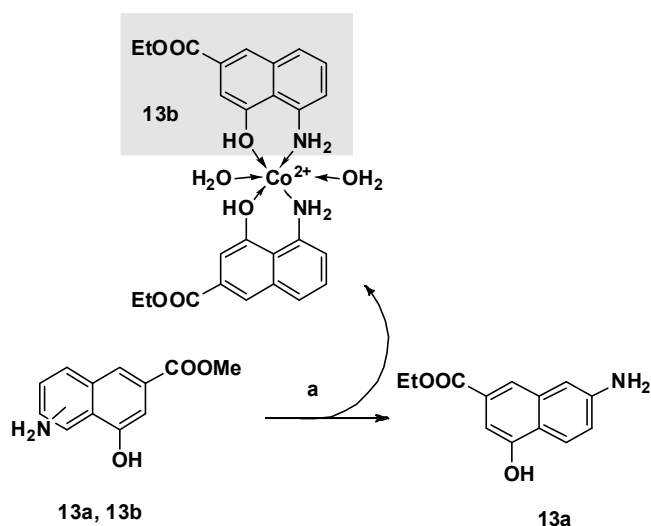
Scheme 3.4. *Reagents and conditions*: $Co(OAc)_2 \cdot 4H_2O$, AcOH/NaOAc pH 5 buffer, methanol.

3.2 Synthesis of 7-amino-4-hydroxy-2-naphtoic acid derivatives

3.2.1 Symmetric derivatives

 The symmetrical ureidic derivative **1a** (Scheme 3.5) was directly obtained by reacting **13a** with diphenyl carbonate in refluxing chlorobenzene in the

Scheme 3.5. ***Reagents and conditions*:** (a) diphenylcarbonate, DMAP, chlorobenzene, reflux, 72 h; (b) aqueous NaOH, pyridine, THF, room temp; (c) aqueous NH$_3$, room temp, 12 h; (d) succinyl chloride, TEA, acetone, room temp, 4 h; (e) diethyl malonate, MW (300 W, 30 min), neat; (f) **12a**, toluene/NMP (10:1), MW (300 W, 3 × 30 min); (g) ClCOCCl$_3$, dichloromethane, room temp, 4 h; (h) R$_1$NH$_2$, K$_2$CO$_3$, DMF, 150 °C, 1 h, sealed tube.

presence of DMAP. The following hydrolysis with aqueous sodium hydroxide and pyridine in tetrahydrofuran furnished the corresponding acid **1b**, whereas the treatment of the ester **1a** with aqueous ammonia gave the bis-amidic derivative **1c**. With regard to bis-amidic derivatives, the reaction of **13a** with succinyl chloride in the presence of triethylamine in acetone as a solvent yielded the ester **3a**, which was hydrolyzed to the acid **3b** (Scheme 3.5) following the aforementioned protocol. On the contrary, the reaction of **13a** with malonyl chloride in the same conditions failed and the malonyl diamide **2a** was obtained in two steps: **13a** (1 equivalent) was first reacted under microwave irradiation with an excess of neat diethyl malonate and then a second equivalent was added as a solution in *N*-methylpyrrolidone-toluene 1:10. Again, subsequent hydrolysis of **2a** gave the corresponding acid **2b** (Scheme 3.5).

3.2.2 Asymmetric derivatives

The unsymmetrical ureidic derivatives were prepared by treating **13a** with trichloroacetylchloride in dichloromethane and reacting the resulting trichloroacetamide **16** with the proper amine to obtain esteric compounds **4a**, **5a** and **6a**, the hydrolysis of which yielded the acids **4b** and **6b**, respectively (Scheme 3.5)

3.3 Synthesis of methyl 4-acetoxy-6-amino-2-naphthoate (18)

The absence of regioselectivity in the preparation of the 7-amino-4-hydroxy-2-naphthoic ester **13a** thus requiring its separation from the 5-amino-

substituted isomer **13b** set hurdles to our intention to build a focused library based on this intermediate with the aim of exploring the two aforementioned pockets that emerged from computational studies. Therefore, we decided to synthesize derivatives the positional isomers of **1a,b**, **2a,b** and **4a,b**, and to evaluate their biological activities.

As a matter of fact, the Wittig reaction between 4-nitrobenzaldehyde and carboxyphosphorane **10**, followed by the microwave-assisted Friedel-Crafts-type ring closure yielded only methyl 4-acetoxy-6-nitro-2-naphthoate **17**, promptly reduced to the key intermediate **18** by heterogeneous catalytic (palladium/activated carbon) hydrogenation (Scheme 3.6).
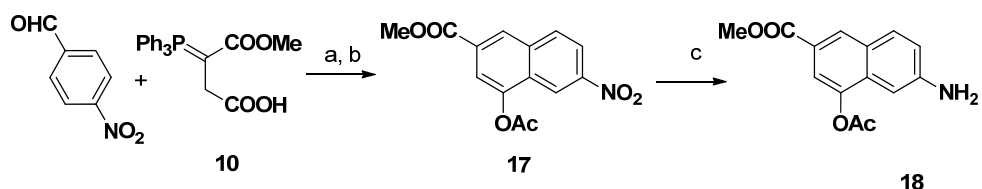
Scheme 3.6. *Reagents and conditions*: (a) benzene, room temp, 48 h; (b) NaOAc, Ac$_2$O, MW (300 W, 5 min); (c) H$_2$, Pd/C, ethanol, 2 h

3.4 Synthesis of methyl 4-acetoxy-6-amino-2-naphthoate derivatives

The reaction of **18** with diphenyl carbonate in refluxing chlorobenzene followed by the hydrolysis of the acetoxy- group with potassium carbonate in ethanol as a solvent gave the symmetrical ureidic derivative **7a**. The subsequent hydrolysis with aqueous sodium hydroxide and pyridine in tetrahydrofuran furnished the corresponding acid **7b** (Scheme 3.7). On the other hand, the unsymmetrical ureidic derivatives were prepared by treating **16** with trichloroacetylchloride in dichloromethane and reacting the resulting crude mixture of the trichloroacetamides **18** with tryptamine to obtain the ester **9a**. The hydrolysis of the latter yielded the corresponding acid **9b**. Finally, the two-step reaction under microwave irradiation between **18** and diethyl

malonate, followed by the hydrolysis of the acetoxy group with potassium carbonate in ethanol, yielded the malonyl diamide **8a**. Again, subsequent hydrolysis of **8a** gave the corresponding acid **8b**.
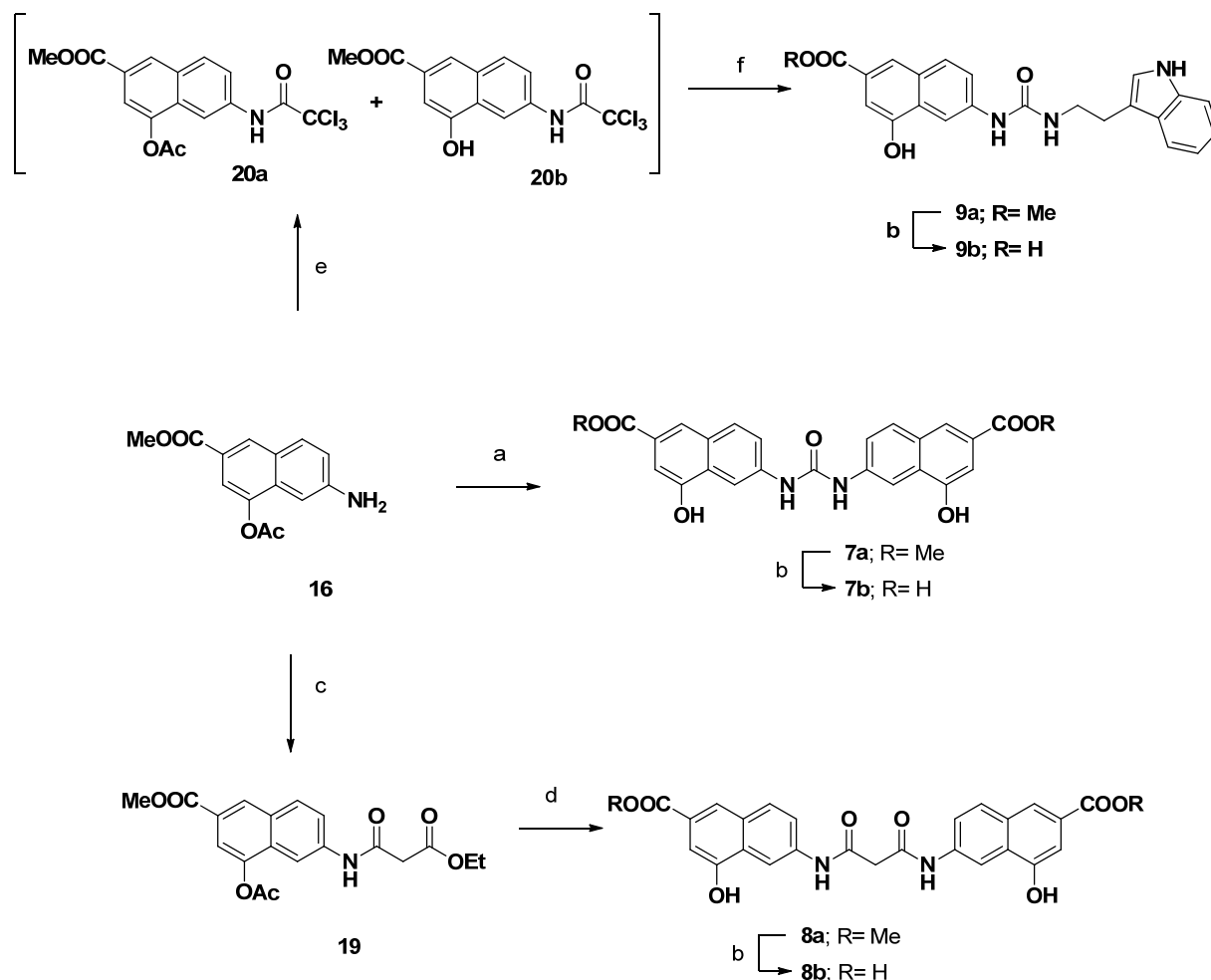
Scheme 3.7. *Reagents and conditions*: (a) 1) diphenylcarbonate, DMAP, chlorobenzene, reflux, 72 h; 2) K$_2$CO$_3$, ethanol, 70 °C, 2 h; (b) aqueous NaOH, pyridine, THF, room temp; (c) diethyl malonate, MW (300 W, 30 min), neat; (d) 1) **16**, toluene/NMP (10:1), MW (300 W, 3 × 30 min); 2) K$_2$CO$_3$, ethanol, 70 °C, 2 h; (e) ClCOCCl$_3$, dichloromethane, room temp, 4 h; (f) tryptamine, K$_2$CO$_3$, DMF, 150 °C, 1 h, sealed tube.

3.5 Indole derivatives

Once that the biological investigation of the first two series of compound was completed (Chapter 4) and our initial hypothesis confirmed, we decided to change the naphtholic ring with an indolic one. This idea, due to the bioisostery between the system (Scheme 3.7), was supported also by docking studies. Moreover the indolic ring is easier to synthesize and handle and would gave us the chance to build a bigger library. So, as done for the 6-substituted naphthol derivatives, we prepared a pool of compound directly linked to the most active of the previous series.
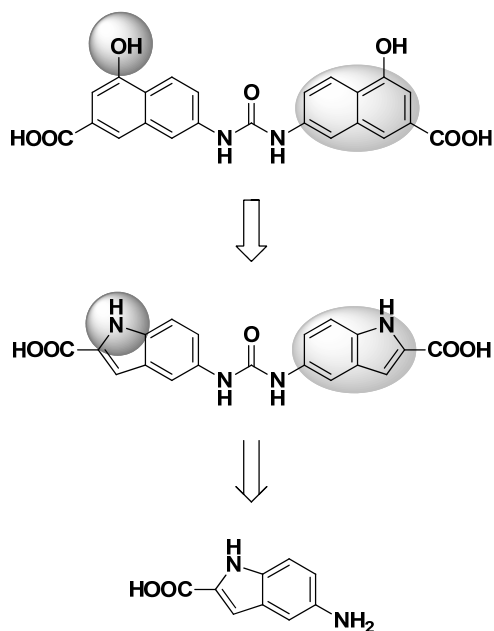
Scheme 3.7. *Bioisosteric substitution of naphthol with indole.*

3.5.1 Symmetric derivatives

Compound **26,** that can be prepared trough Fisher indole synthesis[54], is dimerized in presence of trifosgene and triethylamine bearing in high yield **21a** (Scheme 3..8). Applying the same procedure described for the naphthalene derivatives, aqueous sodium hydroxide and pyridine in tetrahydrofuran, compound **21a** is converted into **21b**.
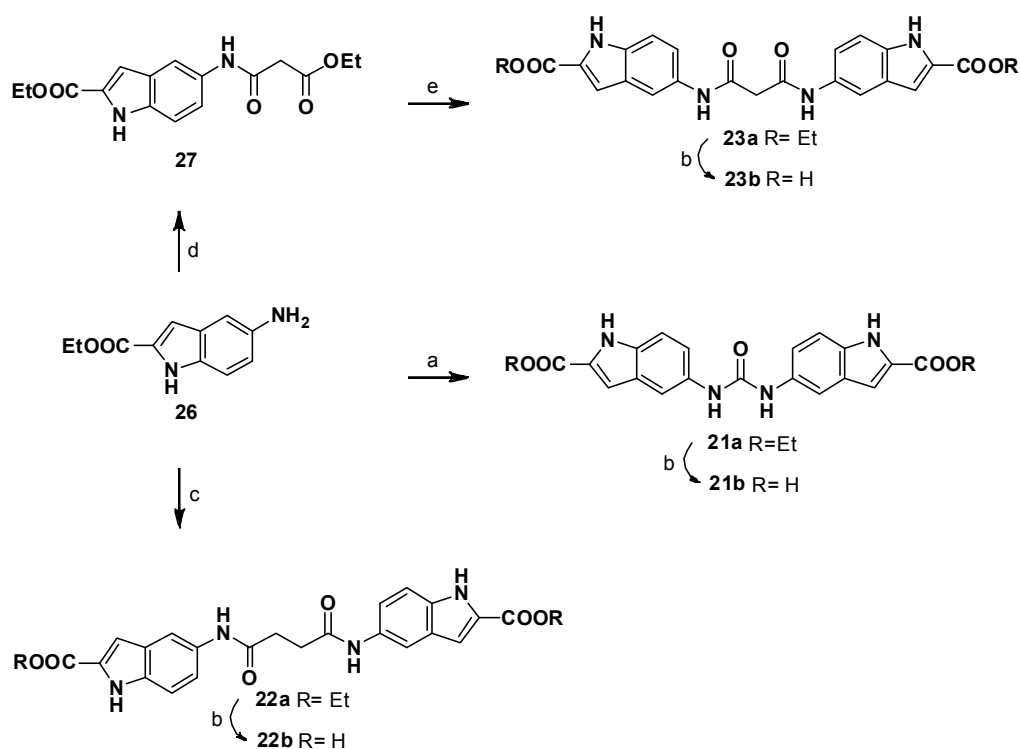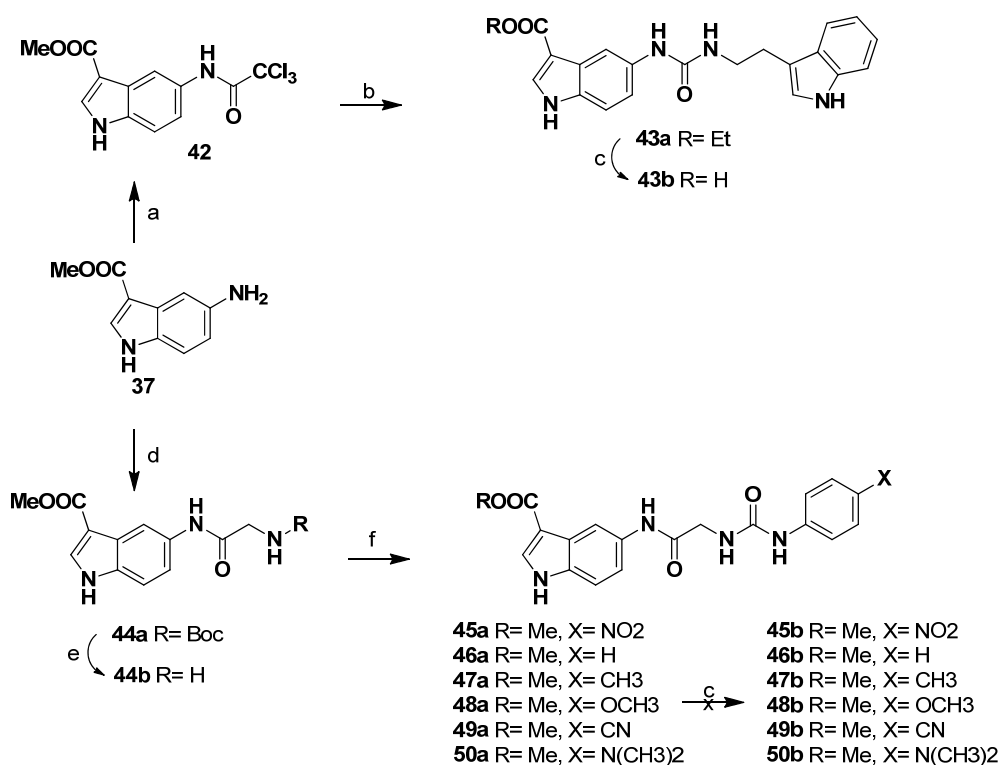

Scheme 3.8. *Reagents and conditions*: (a) trifosgene, TEA, dichloromethane, room temp, 4 h; (b) aqueous NaOH, pyridine, THF, room temp; (c) succinyl chloride, TEA, acetone, room temp, 4 h; (d) diethyl malonate, MW (300 W, 30 min), neat; (f) **26**, toluene/NMP (10:1), MW (300 W, 3 × 30 min).

Similarly, compound **22a** was obtained by reaction of the aminoindole **26** with oxalyl chloride and subsequent hydrolysis gave **22b**. Compound **27** was synthesized by reaction of **26** with neat diethylmalonate by microwave

irradiation and intermediate **23a** was obtained**.** Hydrolysis of the latter brings to **23b**.

3.5.2 Asymmetric derivatives

The asymmetric ureidic derivative has been synthesized as previously done for the naphthalene series. Amine **26** was reacted first with trichloroacetyl chloride to yield **28;** subsequent reaction of the latter with tryptamine yielded **30a** that was then hydrolyzed to **30b** (Scheme 3.9).
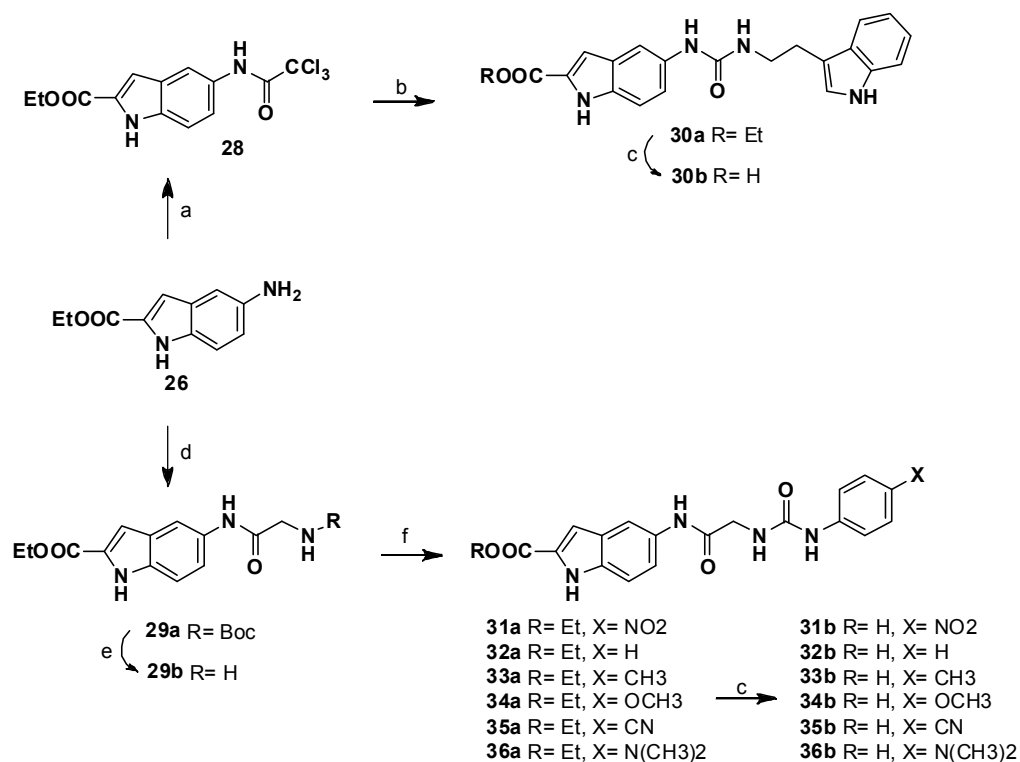
Scheme 3.9. *Reagents and conditions*: (a) ClCOCCl$_3$, dichloromethane, room temp, 4 h; (b) tryptamine, K$_2$CO$_3$, DMF, 150 °C, 1 h, sealed tube; (c) aqueous NaOH, pyridine, THF, room temp; (d) Boc-Gly-OH, TEA, HOBT, HBTU, DMF/THF, 12h, room temperature; (e) TFA/DMC, 1h, room temperature; (f) isocyanate, TEA, DMC, room temperature, 1-3h.

Derivatives **31a-36a** have been prepared reacting glycine derivative **29b** with the proper isocyanate and have been subsequently hydrolyzed to **31b-36b**. Reaction between **26** and Boc-Gly-OH in presence of HOBT and HBTU as coupling agent brings to **29a;** hydrolysis of the Boc protecting group with trifluoroacetic acid yield **29b**.

3.6 Indole derivatives, 2nd series

As emerged from the biological assays (Chapter 4), in the first series of indole derivatives we notice a general loss of inhibitor power and an inversion in the trend ester-acid; all the ester derivatives results more active than the corresponding acid. So we speculate an intramolecular hydrogen bond between the carboxylic acid and the NH of the indole that makes both functions less available to link the enzymatic pocket. So, supported also by energy and stability calculation, we decide to shift the carboxylic acid from 2 to 3 indole position (Scheme 3.10).
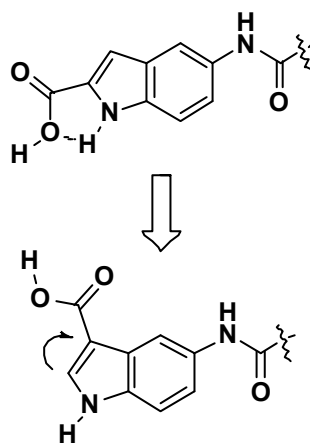
Scheme 3.10. *Hydrogen bond hypothesis* and solution?

3.6.1 Symmetric derivatives

The optimization of an already reported synthesis allows us to obtain easily and with high total yield the methyl 5-amino-1H-indole-3-carboxylate (**37**). All the symmetric derivatives (**38a-40a, 38b** and **39b**) were obtained applying the well established procedure already used for the previous indole series (Scheme 3.11).
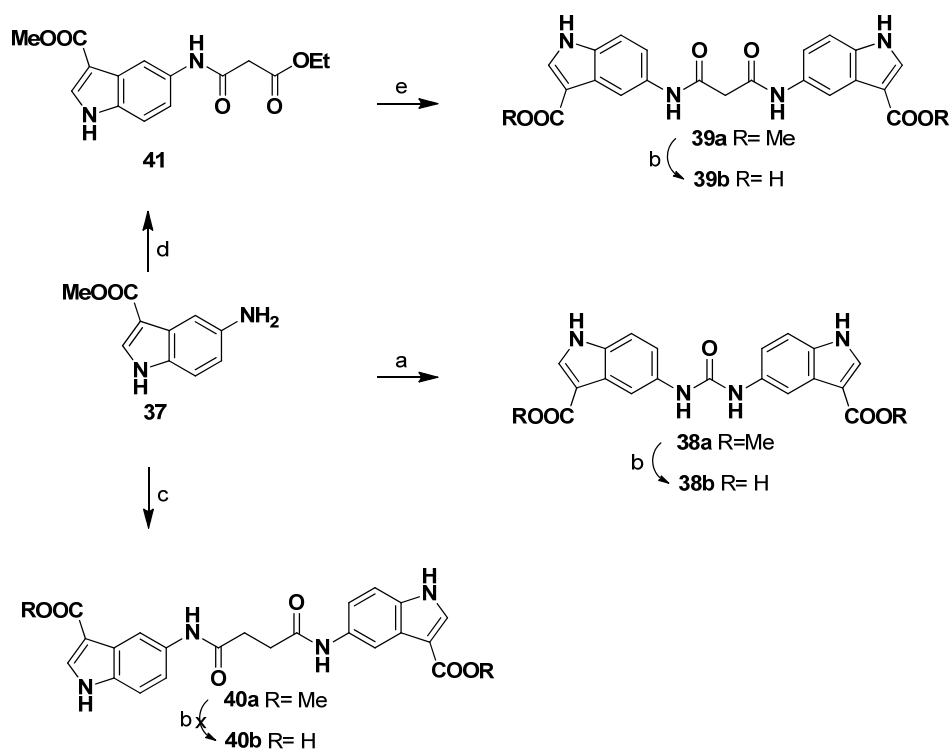
Scheme 3.11. *Reagents and conditions*: (a) trifosgene, TEA, dichloromethane, room temp, 4 h; (b) aqueous NaOH, pyridine, THF, room temp; (c) succinyl chloride, TEA, acetone, room temp, 4 h; (d) diethyl malonate, MW (300 W, 30 min), neat; (f) **41**, toluene/NMP (10:1), MW (300 W, 3 × 30 min).

A notice has to be done for the hydrolysis of compound **40a** which wasn't possible under basic condition. The reaction yield only to the amide bond hydrolysis.

3.6.2 Asymmetric derivatives

Applying the procedure of the 2-substituted carboxyindole compound **43a, 43b,** and **45a-50a** were obtained (Scheme 3.12) while **45b-50b** cannot be recovered through standard basic hydrolysis. For this reason we set up a different route for the synthesis of this compound (Scheme 3.13).

Scheme 3.12. *Reagents and conditions*: (a) ClCOCCl₃, dichloromethane, room temp, 4 h; (b) tryptamine, K₂CO₃, DMF, 150 °C, 1 h, sealed tube; (c) aqueous NaOH, pyridine, THF, room temp; (d) Boc-Gly-OH, TEA, HOBT, HBTU, DMF/THF, 12h, room temperature; (e) TFA/DMC, 1h, room temperature; (f) isocyanate, TEA, DMC, room temperature, 1-3h.

The reaction of the *tert*-butyl ester **51** with oxalyl chloride in acetone yield **53** that was easily hydrolyzed to **40b** using a mixture of dichloromethane and trifluoroacetic acid 1:1 ratio. On the other hand the reaction between Fmoc-Gly-OH and **51** yielded **52a** that was then deprotected on the amine side with dichloromethane/piperidine 2:1 ratio. The so obtained **52b** was reacted with

the proper isocyanate bearing to **55-60**. Acidic hydrolysis of the isocyanate derivatives bring to the desired **45b-50b.** (Scheme 3.13)
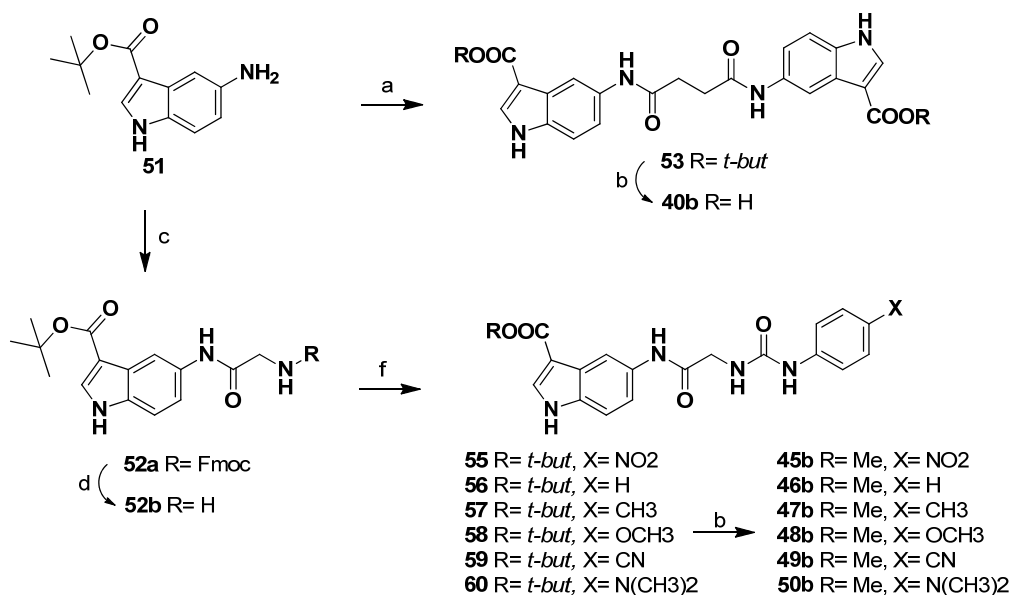
Scheme 3.13. ***Reagents and conditions*:** (a) succinyl chloride, TEA, acetone, room temp, 4 h; (b) TFA/DMC, 1h, room temperature; (c) Fmoc-Gly-OH, TEA, HOBT, HBTU, DMF/THF, 12h, room temperature; (d) DCM/piperidine, 1h, room temperature; (e) isocyanate, TEA, DMC, room temperature, 1-3h.

3.7 The chiral derivatives hypothesis

Once that also the hydrogen bond was validated (Chapter 4) we found a good and easy to handle scaffold for the development of powerful PRMTi.

With the aim of improve the biological activity and selectivity between the PRMTs we start thinking about the insertion inside our molecule of chiral center. So to improve my knowledge in stereoselective synthesis I've been for six months at the SCRIPPS research institute, San Diego, CA, in the laboratory of Prof. Carlos Barbas, III.

During this period I've been involved in a project aimed to the optimization of a highly enantioselective α-amination reactions and to the development of new multifunctional alkaloid catalyst.

3.7.1 Aim of the work

Recently, Barbas group disclosed a novel, dimeric quinidine catalyst and demonstrated its effectiveness in enantioselective aminooxygenation of oxindoles.[55] This multifunctional catalyst, with its seemingly flexible 1,3-dibenzyl tether, was far more effective than other structurally rigid cinchona alkaloid dimers tested (Figure 3.2a). These observations were counterintuitive from a catalyst design perspective and prompted us to explore the use of this catalyst in other asymmetric transformations, particularly in enantioselective α-amination reactions of aryl oxindoles.
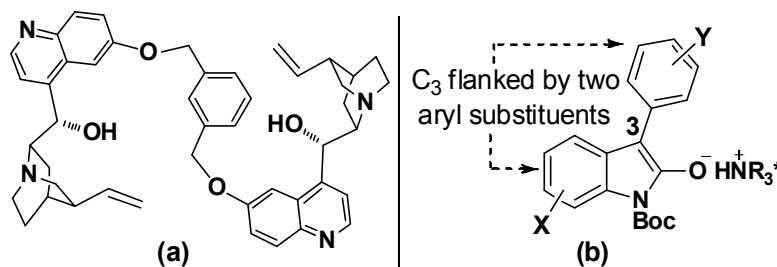
Figure 3.2. *Dimeric quinidine catalyst (a) and (b) aryl oxindole enolates.*

These reactions would provide access to optically active 3-amino aryl oxindoles, common structural motifs present in a variety of bioactive molecules, including NITD609 and SSR-149415, which are drug candidates for the treatment of malaria and stress-related disorders, respectively[56].

To date there was no general catalytic method for the asymmetric synthesis of 3-amino aryl oxindoles, especially those with readily cleavable diazo compounds such as di-*tert*-butyl azodicarboxylates[56c, 57].

Several challenges arise when oxindoles bear an aryl substituent at the C_3 position. First, the aryl group renders the C_3 methine acidic, facilitating a background reaction to occur. Conversely, it sterically hinders this position thereby limiting reactivity. Finally, it is difficult to differentiate the two enantiotopic faces of the oxindole enolate at C_3 when this position is flanked by two aryl groups of a similar size, one of which is the aryl oxindole ring (Figure 3.2b).

3.7.2 Optimization of reaction conditions

Initially, a model reaction using phenyl oxindole **61a** and di-*tert*-butyl azodicarboxylate was examined in the presence of cinchona alkaloid catalysts (Figure 3.3, Table 3.1). With 10 mol % of monomeric quinidine-derived catalyst **I**, **II**, or **III**, the *α*-amination reaction proceeded smoothly at -20 °C to afford product **63a** in good yields, albeit low enantiomeric excess (ee) (entries 1-3). Similarly, commercially available bulky hydroquinidine dimers **IV** and **V** also catalyzed the *α*-amination and provided products in moderate yields with low ee (entries 4-5). Interestingly, these dimers were not as effective as **I** (entry 1 vs. entries 4-5). Previously developed dimeric catalysts **VI-VIII** from Barbas laboratory were also tested, but they did not give satisfactory results with respect to ee (entries 6-8). These catalysts were synthesized by dimerization of quinidine at the C_9 position using different dibromo benzyl linkers. Notably, catalyst **VII** with a free hydroxyl group at C_6 provided

product in higher ee than did catalyst **VI** (entry 7 vs. entry 6). The catalyst with the 1,3-dibenzyl linker was more effective than that with the 1,2-dibenzyl linker (entry 8 vs. entry 6). Not surprisingly, C-$_6$ quinidine dimer **IX** (5 mol%) was most effective among the catalysts examined. These results mirrored those obtained from previously reported catalytic, enantioselective aminooxygenations of alkyl oxindoles.
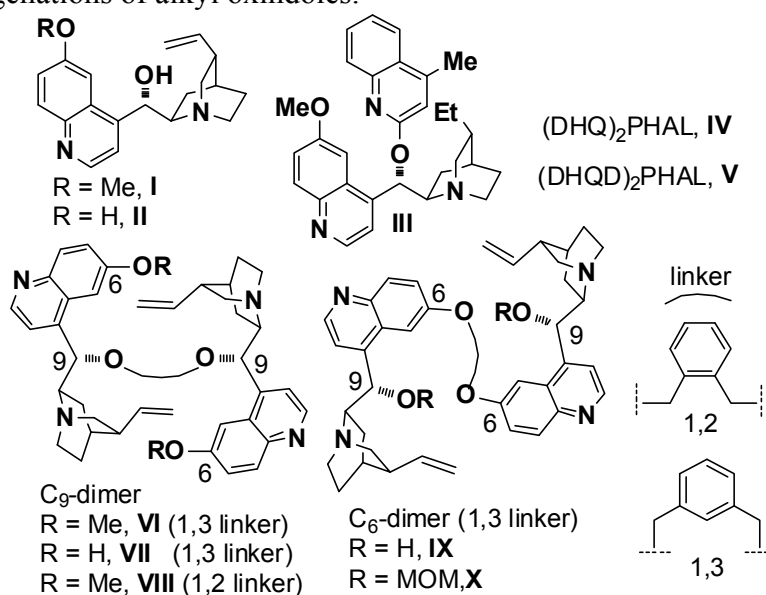
Figure 3.3. *Catalyst screen.*

The moderate enantioselectivity obtained with catalyst **IX** warranted further investigation. We discovered that Boc-protected aryl oxindole **1a** was highly reactive and a competing nonselective reaction occurred (due to the inherent reactivity of aryl oxindoles), thereby compromising the enantioselectivity. This problem was solved by performing the *α*-amination reaction at low temperature (entry 9 vs. entry 10). However, the ee increased only marginally when the temperature was lowered from -50 °C to -70 °C (entry 10 vs. entry 11).

A survey of solvents resulted in conditions that provided excellent yield and ee: the optimal results were obtained when the *α*-amination was performed in toluene at -70 °C for 48 h (entry 15). The long reaction time was required to

ensure good yield and ee of the desired product (24 h, entry 14 vs. 48 h, entry 15). As previously observed, the free hydroxyl groups in catalyst **IX** were important for high yield and enantioselectivity (entry 15 vs. entry 17). These results suggest that these hydroxyl groups might direct or orient the incoming azodicarboxylate electrophile via weak hydrogen bonding before C-N bond formation takes place.
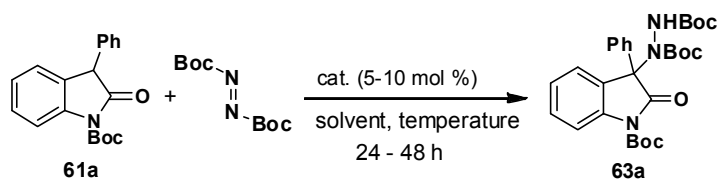
Entry	catalyst	solvent	temperature ^{o}C	yield[a] (%)	ee[b] (%)
1	**I**	THF	-20	86	45
2	**II**	THF	-20	74	27
3	**III**	THF	-20	81	14
4	**IV**	THF	-20	77	0
5	**V**	THF	-20	51	35
6	**VI**	THF	-20	96	5
7	**VII**	THF	-20	94	41
8	**VIII**	THF	-20	84	35
9	**IX**	THF	-20	93	53
10	**IX**	THF	-50	87	83
11	**IX**	THF	-70	78	88
12	**IX**	CH$_2$Cl$_2$	-70	89	79
13	**IX**	Et$_2$O	-70	72	92
14	**IX**	toluene	-70	87	95
15[c]	**IX**	toluene	-70	**93**	**98**
16	**IX**	m-xylene	-70	73	83
17[c]	**X**	toluene	-70	86	83

Table 3.1. *Optimization studies*. Unless otherwise noted, all reactions were run for 24 h. Reactions in entries 1-8 employed 10 mol% catalyst; those entries 9-17 employed 5 mol%. [a] Isolated yields. [b] Determined by chiral HPLC analysis. [c] Reactions run for 48 h

3.7.3 Investigation of oxindole substrates

Having established the optimal reaction conditions, we began to investigate the scope of the *α*-amination reaction with respect to oxindole substrates (Table 3.2). The reaction was general in scope, tolerating aryl oxindoles of different electronic natures and with different aromatic substitution patterns. For example, oxindoles bearing electron-neutral and electron-rich substituents at C_5 afforded the desired products in excellent yields and ee's (entries 1-2). Moreover, reactions with substrates with various aryl groups at the C_3 position also provided products in moderate to good yields with excellent ee's (entries 3-6).
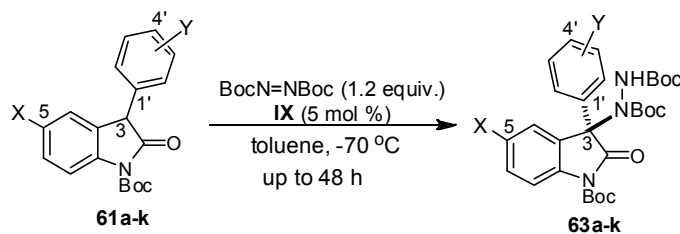
Entry	X	Y	product	yield[a] (%)	ee[b] (%)
1	H	H	**3a**	93	98
2	OMe	H	**3b**	96	95
3	H	4'-Me	**3c**	71	96
4[c]	H	3'-OMe	**3d**	95	97
5	H	4'-tBu	**3e**	76	96
6	H	4'-F	**3f**	87	96
7	OMe	4'-Me	**3g**	94	98
8	OMe	3'-OMe	**3h**	92	97
9	OMe	4'-F	**3i**	91	73
10	OCF$_3$	3'-OMe	**3j**	93	93
11	F	3'-OMe	**3k**	87	87

Table 3.2. *Enantioselective α-aminations of aryl oxindoles*. [a] Isolated yields. [b] Determined by chiral HPLC analysis.

It is noteworthy that oxindole **63f**, which contains a fluorine atom, was obtained in good yield and high ee (entry 6). Enantiomerically enriched

syntheses of fluorine-containing molecules are of importance in drug discovery and development.

Under our optimized conditions, oxindoles with various substituents at C_5 and different substitution patterns on the C_3 substituted aryl ring were all viable substrates (entries 7-11). The yields and ee's of the desired products were high for most of these substrates. The absolute configuration at the newly created center was determined to be *R* by comparison with a known oxindole derivative of **63a**. Finally, we demonstrated that product **63a** could be converted into the corresponding, free amino aryl oxindole in good yield with excellent optical purity.

3.7.4 Understanding the mechanism
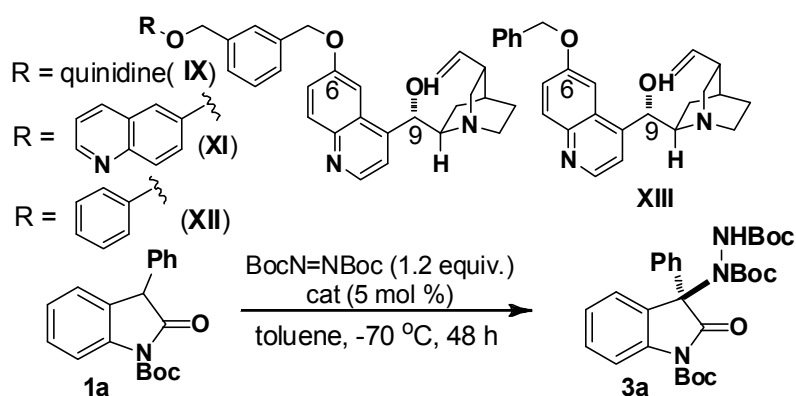
Entry	catalyst	product	yield[a] (%)	ee[b]
1	**IX**	**3a**	93	98
2	**XI**	**3a**	94	98
3	**XII**	**3a**	89	98
4	**XIII**	**3a**	89	94
5	**I**	**3a**	85	79

Table 3.2. *Insight into the role of the dimeric structure*. [a] Isolated yields. [b] Determined by chiral HPLC analysis.

To determine the role of the dimeric structure and the quinidine units in catalysis by **IX**, analogues were synthesized and examined in the enantioselective R-amination of **1a** (Table 3.3).

Catalysts **XI** and **XII** had only one quinuclidine moiety within the catalyst molecule. In **XI**, the 1,3-dibenzyl linker was attached to an electronrich π-quinoline ring, and in **XII**, it was attached to a simple phenyl ring. If π-π interactions between the two quinoline units in **IX** and **XI** were critical for catalysis, one would expect that **XII** would be a less effective catalyst. In catalyst **XIII**, the linker was a single benzyl group. The molecular weight and complexity of catalyst **IX** is greater than those of analogues **XI**, **XII**, and **XIII**. Significantly, catalysts **IX**, **XI**, and **XII** provided the desired product in similar yields with excellent ee's (Table 3.3, entries 1-3). Interestingly, when monomeric catalyst **XIII** was used, the ee was lower (entry 4 vs. entries 1-3). The drop in ee was even more significant when the 1,3-dibenzyl linker was replaced by a methyl group in catalyst **I** (entry 5). The effects of the C6-alcohol protecting group on ee were striking. This effect was not expected as this group is distal to the quinuclidine nitrogen atom where the reactive oxindole enolate is presumably generated. These observations provide valuable information that will aid future catalyst design and development. Our hypothesis is that the hydroxy protecting group at C6 affects the conformation of quinidine; this conformation impacts the stereochemistry-determining step and ultimately the enantioselectivity of the R-amination reaction (Figure 3.4, A-C).

Our proposed transition state structures are consistent with the following experimental observations: (a) the importance of a π-rich moiety that protects the C6 hydroxyl group in the catalyst to maintain high selectivity (Figure 3.4 B), (b) the free hydroxyl group at C9 to ensure high yield and ee, and (c) the same sense of asymmetric induction is observed for both aminooxygenation and R-amination of oxindoles[58].
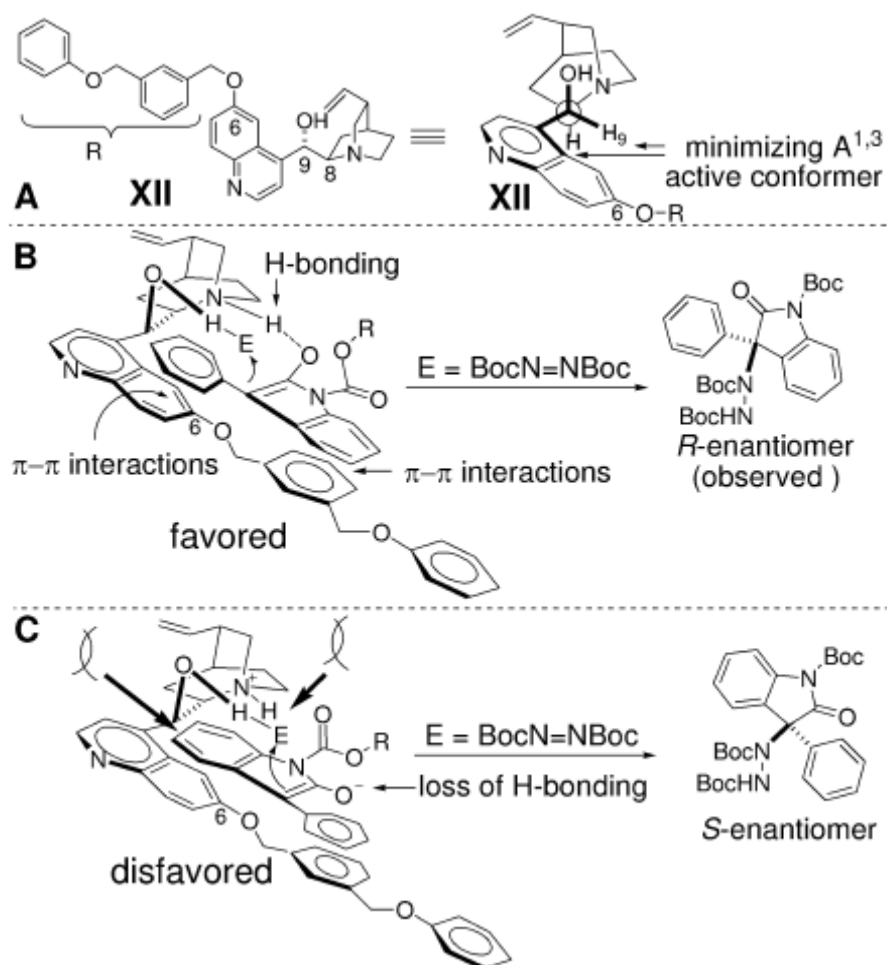
Figure 3.3. *Proposed active conformer (A) and proposed transition state structures with catalyst XII (B and C)[58].*

CHAPTER 4

BIOLOGY

4.1 Biological evaluation of naphthalene derivatives

In accordance with previous reported data by our research group[46b, 47], we first performed a preliminary screening of the activities of compounds **1–9** against Aspergillus nidulans RmtA, a fungal PRMT acting on histone H4 substrate and validated by us as a useful, predictive model for studying PRMT inhibition in mammals. Then we tested the derivatives against human recombinant PRMT1 in vitro, using histone as well as nonhistone (the RNA-binding nuclear shuttling protein, Npl3) proteins as a substrate, to confirm their inhibitory activity and to observe the influence of substrates different from histones on the inhibitory activity. Subsequently, selected compounds were tested (50 μm) against a panel of human PRMTs (PRMT1, PRMT3, CARM1, and PRMT6), using histone H4 (for PRMT1), histone H3 (for CARM1 and PRMT6) or GAR (for PRMT3) motifs as substrates. Furthermore, to assess the selectivity of our compounds against lysine methyltransferases, we also tested our compounds against the HKMT SET7/9 using histone H3 as a substrate.

All the biological assays have been performed by Prof. Gerald Brosch (Division of Molecular Biology, Biocenter-Innsbruck Medical University) and Prof. Mark T. Bedford (University of Texas M.D. Anderson Cancer Center Science Park-Research Division Smithville, Texas, USA).

4.1.1 Inhibitory activities against RmtA and PRMT1

Compounds **1-9** were preliminarily tested against Aspergillus nidulans RmtA, a fungal PRMT with significant sequence similarity to human PRMT1 and specific for methylation at Arg 3 of histone H4[15a], and against hPRMT1, using core histones as substrate as previously reported[15a, 47]. The inhibition (%)

at a fixed dose (nearly 100 µm) were first determined, and then the IC_{50} values for the active compounds were established (Table 4.1). Moreover, the derivatives were also tested against hPRMT1, using the heterogeneous nuclear ribonucleoprotein (hnRNP) Npl3p, an in vivo substrate of HMT1 from Saccharomyces cerevisiae[59], as a substrate. The inhibition (%) at fixed doses (10 and 50 µm) was determined (Table 4.2). **AMI-1** was used as reference compound in both assays.

The first result that emerged from both assays was that the substitution of the **AMI-1** sulfonic group with its carboxylic isoster gave only a slight decrease in inhibiting activity (cf. **AMI-1** and **1b**, Tables 4.1 and 4.2). Conversely, the replacement of the carboxylic group with an ester or an amide function diminished the activity against PRMT1. There was no difference in the order of activity when histone or nonhistone proteins were used as the substrate (**1b**>**1c**>**1a**), however, a slightly different order resulted when compared to the results obtained against RmtA (**1b**>**1a**>**1c**).

The substitution of the ureidic group with bisamidic moieties was detrimental to the inhibitory potency of the resulting derivatives, with the decrease being proportional to the length of the aliphatic spacer (cf. inhibition (%) values of compounds **1b, 2b** and **3b**).

The introduction of the tyramine nucleus in place of one of the two naphthalenic moieties resulted in derivatives with activities comparable to those of their counterparts (cf. activities of **1a** and **4a**, or **1b** and **4b**). On the other hand, replacement with the isosteric indole-2-carboxylic moiety gave less homogeneous results. In fact, indolic derivatives **6a** and **6b** showed decreased RmtA inhibition (Table 4.1) in comparison with their naphthalenic counterparts **1a** and **1b**, respectively, but the activities against PRMT1 were
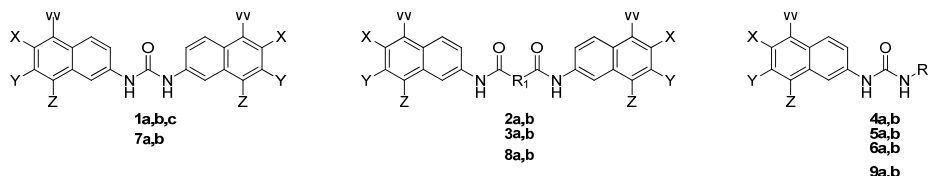
Com.	W	X	Y	Z	R₁	R₂	IC$_{50}$ (μM) or % inhbtn	
							RmtA	**PRMT1**
1a	OH	H	COOEt	H	-	-	191	448
1b	OH	H	COOH	H	-	-	138	298
1c	OH	H	CONH$_2$	H	-	-	445	406
2a	OH	H	COOEt	H	-CH$_2$-	-	121	233
2b	OH	H	COOH	H	-CH$_2$-	-	ND^c	ND^c
3a	OH	H	COOEt	H	-CH$_2$CH$_2$-	-	272	676
3b	OH	H	COOH	H	-CH$_2$CH$_2$-	-	123	343
4a	OH	H	COOEt	H	-	(indole)	196	346
4b	OH	H	COOH	H	-	(indole)	170	262
5a	OH	H	COOEt	H	-	(amine)	180	875
6a	OH	H	COOEt	H	-	(indole-COOEt)	620	510
6b	OH	H	COOH	H	-	(indole-COOH)	330	0 at 230 μM
7a	H	COOMe	H	OH	-	-	204	195
7b	H	COOH	H	OH	-	-	95	112
8a	H	COOMe	H	OH	-CH$_2$-	-	205	133
8b	H	COOH	H	OH	-CH$_2$-	-	395	272
9a	H	COOMe	H	OH		(indole)	290	320
9b	H	COOH	H	OH		(indole)	227	205
AMI-1	OH	H	SO$_3$H	H	-	-	88^d	92^d

Table 4.1. *Inhibition activities (IC$_{50}$) of 1-9 against hPRMT1 and RmtA using histone substrate^{a,b}*. ^{a}Chicken erythrocyte core histones were used as substrate; ^{b}Values are means determined for at least two separate experiments; ^{c}Not determined. ^{d} Literature value: 33.2±7.8 μm (RmtA) and 1.2±0.5 μm (PRMT1), fluorescence assay.

similar (Table 4.1 and Table 4.2). Strangely, in this case, carboxylic acid **6b** was less active than the corresponding ester **6a**.
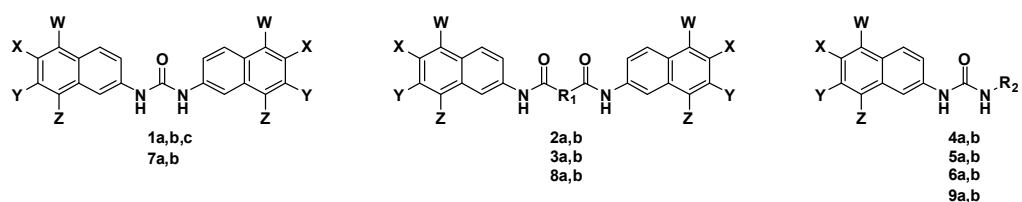
Com.	W	X	Y	Z	R$_1$	R$_2$	% inhib hPRMT1/Npl3	
							50 μM	10 μM
1a	OH	H	COOEt	H	-	-	40.81	4.91
1b	OH	H	COOH	H	-	-	75.16	41.73
1c	OH	H	CONH$_2$	H	-	-	63.47	0.13
2a	OH	H	COOEt	H	-CH$_2$-	-	34.65	10.77
2b	OH	H	COOH	H	-CH$_2$-	-	60.22	21.73
3a	OH	H	COOEt	H	-CH$_2$CH$_2$-	-	31.66	0.92
3b	OH	H	COOH	H	-CH$_2$CH$_2$-	-	30.85	-0.41
4a	OH	H	COOEt	H	-	(indole-propyl)	61.24	30.21
4b	OH	H	COOH	H	-	(indole-propyl)	71.65	20.21
5a	OH	H	COOEt	H	-	(dimethylaminopropyl)	-7.20	-1.70
6a	OH	H	COOEt	H	-	(methylindole-COOEt)	53.20	27.73
6b	OH	H	COOH	H	-	(methylindole-COOH)	32.47	8.01
7a	H	COOMe	H	OH	-	-	59.07	19.62
7b	H	COOH	H	OH	-	-	100.00	75.29
8a	H	COOMe	H	OH	-CH$_2$-	-	52.07	25.13
8b	H	COOH	H	OH	-CH$_2$-	-	90.99	-8.59
9a	H	COOMe	H	OH		(indole-propyl)	83.78	20.47
9b	H	COOH	H	OH		(indole-propyl)	73.17	20.15
AMI-1	OH	H	SO$_3$H	H	-	-	100.00	66.89

Table 4.2. **Inhibitory activities of compounds 1–9 against hPRMT1 using nonhistone substrates**[a,b]. [a]Npl3p was used as a nonhistone substrate, SAM as a cofactor. [b]Values given are means determined for at least two separate experiments.

This outcome could be justified by the formation of an intramolecular H bond between the indole NH and the COOH group, thus reducing the availability of both groups for interaction with the binding pocket of the

enzyme. Regarding compounds resulting from the formal shift of the ureidic function from the C-7 to the C-6 position of the naphthalene ring, it is noteworthy that their inhibitory activity was greatly enhanced. In fact, compounds **7**, **8**, and **9** were more potent than their positional isomers.
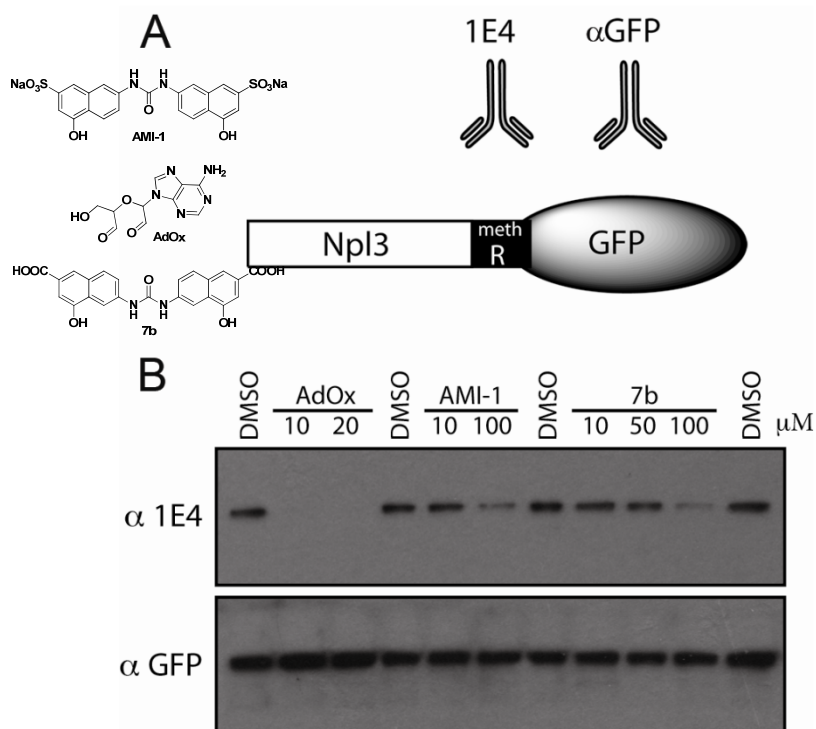
Figure 4.1. *Effects of compounds on cellular arginine methyltransferase activity*: a) a depiction of the GFP–Npl3 fusion protein with the position of methylated region and the antibodies that recognize it; b) HeLa cells were grown in 12-well plates and then transiently transfected with d2GFP–Npl3. Three hours post-transfection, the cells were incubated with the indicated compounds for 24 h. The cells were lysed in RIPA buffer, and Western analysis was performed with either the 1E4 antibody (top panel) or aGFP antibody (bottom panel). The effects of the compounds on GFP-Npl3 methylation status were established with the methyl-specific antibody, 1E4. The aGFP antibody showed the protein levels of GFP-Npl3. DMSO (0.25% v/v) was used as a vehicle (lanes 1, 4, 7, 11); compounds concentrations: AdOx (10 and 20 μm, lane 2,3), AMI-1 (10 and 100 μm, lanes 5,6), 7b (10, 50, and 100 μm, lanes 8–10).

Moreover, the biscarboxylic acid derivative **7b**, the isomer of **1b**, showed the highest inhibitory efficacy, comparable (Table 4.1) or even better (Table

4.2) than **AMI-1**. Finally, the introduction of a tertiary amine, like the dimethyl-aminopropyl moiety in compound **5a**, led to a substantial decrease of the inhibitory potency against hPRMT1 (Table 4.2). To determine whether the compounds that showed arginine methyltransferase inhibitory properties were able to inhibit PRMT activity within a cellular context, we used a fusion between green fluorescence protein (GFP) and the yeast protein Npl3. We previously established that mammalian PRMT1 can methylate Npl3 in vitro, thus we reasoned that this reaction could also take place within a mammalian cell line. A destabilized GFP variant was used that displays rapid turnover rates. This shorter half-life makes destabilized variants suitable for use in quantitative reporter assays. The GFP–Npl3 was transiently transfected into HeLa cells; post-transfection the cells were treated for 24 h with derivatives **1b**, **7b**, **8b** and **9b** (10, 50, and 100 μm), using AMI-1 and 2',3'-acycloadenosine-2',3'-dialdehyde (adenosine dialdehyde, AdOx), an indirect methyltransferase inhibitor, as reference compounds.

Because GFP and Npl3 are fused, the aGFP antibody was used to establish equal loading and aNpl3 antibody (1E4) acted as the methylation sensor (Figure 4.1a). Thus, the relative degree of arginine methylation in the presence of the different inhibitors can be established. Using this assay system we demonstrated that all tested derivatives were able to inhibit methylation of the GFP-Npl3 fusion, even if to varying extents. We thus focused our attention on **7b**, the compound that showed the highest inhibitory efficacy in enzymatic assays. A concentration gradient of **7b** (10, 50, 100 μm) was used to treat GFP–Npl3 transiently transfected HeLa cells for 24 h, using AMI-1 (10 and 100 μm) and AdOx (10 and 20 μm) as reference compounds. Total cell extracts were then subjected to Western analysis with aGFP and 1E4 (methyl-sensitive aNpl3) antibodies. Derivative **7b** inhibited the methylation of Npl3 within the cell in a dose-dependent manner and more effectively than the

reference AMI-1 (Figure 4.1b). In addition, the inhibitor of global methylation, AdOx, also reduced the methylation status of this reporter.

4.1.2 Inhibitory activities against a panel of arginine methyltransferases

The most active derivatives were selected and tested at 50 μm against a panel of arginine methyltransferases, as well as against a lysine methyltransferase, to assess their selectivity. Compounds **1b, 1c, 2b, 4a, 4b, 7b, 8b, 9a**, and **9b** were tested against the human recombinant arginine methyltransferases PRMT1, PRMT3, CARM1 and PRMT6, using histone H4, GAR motifs and histone H3 (for both CARM1 and PRMT6) as substrates, respectively, and also against the lysine methyltransferase SET7/9, using histone H3 as a substrate. AMI-1 was used as reference compound in all assays. As seen in Table 4.3, all of the derivatives tested are generally more selective for arginine methyltransferases than AMI-1. In fact, they are practically inactive against the lysine methyltransferase SET7/9, whereas AMI-1 shows a minor inhibition of this HKMT enzyme. This, together with its capability to inhibit all tested PRMTs, support the pleiotropic nature of the interactions established by the sulfonic groups. In contrast, compound **1b**, the carboxylic analogue of AMI-1, is inactive against SET7/9 but its activity is fairly comparable to that of its sulfonic counterpart against PRMT3, and to a lesser degree against CARM1. Interestingly, the use of histone H4 instead of core histones or the nonhistone protein Npl3p as a substrate for the PRMT1 assay yielded an appreciably weaker inhibition of PRMT1. The malonic bisamidic derivative **2b** exhibited a similar activity profile against the enzyme panel (Table 4.3). The bisamide **1c** was consistently less active than **1b** and **2b** against both PRMT3 and CARM1, but was the only compound among those tested that was able to inhibit PRMT6, with potency comparable to that of **AMI-1** or even higher. Regarding compound **7b**, the positional isomer of **1b**, this compound was confirmed as the most active in the series showing very

good inhibitory activities against PRMT1, PRMT3, and CARM1, and was comparable or even better than that exhibited by **AMI-1**. However, it was practically inactive against both PRMT6 and SET7/9 (Table 4.3). The bisamidic malonic analogue **8b** was consistently less active than **7b** against both PRMT1 and PRMT3, yet displayed a positive modulating effect on the enzymatic activity of CARM1 (Table 4.3). Similarly, the tryptamine derivatives **9a,b** showed little or no activity against PRMT1, PRMT3 and PRMT6, but strongly increased enzymatic activity of CARM1. In contrast, the isomeric derivatives **4a,b** showed only weak inhibition against all enzymes.
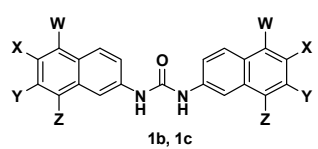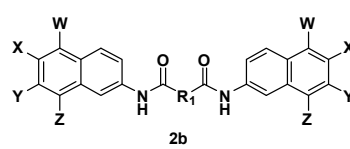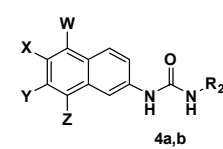
Com.	W	X	Y	Z	R_1	R_2	% inhib at 50 μM				
							PRMT1 /H4[b]	PRMT3 /GAR[c]	CARM1 /H3[d]	PRMT6 /H3[d]	SET7/9 /H3[d]
1b	OH	H	COOH	H	-	-	12.36	90.92	53.06	-7.23	-8.07
1c	OH	H	CONH$_2$	H	-	-	42.42	29.46	9.26	43.77	13.36
2b	OH	H	COOH	H	CH$_2$-	-	48.44	91.94	54.96	6.40	-1.40
4a	OH	H	COOEt	H	-	(indole)	24.73	42.13	-46.56	-12.40	6.65
4b	OH	H	COOH	H	-	(indole)	9.86	13.98	39.53	18.30	-5.13
7b	H	COOH	H	OH	-	-	61.65	72.81	83.07	-21.72	3.80
8b	H	COOH	H	OH	CH$_2$-	-	16.76	32.56	-298.99	-2.09	14.44
9a	H	COOMe	H	OH	(indole)		20.50	-5.03	-328.49	9.70	-8.46
9b	H	COOH	H	OH	(indole)		38.89	-8.17	-217.98	-11.13	-10.41
AMI-1	OH	H	SO$_3$H	H	-	-	87.67	101.33	74.76	40.69	34.34

Table 4.3. *Inhibition activities of selected compounds against different methyltransferases.*[a] [a]Values given are means determined for at least two separate experiments; [b]Histone H4 (1.5 μm) and SAM (0.42 μm) were used as substrates; [c]Glycine- and arginine-rich (GAR) motifs (0.41 μm) and SAM (0.42 μm) were used as substrates; [d]Histone H3 (1.1 μm) and SAM (0.42 μm) were used as substrates.

4.2 Biological evaluation of indole derivatives

4.2.1 Inhibitory activities against PRMT1

Compounds **21-23, 30**, **38-40**, **43**, were preliminarily tested against hPRMT1, using the heterogeneous nuclear ribonucleoprotein (hnRNP) Npl3p, an in vivo substrate of HMT1 from Saccharomyces cerevisiae[59], as a substrate. The inhibition (%) at fixed doses (10 and 50 μm) was determined (Table 4.4). **AMI-1** was used as reference compound in both assays.

Com	X	Y	R1	R2	% inhib hPRMT1/Npl3	
					50 μM	10 μM
21a	COOEt	H	-	-	32.16	10.10
21b	COOH	H	-	-	19.84	-21.68
22a	COOEt	H	-CH$_2$-	-	61.63	1.45
22b	COOH	H	-CH$_2$-	-	70.59	0.00
23a	COOEt	H	-CH$_2$CH$_2$-	-	17.01	-22.16
23b	COOH	H	-CH$_2$CH$_2$-	-	-17.21	-32.19
30a	COOEt	H	-	(indole propyl)	42.02	-6.27
30b	COOH	H	-	(indole propyl)	9.93	-2.36
31a	COOEt	H	-	(acyl-NO$_2$-phenyl)	63,21	6,70
38a	H	COOMe	-	-	58,82	17,64
38b	H	COOH	-	-	82,35	70.59
39a	H	COOMe	-CH$_2$-	-	88.24	64.71
39b	H	COOH	-CH$_2$-	-	94.12	47.06
40a	H	COOMe	-CH$_2$CH$_2$-	-	29.41	-11.76
40b	H	COOH	-CH$_2$CH$_2$-	-	70.59	64.71
43a	H	COOMe	-	(indole propyl)	47.06	0.00
43b	H	COOH	-	(indole propyl)	82.35	0.00
AMI-1	-	-	-	-	100.00	66.89
7b	-	-	-	-	100.00	75.29

Table 4.4. *Inhibitory activities of compounds 21-23, 30, 38-40, 43 against hPRMT1 using nonhistone substrates[a,b].* [a]Npl3p was used as a nonhistone substrate, SAM as a cofactor. [b]Values given are means determined for at least two separate experiments..

The data emerging from the first series of indole derivatives (**21-23a,b** and **30a,b**) were not exciting (Table 4.4). To a first look all the derivatives result less active of the corresponding naphthalene analogue.

The most important data is a general inversion of activity trend between ester and acid. In the 1st indole series the ester derivatives result more active than the corresponding acid (**21a**>**21b**, **23a**>**23b** and **30a**>**30b**). On the other hand, in contrast with the naphthalene data (Table 4.2), the substitution of the ureidic moiety with a bisamidic one bring to an improvement of activity (**21a**<**22a**) that dramatically drop with the increase of the spacer length (**22a**>**23a**). Asymmetric derivative obtained by substitution of the aminoindole with the tyramine nucleus bring to a slightly increase of activity in the ester derivatives (cf. activities of **21a** and **30a**) while the relation is the opposite looking at the acid (**21b**>**30b**). Notably mixed amid-urea derivative **31a** showed a nice inhibitor power, being the most active compound of this series.

As regards to the 2nd indole series, our hypothesis of intramolecular hydrogen bond seems to be valid. Not only all the 3-substituted carboxyindol are better PRMT-1 inhibitors, in this assay, than the 2-carboxy ones but also the activity trend between ester and acid has been recovered (Table 4.4). As the previous compound the replacement of the ureidic function with a bisamidic one improve the PRMT-1 inhibition in a length depending manner. The spacer has to be one *CH$_2$* (**39b**>**38b**>**40b**). Again the asymmetric derivatives show almost the same power of the symmetric ones (cf. activities of **38b** and **43b**). Moreover, the bisamidic derivative **39b** shows an inhibitor power similar to **AMI-1** and **7b**, our best inhibitors.

4.2.2 Inhibitory activities against a panel of arginine methyltransferases

Applying the same procedure developed for the naphthalene derivatives[53], the most active indole compound were selected and tested at 50 μm against a panel of arginine methyltransferases, as well as against a lysine methyltransferase, to assess their selectivity (Table 4.5).

Com	X	Y	R_1	R_2	% inhib at 50 μM					
					PRMT 1/H4[b]	PRMT 3/GAR[c]	CARM1 /H3[d]	PRMT6 /H3[d]	SET7/ 9/H3[d]	G9a / H3[d]
38b	H	COOH	-	-	-20.89	59.83	nd	nd	-8.07	26.10
39a	H	COOMe	CH_2	-	6.61	75.54	nd	nd	70.73	28.83
39b	H	COOH	CH_2	-	-9.38	80.97	nd	nd	56.78	-3.41
40b	H	COOH	$(CH_2)_2$	-	1.16	82.18	nd	nd	63.92	-3.62
43b	H	COOH	-	(structure)	-66.19	72.84	nd	nd	61.70	-3.79
31a	COOEt	H	-	(structure)	27.73	55.89	-377.12	-19.49	10.25	nd
7b	-	-	-	-	61.65	72.81	83.07	-21.72	3.80	nd
AMI-1	-	-	-	-	87.67	101.3	74.76	40.69	34.34	

Table 4.5. *Inhibition activities of selected compounds against different methyltransferases.*[a] [a]Values given are means determined for at least two separate experiments; [b]Histone H4 (1.5 μm) and SAM (0.42 μm) were used as substrates; [c]Glycine- and arginine-rich (GAR) motifs (0.41 μm) and SAM (0.42 μm) were used as substrates; [d]Histone H3 (1.1 μm) and SAM (0.42 μm) were used as substrates

Compounds **38b, 39a, 39b, 40b, 43b** and **31a** were tested against the human recombinant arginine methyltransferases PRMT1, PRMT3, CARM1 and PRMT6, using histone H4, GAR motifs and histone H3 (for both CARM1 and PRMT6) as substrates, and also against the lysine methyltransferase

SET7/9 and G9a, using histone H3 as a substrate. Data quantization has been done by liquid scintillization counting or densiometric measurement (Quantity One Software). Where not showed, the data does not fit with measurement on film (Figure 4.2 and Figure 4.3).
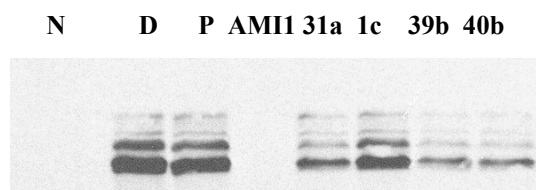
Figure 4.2. *Inhibition activities of selected compounds against CARM-1/H3*
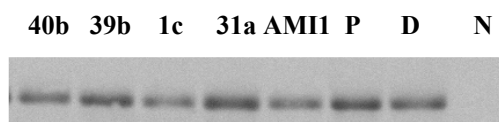
Figure 4.3. *Inhibition activities of selected compounds against PRMT-6/H3*

The first important result emerging from the selectivity assays of the indole derivatives is a good inhibition of PRMT3. Derivatives **38b, 39a, 39b, 40b** at 50 μm inhibit almost only PRMT3 among the PRMTs. On the other hand the same compounds are less selective than the reference **7b** towards different methyltransferases. Seems that the indole structure, strictly linked to the SAM, bring to a decrease of selectivity. Interestingly **39b** and **40b**, the most powerful inhibitors of the indole series, show a good selectivity between lysine methyltransferases: good inhibition of SET7/9/H3 but are completely inactive on G9a/H3.

4.2.2 Activation activities against a panel of arginine methyltransferases

Another important results emerging from the selectivity assays is the peculiar activity of **31a**: this compound, almost inactive towards PRMTs, shows a really strong and selective activation of CARM-1. This data, reported for the first time in literature and that may seems an outlier, bring us to build and test a small focused library of compound strictly correlated to **31a** to validate our hypothesis (Table 4.6).
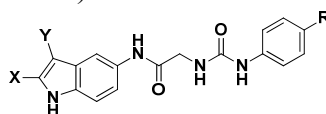
Com	X	Y	R	% inhib hPRMT1/Npl3		% activ CARM1 /H3	% activ CARM1 /PABP
				50 μM	10 μM	50 μM[a]	50 μM[b]
31a	COOEt	H	NO_2	63,21	6,70	184,37	175,50
31b	COOH	H	NO_2	0.00	0.00	142,54	85,29
32a	COOEt	H	H	0,00	0,00	136,20	10,00
32b	COOH	H	H	4,74	3,68	166,09	171,76
33a	COOEt	H	CH_3	11,58	0,00	127,22	382,35
33b	COOH	H	CH_3	0,00	0,00	111,03	148,82
34a	COOEt	H	OCH_3	6,84	0,00	184,27	74,71
34b	COOH	H	OCH_3	37,89	0,00	211,45	96,47
35a	COOEt	H	CN	13,68	0,00	115,35	357,65
35b	COOH	H	CN	4,74	0,00	142,69	81,18
36a	COOEt	H	$N(CH_3)_2$	47,37	0,00	102,14	70,59
36b	COOH	H	$N(CH_3)_2$	6,64	0,00	48,34	134,71
45a	H	COOMe	NO_2	41,18	23,53	133,98	114,71
46a	H	COOMe	H	6,37	0,00	74,61	26,47
47a	H	COOMe	CH_3	17,89	0,00	39,86	4,71
48a	H	COOMe	OCH_3	10,57	0,00	62,70	28,24
49a	H	COOMe	CN	0.00	0,00	134,82	38,82
50a	H	COOMe	$N(CH_3)_2$	0,41	0,00	125,20	7,65
Positive						260	300
DMSO						100	100

Table 4.6. *Activation of CARM-1 and inhibition of hPRMT1* [a]Histone H3 (1.1 μm) and SAM (0.42 μm) were used as substrates, [b]PABP (1.1 μm) and SAM (0.42 μm) were used as substrates.

The value of activation has been measured on two different substrate, one histonic and one non-histonic. Regards to the H3 substrate the better activator are 34a and **31a** while on PABP-1 are **33a** and **35a**.

An interesting result is the inversion of activity between ester and acid. For the activation the better compounds are all ester, while the acid works better for the inhibitions. Moreover all the 2-substituted carboxyindole are better activator than 3-derivatives, while for the inhibitors was the exact opposite (cf. activity of **31a, 33a** and **35a,** with **45a**, **47a** and **49a**). For the further development of activators the substituent on the phenyl ring has to be taken in account. An electron poor ring is needed to improve activation of CARM1 (**35a** and **31a** are better than **32a** and **36a**) as well as a para-substitution (compare **33a** and **32a**).

The activation data became more interesting if consider that DMSO alone inhibits the substrates methylation of about 2.5-3 fold.

Another interesting data comes from the dose dependent assay of **31a** (Figure 4.4).
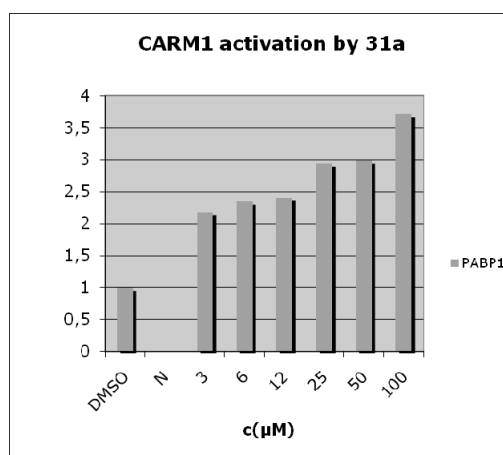
Figure 4.4. *Dose response data of 31a on CARM1/PABP*

A strong activation effect (200%) starts already at 3µm and increase until 360% at a dose of 100 µm. Additional studies are on run to determine the AC_{10} (activator concentration at 10% maximal activation level)[60] **31a**.

As previously done with the best PRMTi, also for compound showing the best activator power (**33a** and **35a**) in cell assays has been done.

In this case as substrates PABP-1 has been used because CARM-1 doesn't methylate NPL3. Importantly, CARM1 is the only enzyme that methylates PABP1, and in CARM1 knockout cells PABP1 is hypomethylated. For this study, a methyl-specific antibodies against the PABP1 sequence CGAIR*PAAPR*PPFS (where R* represents an asymmetrically dimethylated arginine residue) has been developed. Moreover, as yet, no arginine deme-thylases have been discovered, this methyl-mark is thus extremely stable. To test the efficacy of potential PRMT modulators in cells could require days of treatment to allow for the methylated substrates to turnover. Under these conditions, compounds with pleiotropic effects would be difficult to investigate in a cell-based assay. To bypass this problem a PABP1 inducible cell line has been developed. Upon treatment with tetracycline (Tet), these HEK293 cells express a flag-tagged form of full-length PABP1 (fPABP1). This tag allows the induced form of PABP1 to migrate more slowly by SDS-PAGE. We can, thus, easily distinguish between the endogenous PABP1 and the newly synthesized fPABP1. When fPABP1 expression is induced with Tet in the presence of a potential CARM1 activator, we can gauge the degree of fPABP1 methylation, using the methyl-specific anti-PABP1 antibody.

As can be easily seen (Figure 4.5), **33a** and **35a** induce a strong increment in methylation of newly synthesized PABP-1 (higher bands). So our activators as well as our inhibitors are active not only in vitro, but also in cellular assays.

+	-	-	-	+	+	Tetraciclin (1 µg/ml)
-	-	+	-	+	-	**33a** (50 µM)
-	-	-	+	-	+	**35a** (50 µM)
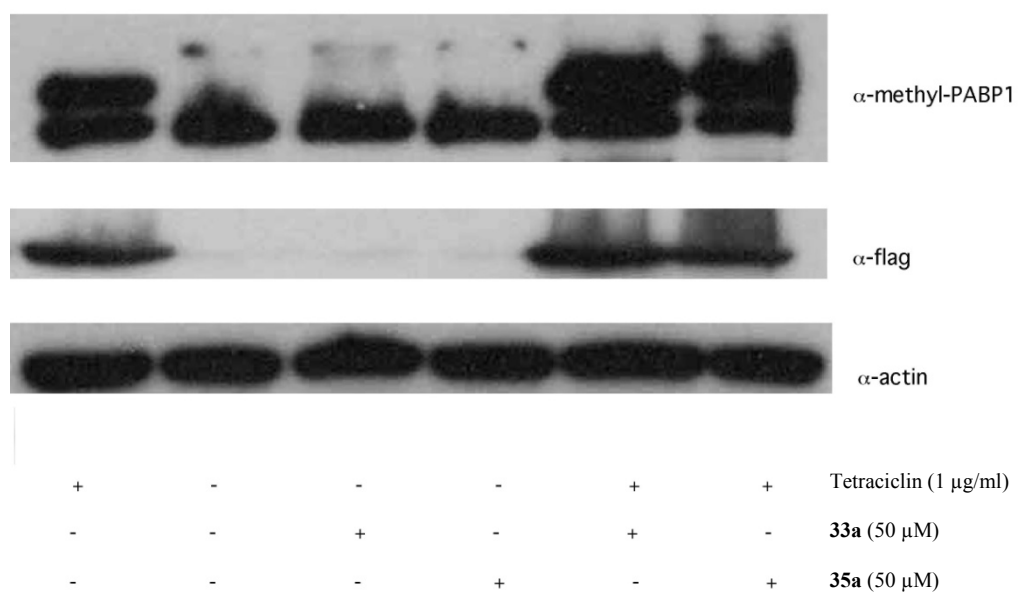
Figure 4.5 *In cell assays of CARM-1 activators*

CHAPTER 5

DOCKING AND BINDING MODE

5.1 Docking and binding mode of naphthalene derivatives

The binding modes of selected PRMT inhibitors were carried out in an attempt to rationalize their differences in terms of activity. To this aim, compounds **1b**, **7b**, and AMI-1 were docked (Autodock 3 program)[61] into the homology model of the PRMT1 orthologue RmtA, previously reported by us[47] and used to describe three different binding modes of PRMT inhibitors: (a) molecules *docked in the Arg pocket* (DAP), (b) molecules *docked in the SAM pocket* (DSP), and (c) molecules partially overlapping with both sites (*docked in both pockets*, DBP).[47] The analysis of the Autodock conformations selected by the X-Score[62] external scoring function showed that **1b** belongs to the DSP group, while **7b** seems to bind preferentially in the DBP (Figure 5.1). In particular, the binding conformation selected for **1b** is similar to the one observed for the SAM co-factor (Figure 5.2). In fact, one naphthalenic group lays in a sandwich-like mode between Met69 and Met123 side chains (SAM adenine binding site) making positive van der Waals interactions, while the corresponding carboxylate group makes a weak hydrogen bond with Thr126-OH. The other aromatic moiety is placed in the SAM methionine pocket, delimited by Arg22, Asp44, Gly46, Cys47, Ile51, Leu52 and Glu112, and the respective carboxylate function establishes either an electrostatic or a hydrogen bond interaction with the Arg22 side chain. Moreover, the two ureidic NH are within hydrogen bonding distance of Asp68 carboxylate group (Figure 5.2B), thus mimicking the two OH of the SAM ribosyl moiety (compare Figures 6A5.2A and 5.2B).
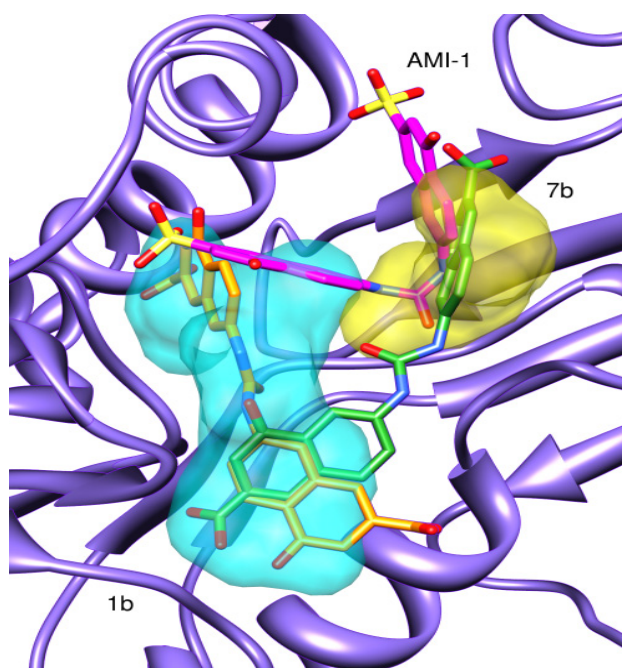
Figure 5.*1 Autodock/X-Score selected binding conformations of compounds 1b (orange), 7b (green) and AMI-1 (magenta)* docked into RmtA catalytic site. The volumes occupied by Arg and SAM are represented in yellow and cyan, respectively

Regarding derivative **7b**, it is noteworthy that it displays a substantially different binding scenario from the one above described for its positional isomer **1b**, as the binding conformation selected by X-Score was docked into the DBP pocket (Figure 5.3). Significant hydrogen bonds may be observed between **7b** with both the arginine anchoring residues Glu112 and Glu121 and with Asp68 (Figure 5.3B). The differences in affinity values among derivatives structurally highly correlated to each other (like **1b**, **7b** and AMI-1) could be better highlighted by the direct comparison of their respective binding modes while maintaining the same protein orientation (Figure 5.4), and by comparison of the bonding interactions (listed in Table 5.1) made by each inhibitor with the residues in RmtA binding pockets.
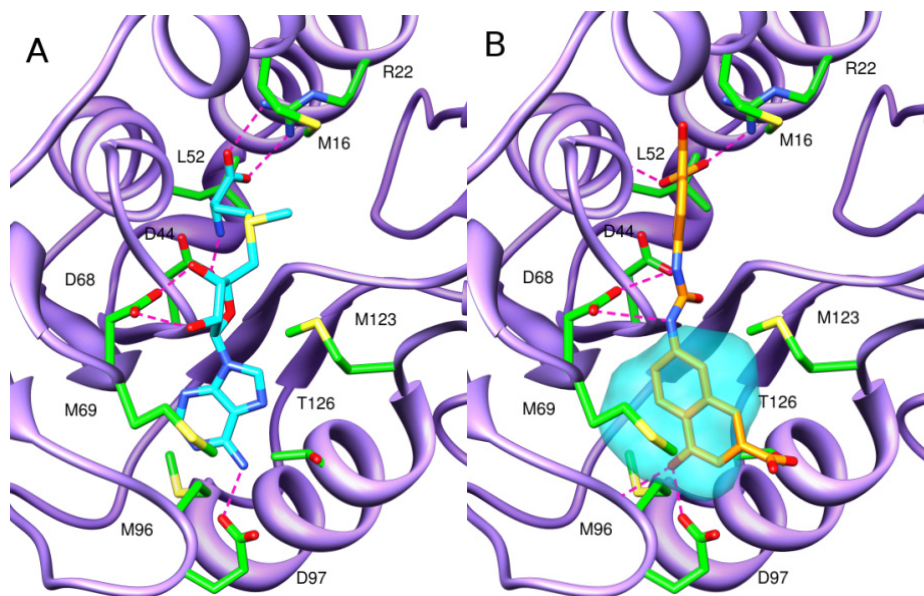
Figure 5.*2 Comparison between binding conformations of SAM cofactor and compound 1b into RmtA catalytic site.* A) SAM cofactor (cyan colored carbon atoms); B) 1b (orange colored carbon atoms). The RmtA residues within 4.0 Å from the docked compounds are reported in green. For the sake of clarity, hydrogen atoms are not displayed.

Like AMI-1, derivative **7b** can be classified as a DBP binding compound, even though it shows a stretched conformation, while AMI-1 was found to bind in a bended shape. In fact, similar to AMI-1, half of **7b** structure is buried into a hydrophobic pocket delimited by Trp262, His261, and Tyr116 side chains. However, the second half of **7b** is located in the SAM adenine binding pocket, while the second half of AMI-1 is placed into the SAM methionine site.

On the other hand, **1b** is a DSP binding derivative and thus shares fewer interactions with AMI-1 than **7b** does. Interestingly, the binding profile of **1b** seems to be intermediate between those displayed by **7b** and AMI-1. In fact, half of its structure is docked in the SAM methionine site, similar to AMI-1, and the other half occupies the same SAM adenine binding region that is also

filled by one of **7b**'s two substituted naphthyl groups (Figure 5.1 and Figure 5.4).
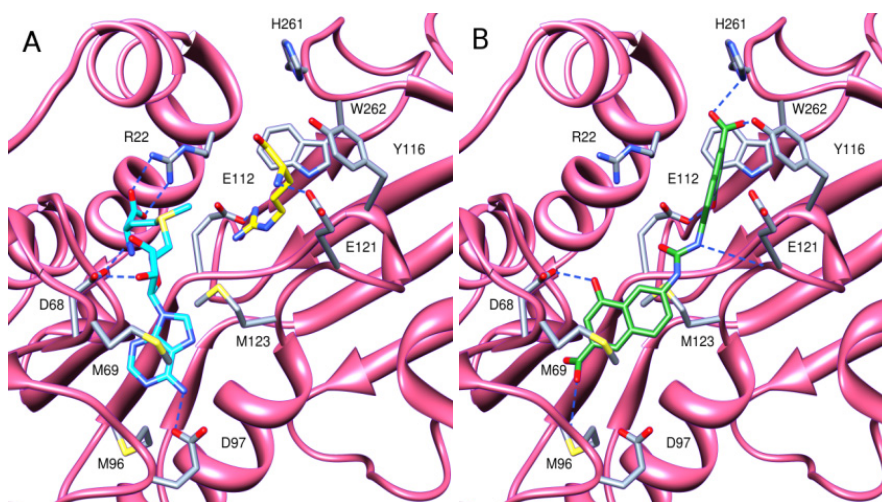
Figure 5*.3 **Binding conformations of compound 7b into RmtA catalytic site.** A) SAM cofactor (cyan colored carbon atoms) and Arginine substrate (yellow colored carbon atoms); B) 7b (green colored carbon atoms). The RmtA residues within 4.0 Å from the docked compounds are reported in cornflower blue. For the sake of clarity, hydrogen atoms are not displayed

In all three derivatives either sulfonic or carboxylic acid groups act as anchoring points to the protein establishing relevant interactions. In particular, one AMI-1 sulfonic group interacts with Arg22 (guanidinic side chain) and Thr49 (amidic NH) (Table 1) and the second with main chain His261 amidic NH. On the other hand, **1b** and **7b** carboxylic groups, while sharing some interactions with AMI-1 sulfonic group (H-bonds with Arg22 and His261 for **1b** and **7b**, respectively, Table 1), establish new interactions with both Tyr116 and Met96 (**7b**) or Leu52 and Tyr126 (**1b**).

A deeper analysis of the above described binding modes could help explain the observed activity trend. The lower activity of **1b** in respect to those observed for **7b** and AMI-1 could be due to its minor interaction with the important Ile12-His13-His16-Thr49 pocket, as well as to the lack of any

interaction with the arginine anchoring residues Glu112 and Glu121 that seem to play an important role in the enzyme inhibition.
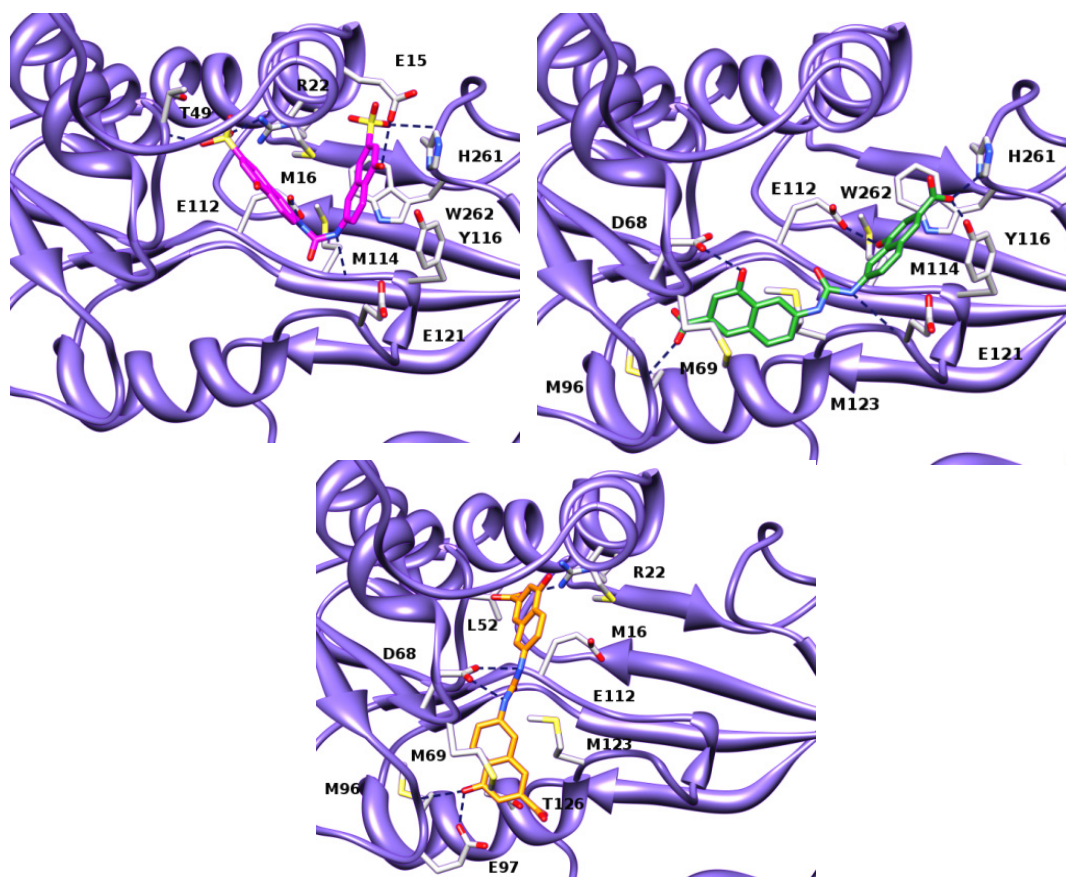
Figure 5.*4 Comparison between binding conformations of AMI-1 (magenta), 7b (green) and 1b (orange) into RmtA catalytic site.).* The RmtA residues within 4.0 Å from the docked compounds are reported in white. For the sake of clarity, hydrogen atoms are not displayed.

	AMI-1		7b		1b	
	d (Å)	residue···substituent	d (Å)	residue···substituent	d (Å)	residue···substituent
electrostatic/H-bond interactions	2.9	Glu15···OH				
	3.1	Arg22···SO_3^{2-}			2.7	Arg22···CO_2^-
	2.9	His261···SO_3^{2-}	3.2	His261···CO_2^-		
			3.2	Tyr116···CO_2^-		
	3.3	Met114···NH				
	2.8	Glu112···NH	3.6	Glu112···OH		
			2.8	Glu121 NH		
	2.7	Thr49 NH···SO_3^{2-}				
			2.9	Asp68···OH	2.8	Asp68···NH
			2.7	Met96-NH···CO_2^-	2.8	Met96-NH···OH
					2.3	Glu97···OH
					3.3	Leu52-NH···CO_2^-
					2.9	Tyr126···CO_2^-
Hydrophobic interactions	Met16-Thr49-Gly46		-		Met16-Thr49-Gly46	
	Trp262-His261-Tyr116		Trp262-His261-Tyr116		-	
	-		Met123-Met69		Met123-Met69	

Table 5.*1 Summary report of the interactions between AMI-1, 7b, 1b and RmtA amino acid residues*

CHAPTER 6

CONCLUSIONS

Conclusion

We started by stating the rationale by which 7,7'-carbonylbis-(azanediyl) bis(4-hydroxynaphthalene-2-sulfonic acid) (**AMI-1**), a selective PRMT inhibitor with a bisanionic structure that is related to compounds known to generate pleiotropic interactions with many proteins, should be further optimized before exploring additional binding pockets. On the basis of these observations, we have synthesized two series of analogue structurally related to the **AMI-1** and characterized by the substitution of the sulfonic groups with the bioisosteric carboxylic groups, the replacement of the ureidic function with a bisamidic moiety, the introduction of a *N*-containing basic moiety or the positional isomerization of the aminohydroxynaphthoic moiety as well as the substitution of the naphthol structure with an indolic one. We assessed their biological activity against a panel of arginine methyltransferases (fungal RmtA, hPRMT1, hCARM1, hPRMT3, hPRMT6), as well as against SET7/9 and G9a lysine methyltransferase, using histone and nonhistone proteins as substrates. All the data obtained allowed us to understand a preliminary structure–activity relationships.

Substitution of the **AMI-1** sulfonic group with the carboxylic isoster gave compound **1b**, which maintained a fairly good activity. Moreover, derivatives resulting from the formal shift of the ureidic function from the C-7 to the C-6 position of the naphthalene ring (compounds **7, 8,** and **9**) were more potent than their positional isomers. The biscarboxylic acid **7b**, an isomer of **1b**, showed the highest inhibitory efficacy in vitro and was able to prevent arginine methylation of cellular proteins in whole-cell assays, with activities comparable or even better than **AMI-1**. As regard to the indole moiety, the 2-substituted showed a general decree of activity compared to the naphthalene counterpart due to an intramolecular hydrogen bond. This problem was solved

shifting the carboxylic moiety from 2 to 3 position; compound 39b showed an inhibitor power similar to **7b**.

All naphthalene derivatives evaluated were found to be selective for arginine methyltransferases, and practically inactive against the lysine methyltransferase SET7/9, whereas **AMI-1**, due to the pleiotropic nature of the interactions established by the sulfonic groups, inhibits all the enzymes tested, albeit with different potencies, including a minor inhibition of the HKMT SET7/9. Differently, indole derivatives showed a general selective inhibition of PRMT-3 and HKMT SET7/9 among other PRMTs and HKMTs. This decrease in selectivity, probably due to the analogy between indole and SAM, may be overtaken by further fictionalization.

Finally we identified, for the first time, CARM-1 selective activator. Compound **33a** and **35a** were the most powerful CARM-1 activator using non histone substrate PABP-1, and compound **31a** showed a dose dependent activation of this enzyme.

CHAPTER 7

EXPERIMENTAL SECTION

7.1 Naphthalene and indole derivatives

All chemicals were purchased from Aldrich Chimica (Milan, Italy) or from Alfa Aesar GmbH (Karlsruhe, Germany) and were of the highest purity. All solvents were reagent grade and, when necessary, were purified and dried by standard methods. All reactions requiring anhydrous conditions were conducted under a positive atmosphere of nitrogen in oven-dried glassware. Standard syringe techniques were used for anhydrous addition of liquids. All microwave reactions were conducted using a CEM Corporation (Cologno al Serio (BG), Italy) Discover LabMate system using the standard 10 mL reaction vessel. Reactions were routinely monitored by TLC performed on aluminum-backed silica gel plates (Merck DC, Alufolien Kieselgel 60 F_{254}) with spots visualized by UV light ($\lambda = 254$, 365 nm) or using a $KMnO_4$ alkaline solution. Concentration of solutions after reactions and extractions involved the use of a rotary evaporator operating at a reduced pressure of ~10 Torr. Organic solutions were dried over anhydrous sodium sulfate. Chromatographic separations were performed on silica gel (Silica gel 60, 0.063-0.200 mm; Merck DC) or on alumina (aluminium oxide 90, active, neutral, 0.063-0.200 mm; Merck DC) columns. Melting points were determined on a Gallenkamp melting point apparatus in open capillary tubes and are uncorrected. Infrared (IR) spectra (KBr) were recorded on a Shimadzu FTIR-8000 instrument. ^{1}H NMR spectra were recorded at 300 MHz on a Bruker Avance 300 spectrometer; chemical shifts are reported in δ (ppm) units relative to the internal reference tetramethylsilane (Me_4Si). Mass spectra were recorded on a Finnigan LCQ DECA TermoQuest (San Jose, CA, USA) mass spectrometer using an electrospray ion source (ESI-MS). Combustion analysis on target compounds were performed by our Analytical Laboratory at the University of Salerno. All compounds showed ≥98% purity. When the elemental analysis is not included, crude compounds were used in the next

step without further purification. As a rule, samples prepared for physical and biological studies were dried in high vacuum over P_2O_5 for 20 h at temperatures ranging from 25 to 110 °C, depending on the sample melting point.

Preparation of ethyl 7-amino-4-hydroxy-2-naphthoate (13a)
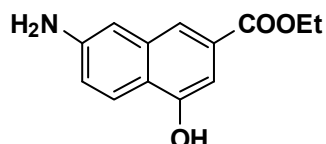
The mixture (3.00 g, 12.97 mmol) of ethyl 7-amino-4-hydroxy-2-naphthoate **12a** and ethyl 5-amino-4-hydroxy-2-naphthoate **12b**, obtained as previously described,[53] was dissolved in 150 mL of methanol and a solution of cobalt(II) acetate tetrahydrate (4.00 g, 16.06 mmol) in 20 mL of AcOH/AcONa pH 5 buffer was added dropwise in 30 min. The resulting slurry was heated to 50 °C for 3 h and then left at room temperature for additional 3 h. The black solid was filtered off and the solution was concentrated under reduced pressure. Saturated aqueous $NaHCO_3$ solution (150 mL) was added to the resulting oil and the mixture was extracted with ethyl acetate (3 × 75 mL). The organic phase was dried over anhydrous sodium sulfate and concentrated under vacuum to give **12a** as a white solid (0.96 g, 33%); mp 245.5-246.5 °C (dec); ^{1}H NMR (CDCl$_3$) δ 10.57 (s, 1H), 8.03 (d, J = 8.0 Hz, 1H), 7.92 (d, J = 1.2 Hz, 1H), 7.18 (d, J = 1.2 Hz, 1H), 7.02– 6.96 (m, 2H), 5.50 (br s, 2H), 4.40 (q, J = 7.3 Hz, 2H), 1.41 (t, J = 7.3 Hz, 3H); MS (ESI) *m/z* (%): 232 (M+H)[+].

Preparation of diethyl 7,7′-carbonylbis(azanediyl)bis(4-hydroxy-2-naphthoate) (1a)
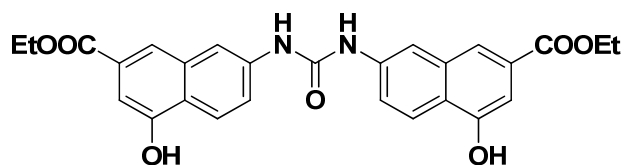
Diphenylcarbonate (0.463 g, 2.16 mmol) and 4-dimethylaminopyridine (0.053 g, 0.43 mmol) were added to a solution of **12a** (1.0 g, 4.32 mmol) in chlorobenzene (20 mL) and the mixture was refluxed for 72 h. The solvent was evaporated under reduced pressure, and the dark brown solid obtained was washed twice with petroleum benzene. The solid was taken up with 100 mL of ethyl acetate and washed with 3N HCl solution (3 × 70 mL). The organic phase was then washed with brine, dried and evaporated. The crude residue was purified by column chromatography on silica gel (gradient, dichloromethane/methanol, 98:2 to 90:10) to afford pure **1a** as a white solid (0.633 g, 60%); mp 266.2-266.8 °C (dec); ^{1}H NMR (DMSO-d$_6$) δ 10.43 (s, 2H), 9.11 (s, 2H), 8.16 (s, 2H), 8.10 (d, J = 8 Hz, 2H), 7.94 (s, 2H), 8.33 (d, J = 8 Hz, 2H), 7.25 (s, 2H), 6.45 (q, J = 7 Hz, 4H), 1.36 (t, J = 7 Hz, 6H); MS (ESI) m/z (%)*:* 489 (M+H)$^+$; Anal. calcd for C$_{27}$H$_{24}$N$_2$O$_7$: C 66.39, H 4.95, N 5.73, found: C 66.52, H 4.94, N 5.72.

General Procedure for the Preparation of Acids 1b, 2b, 3b, 4b and 6b.[63]
Example: Preparation of 7,7′-carbonylbis(azanediyl)bis(4-hydroxy-2-naphthoic acid) (1b)
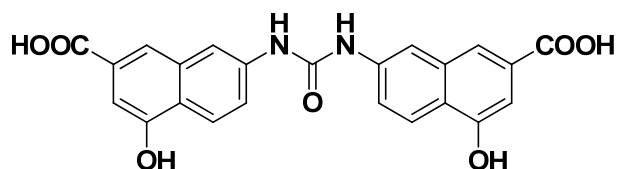
The ester **1a** (0.3 g, 0.61 mmol) was dissolved in a mixture of THF (4 mL) and pyridine (1.22 mmol, 98 μL). Aqueous 1 N sodium hydroxide (12 mL) was added dropwise and the mixture was stirred at room temperature until starting material disappeared (silica TLC, AcOEt/AcOH 99/1). After removing THF by means of nitrogen flow, 2N HCl solution (10 mL) was added and the white precipitate was collected by filtration (0.260 g, 98%); mp >290 °C; ^{1}H NMR (DMSO-d$_6$) δ 10.37 (s, 2H), 9.09 (s,2H), 8.13-8.10 (m, 4H), 7.93 (s, 2H), 7.67 (dd, J_1 = 9Hz, J_2 = 1 Hz, 2H), 7.25 (d, J = 1 Hz, 2H); MS (ESI) *m/z* (%)*:* 433 (M+H)$^+$; Anal. calcd for $C_{23}H_{16}N_2O_7$: C 63.89, H 3.73, N 6.48, found: C 64.04, H 3.73, N 6.47.

The acids 7-(3-(7-carboxy-5-hydroxynaphthalen-2-ylamino)-3-oxopropan-amido)-4-hydroxy-2-naphthoic (**2b**), 7-(4-(7-carboxy-5-hydroxynaphthalen-2-ylamino)-4-oxobutanamido)-4-hydroxy-2-naphthoic (**3b**), 7-(3-(2-(1*H*-indol-3-yl)ethyl)ureido)-4-hydroxy-2-naphthoic (**4b**), and 5-(3-(7-carboxy-5-hydroxynaphthalen-2-yl)ureido)-1*H*-indole-2-carboxylic (**6b**) were obtained from the corresponding esters **2a**, **3a**, **4a**, and **6a**, respectively, following the same procedure.

2b:
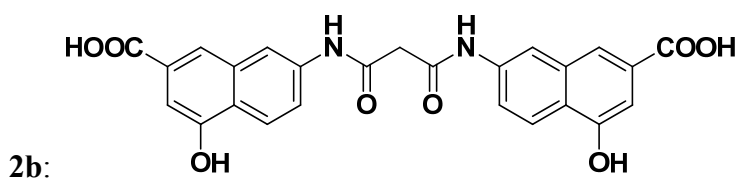
white solid (yield 96%); mp >290 °C; ^{1}H NMR (DMSO-d$_6$) δ 10.50 (s, 2H), 10.45 (s, 2H), 8.33 (s, 2H), 8.14 (d, J = 9 Hz, 2H), 7.93 (s, 2H), 7.73 (d, J = 9 Hz, 2H), 7.29 (s, 2H), 3.64 (s, 2H); MS (ESI) *m/z* (%)*:* 475 (M+H)$^+$; Anal. calcd for $C_{25}H_{18}N_2O_8$: C 63.29, H 3.82, N 5.90, found: C 63.38, H 3.82, N 5.89.
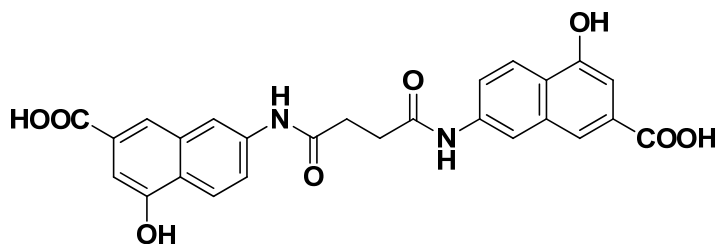
3b:

white solid (yield 90%); mp >290 °C; ^{1}H NMR (D_2O + NaOD) δ 7.92 (d, J = 9 Hz, 2H), 7.55 (d, J = 9 Hz, 2H), 7.27 (s, 2H), 7.12-7.07 (m, 4H), 2.55 (s, 4H); MS (ESI) *m/z* (%)*:* 489 (M+H)[+]. Anal. calcd for $C_{26}H_{20}N_2O_8$: C 63.93, H 4.13, N 5.74, found: C 64.03, H 3.75, N 5.73.
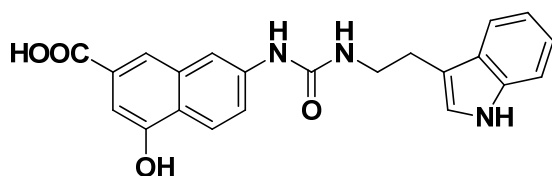
4b:

white solid (yield 98%); mp > 290 °C; ^{1}H NMR ^{1}H NMR (DMSO-d_6) δ 11.77 (s, 1H), 10.83 (s, 1H), 10.25 (s, 1H), 8.75 (s, 1H), 8.00 (d, J = 7 Hz,1H), 7.98 (s, 1H), 7.81 (s, 1H), 7.57 (d, J = 8 Hz, 1H), 7.53 (dd, J_1 = 9 Hz, J_2 =2 Hz, 1H), 7.33 (d, J = 8 Hz, 1H), 7.17 (d, J = 2 Hz, 1H), 7.15 (d, J = 1 Hz, 1H), 7.08-7.03 (m, 1H), 6.99-6.94 (m, 1H) 6.24 (t, J = 12 Hz, 1H), 3.45-3.49 (m, 2H), 2.87 (t, J = 14 Hz, 2H); MS (ESI) *m/z* (%)*:* 390 (M+H)[+]; Anal. calcd for $C_{22}H_{19}N_3O_4$: C 67.86, H 4.92, N 10.79, found: C 67.98, H 4.92, N 10.78.
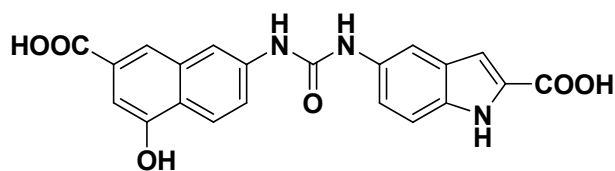
6b:

white solid (yield 70%); mp >290 °C; ^{1}H NMR (DMSO-d_6) δ 11.62 (s, 1H), 10.31 (s, 1H), 8.91 (s, 1H), 8.67 (s, 1H), 8.08-8.03 (m, 2H), 7.88-7.85 (m, 2H), 7.63 (d, J = 8 Hz, 1H), 7.37 (d, J = 8Hz, 1H), 7.26 (s, 1H), 7.21 (s, 1H), 7.02

(s, 1H); MS (ESI) *m/z* (%): 406 (M+H)$^+$; Anal. calcd for $C_{25}H_{23}N_3O_6$: C 65.07, H 5.02, N 9.11, found: C 65.19, H 5.01, N 9.10.

Preparation of 7,7′-carbonylbis(azanediyl)bis(4-hydroxy-2-naphthamide) (1c)
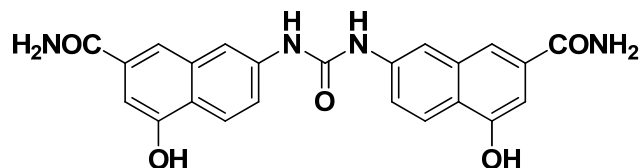
A mixture of compound **1a** (0.3 g, 0.61 mmol) and ammonium hydroxide 30% w/w (20 ml) was stirred at room temperature for 12 h. The solution was then acidified to pH 5 with 3N HCl and the light brown solid thus obtained was recovered by filtration to obtain pure **1c** (0.157 g, 60%); mp >290 °C; ^{1}H NMR (DMSO-d$_6$) δ 10.23 (s, 2H), 9.13 (s, 2H), 8.15, (s, 2H), 8.07 (d, *J* = 9 Hz, 2H), 7.98 (s, 2H), 7.81 (s, 2H), 7.54 (d, *J* = 9 Hz, 2H), 7.31 (s, 2H), 7.18 (s, 2H); MS (ESI) *m/z* (%): 431 (M+H)$^+$. Anal. calcd for $C_{23}H_{18}N_4O_5$: C 64.18, H 4.22, N 13.02, found: C 64.29, H 4.21, N 13.00.

Preparation of ethyl 7-(3-ethoxy-3-oxopropanamido)-4-hydroxy-2-naphthoate (15)
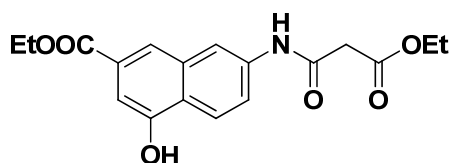
Intermediate **12a** (1.0 g, 4.32 mmol) was suspended in 6.5 mL of diethyl malonate into a 10 mL microwave vessel and the mixture was irradiated for 30 min at 300 W keeping temperature below 100 °C (air flow cooling). Ethyl acetate (100 mL) was added and the solution was washed with 6N HCl (3 × 70 mL). The organic phase was dried, evaporated under reduced pressure, and the

crude residue was purified by column chromatography on silica gel (gradient, dichloromethane/methanol, 99:1 to 95:5) to give a light yellow solid (1.34 g, 90%); mp 201-202 °C; ^{1}H NMR (DMSO-d$_6$) δ 10.47 (s, 1H), 10.44 (s, 1H), 8.29 (s, 1H), 8.10 (d, J = 9 Hz, 1H), 7.92 (s, 1H), 7.64 (d, J_1 = 9 Hz, 1H), 7.27 (s, 1H), 4.32 (q, J = 7 Hz, 2H), 4.12 (q, J = 7 Hz, 2H), 3.51 (s, 2H), 1.34 (t, J = 7 Hz, 3H), 1.20 (t, J = 7 Hz, 3H); MS (ESI) *m/z* (%): 346 (M+H)$^+$.

Preparation of ethyl 7-(3-(7-(ethoxycarbonyl)-5-hydroxynaphthalen-2-ylamino)-3-oxopropanamido)-4-hydroxy-2-naphthoate (2a)
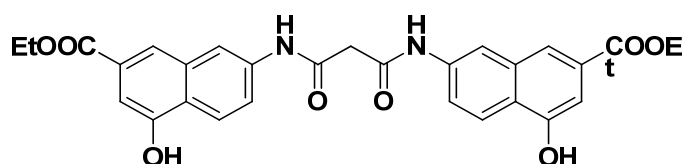
Compound **12a** (0.740 g, 3.19 mmol) was added to a solution of derivative **13** (1.00 g, 2.90 mmol) in toluene (10 mL) and 1-methyl-2-pyrrolidinone (1 mL) into a 10 mL microwave vessel, and the resulting mixture was irradiated (3 × 30 min) at 300 W keeping temperature below 120 °C (air flow cooling). After solvent removal under reduced pressure, the resulting oil was taken up with ethyl acetate (150 mL), washed with 1N HCl (3 × 60 mL), dried, evaporated under vacuum. The crude residue was purified by column chromatography on silica gel (gradient, dichloromethane/methanol, 99:1 to 90:10) to give a white solid (0.770 g, 50%); mp 282.2-282.7 °C; ^{1}H NMR (DMSO-d$_6$) δ 10.50 (s, 2H), 10.47 (s, 2H), 8.34 (s, 2H), 8.11 (d, J = 9 Hz, 2H), 7.92 (s, 2H), 7.70(dd, J_1 = 9 Hz, J_2 =1 Hz, 2H), 7.27 (s, 2H), 4.32 (q, J = 7 Hz, 4H), 3.61 (s, 2H), 1.33 (t, J = 7 Hz, 6H); MS (ESI) *m/z* (%): 531 (M+H)$^+$; Anal. calcd for C$_{29}$H$_{26}$N$_2$O$_8$: C 65.65, H 4.94, N 5.28, found: C 65.76, H 4.93, N 5.27.

Preparation of ethyl 7-(4-(7-(ethoxycarbonyl)-5-hydroxynaphthalen-2-ylamino)-4-oxobutanamido)-4-hydroxy-2-naphthoate (3a)
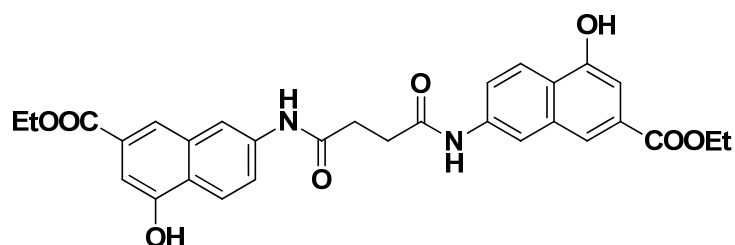
A solution of **12a** (1.0 g, 4.32 mmol) in acetone (6 mL) was cooled to -15 °C and an acetone solution (12 mL) of succinil dichloride (0.401 g, 2.59 mmol) was added dropwise in 30 min. The resulting solution was stirred for 12 h at room temperature, then aqueous $NaHCO_3$ solution (6 mL) was added and the mixture concentrated under vacuum. The residual oil was taken up with aqueous $NaHCO_3$ (100 mL) and extracted with ethyl acetate (3 × 60 mL). The combined organic phases were washed with 2N HCl (3 × 60 mL), dried and evaporated under reduced pressure. The solid thus obtained was purified by flash chromatography on silica gel (gradient, dichloromethane/methanol, 99:1 to 90:10) to give a white solid (0.470 g, 40%); mp >290 °C. ^{1}H NMR (DMSO-d$_6$) δ 10.50 (s, 2H), 10.37 (s, 2H), 8.33 (s, 2H), 8.07 (d, J = 9 Hz, 2H), 7.87 (s, 2H), 7.68 (d, J = 9 Hz, 2H), 7.31 (s, 2H), 4.31 (q, J = 7 Hz, 4H), 2.83 (s, 2H), 1.33 (t, J = 7 Hz, 6H). MS (ESI) *m/z* (%)*:* 545 (M+H)$^+$. Anal. calcd for $C_{25}H_{23}N_3O_6$: C 65.07, H 5.02, N 9.11, found: C 65.15, H 5.01, N 9.10.

Preparation of ethyl 4-hydroxy-7-(2,2,2-trichloroacetamido)-2-naphthoate (16)
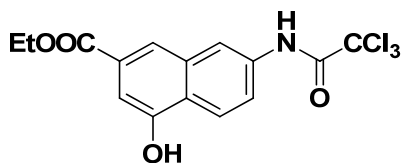
Triethylamine (0.674 g, 6.67 mmol) was added to a solution of compound **13a** (1.0 g, 4.32 mmol) in dry dichloromethane (100 mL) under nitrogen flow. After 30 min trichloroacetylchloride (1.212 g, 6.67 mmol) was added dropwise in 10 min under nitrogen flow and the reaction was stirred at room temperature for 4 h. The solution was then washed with saturated aqueous NaHCO$_3$ solution (3 × 40mL), 3N HCl (3 × 40 mL), dried and concentrated under reduced pressure, and purified by column chromatography on silica gel (gradient, dichloromethane/methanol, 99:1 to 90:10) to give a light yellow solid (1.34 g, 83%); mp 232.0-232.7 °C; ^{1}H NMR (DMSO-d$_6$) δ 11.06 (s, 1H), 10.56 (s, 1H), 8.29 (s, 1H), 8.16 (d, J = 9 Hz, 1H), 7.99 (s, 1H), 7.80 (d, J = 9 Hz, 1H), 7.33 (s, 1H), 4.34 (q, J = 7 Hz, 2H), 1.34 (t, J = 7 Hz, 3H); MS (ESI) (+) *m/z* (%): 376 (M+H, 100); 378 (M+H+2, 96); 380 (M+H+4, 36); 382 (M+H+6, 4).

General Procedure for the Preparation of Derivatives 4a, 5a and 6a. Example: ethyl 7-(3-(2-(1*H*-indol-3-yl)ethyl)ureido)-4-hydroxy-2-naphthoate (4a)
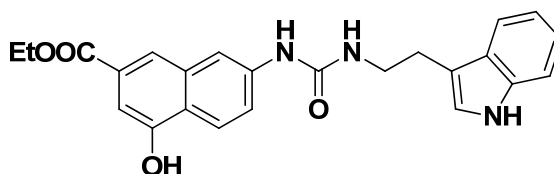
Sodium carbonate (1.40 g, 13.25 mmol) and tryptamine (0.467 g, 2.91 mmol) were added to a solution of derivative **16** (1.0 g , 2.65 mmol) in dry DMF (10 mL) in a sealed tube. The resulting mixture was heated at 150 °C for 1 h, the solvent was removed under reduced pressure, and ethyl acetate (150 mL) was added to the residual oil. The solution was then washed with 2N HCl (3 × 50mL) and saturated aqueous NaHCO$_3$ solution (3 × 50mL), dried, evaporated under reduced pressure, and purified by column chromatography on silica gel (gradient, dichloromethane/methanol, 99:1 to 90:10) to give a white solid (0.696 g, 63%); mp 214.7-215.5 °C; ^{1}H NMR (DMSO-d$_6$) δ 10.82 (s, 1H), 10.39 (brs, 1H), 8.79 (d, $J = 4$ Hz, 1H), 8.03-7.99 (m, 2H), 7.84 (s, 1H), 7.59-7.51 (m, 2H), 7.34 (d, $J = 9$ Hz, 1H), 7.19-7.18, (m, 2H), 7.06-7.03 (m, 1H), 6.97-6.95 (m, 1H), 6.29 (t, $J = 6$ Hz, 1H), 4.31 (q, $J = 7$ Hz, 2H), 4.43-4.41 (m, 2H), 2.91 (t, $J = 7$ Hz, 2H), 1.33 (t, $J = 7$ Hz, 3H); MS (ESI) *m/z* (%): 418 (M+H)$^+$; Anal. calcd for C$_{24}$H$_{23}$N$_3$O$_4$: C 69.05, H 5.55, N 10.07, found C 69.14, H 5.54, N 10.06.

Ethyl 7-(3-(2-(dimethylamino)propyl)ureido)-4-hydroxy-2-naphthoate (**5a**) and ethyl 5-(3-(7-(ethoxycarbonyl)-5-hydroxynaphthalen-2-yl)ureido)-1*H*-indole-2-carboxylate (**6a**) were obtained following the same procedure starting from **16** and *N^1,N^1*-dimethylpropane-1,3-diamine or ethyl 5-amino-1*H*-indole-2-carboxylate, respectively, as nucleophile.

5a:
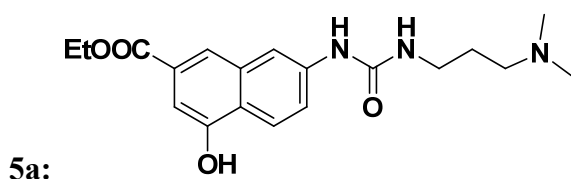
white solid (yield 63%); mp 161-163 °C; ^{1}H NMR (DMSO-d$_6$) δ 10.36 (s, 1H), 8.76 (s, 1H), 8.03-8.00 (m, 2H), 7.85 (s, 1H), 7.55 (dd, $J_1 = 9$ Hz, $J_2 = 1$ Hz, 1H), 7.19 (s, 1H), 6.34 (t, $J = 9$ Hz, 1H), 4.33 (q, $J = 7$ Hz, 2H), 3.17-3.11 (m, 2H), 2.36-2.31 (m, 2H), 2.20 (s, 6H), 1.63-1.58 (m, 2H), 1.34 (t, $J = 7$ Hz,

3H); MS (ESI) *m/z* (%)*:* 360 (M+H)$^+$; Anal. calcd for C$_{19}$H$_{25}$N$_3$O$_4$: C 63.49, H 7.01, N 11.69, found: C 63.57, H 7.00, N 11.67.

6a:
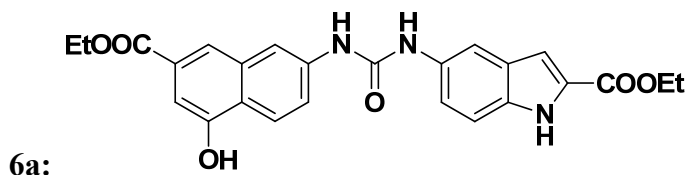
white solid (yield 50%); mp 210.8-211.7 °C; ^{1}H NMR (DMSO-d$_6$) *δ* 11.74 (s, 1H), 10.39 (s, 1H) 8.98 (s, 1H), 8.75 (s, 1H), 8.17 (s, 1H), 8.08 (d, *J* = 9Hz, 1H), 7.94-7.88 (m, 2H), 7.64 (d, *J* = 8 Hz, 1H), 7.39 (d, *J* = 8 Hz, 1H) 7.27 (d, *J* = 9 Hz, 1H), 7.23 (s, 1H), 7.07 (s, 1H), 4.35 (m, 4H), 1.38-1.32 (m, 6H); MS (ESI) *m/z* (%)*:* 462 (M+H)$^+$; Anal. calcd for C$_{25}$H$_{23}$N$_3$O$_6$: C 65.07, H 5.02, N 9.11, found: C 65.17, H 5.01, N 9.10.

Preparation of (*E*)-3-(methoxycarbonyl)-4-(4-nitrophenyl)but-3-enoic acid
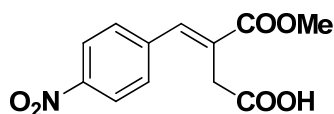
Carboxyphosphorane **10**[50] (13.0 g, 35.2 mmol) was suspended in dry benzene (150 mL) and 4-nitrobenzaldehyde (5.74 g, 38.0 mmol) was then added. The resulting mixture was stirred at room temperature for 48 h and then extracted with saturated NaHCO$_3$ solution (3 × 70 mL). The aqueous phase was washed with ethyl ether, acidified with concentrated HCl and the white solid formed was recollected by filtration (8.60 g, 92%) and directly used in the following step without further purification; mp ^{1}H NMR (DMSO-d$_6$) *δ* 8.30 (d, *J* = 9 Hz, 2H), 7.86 (s, 1H), 7.69 (d, *J* = 9 Hz, 2H), 3.78 (s, 3H), 3.43 (s, 2H); MS (ESI) *m/z* (%)*:* 266 (M+H)$^+$.

Preparation of methyl 4-acetoxy-6-nitro-2-naphthoate (17)
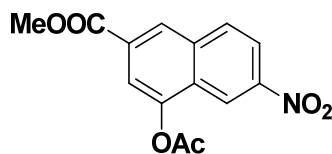
A round-bottomed flask containing a magnetic stirring bar and fitted with a reflux condenser was charged with a mixture of (*E*)-3-(methoxycarbonyl)-4-(4-nitrophenyl)but-3-enoic acid (5.0 g, 18.85 mmol), Ac_2O (35 mL) and NaOAc (2.30g, 28.27 mmol). The flask was subjected to MW irradiation (power 300 W) for 5 min keeping temperature below 120 °C (air flow cooling). The reaction mixture was filtered and the solvent evaporated to give a pure yellow solid (5.17 g, 95%); mp 167-168 °C; ^{1}H NMR (CDCl$_3$) δ 8.89 (d, J = 2 Hz, 1H), 8.62 (s, 1H), 8.38 (dd, J_1 = 9 Hz, J_2 = 2 Hz, 1H), 8.17 (d, J = 9 Hz, 1H), 8.05 (s, 1H), 4.05 (s, 3H), 2.59 (s, 3H); MS (ESI) *m/z* (%)*:* 290 (M+H)$^+$.

Preparation of methyl 4-acetoxy-6-amino-2-naphthoate (18)
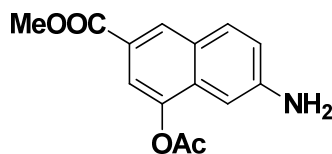
Pd/C (5 wt % palladium on activated carbon, 0.1 eq) was added to a solution of **17** (3.0 g, 10.37 mmol) in ethanol (100 mL), and the reaction was stirred under 1 atm of H$_2$ (balloon) for 2h. The reaction mixture was filtered and, after solvent evaporation, a light yellow solid was recollected (2.66 g, 99%); mp 195-196 °C; ^{1}H NMR (DMSO-d$_6$) δ 8.28 (s, 1H), 7.86 (d, J = 9 Hz, 1H), 7.54 (s, 1H), 7.06 (d, J = 9 Hz, 1H), 6.79 (s, 1H), 6.04 (s, 2H), 3.87 (s, 3H), 2.42 (s, 3H); MS (ESI) *m/z* (%)*:* 260 (M+H)$^+$.

Preparation of dimethyl 6,6′-carbonylbis(azanediyl)bis(4-hydroxy-2-naphthoate) (7a)
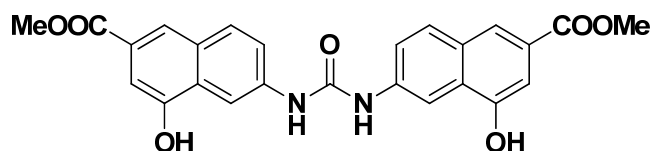
Diphenylcarbonate (0.411 g, 1.92 mmol) and 4-dimethylaminopyridine (0.046 g, 0.38 mmol) were added to a solution of **18** (1.0 g, 3.85 mmol) in chlorobenzene (20 mL) and the mixture was refluxed for 72 h. The solvent was evaporated under reduced pressure, and the dark brown solid obtained was washed twice with petroleum benzene. The crude product obtained was dissolved in ethanol (50 mL) and K_2CO_3 (0.585 g, 4.23 mmol) was added. The mixture was heated at 70 °C for 2 h, then evaporated, taken up with 100 mL of ethyl acetate and washed with 3N HCl solution (3 × 70 mL). The organic phases were collected, washed with brine, dried and evaporated. The crude residue was purified by column chromatography on silica gel (gradient, dichloromethane/methanol, 98:2 to 90:10) to afford pure **7a** as a white solid (0.443 g, 50%); mp 276.6-277.6 °C; ^{1}H NMR (DMSO-d_6) δ 10.39 (s, 2H), 9.13 (s, 2H), 8.42 (d, J = 2 Hz, 2H), 8.00 (s, 2H), 7.95 (d, J = 9 Hz, 2H), 7.56 (dd, J_1 = 9 Hz, J_2 = 2 Hz, 2H), 7.33 (s, 2H), 3.85 (s, 6H); MS (ESI) *m/z* (%): 461 (M+H)$^+$; Anal. calcd for $C_{25}H_{20}N_2O_7$: C 65.21, H 4.38, N 6.08, found: C 65.29, H 4.37, N 6.07.

General Procedure for the Preparation of acids 7b, 8b and 9b.

The acids 6,6′-carbonylbis(azanediyl)bis(4-hydroxy-2-naphthoic acid) (**7b**), 6-(3-(6-carboxy-8-hydroxynaphthalen-2-ylamino)-3-oxopropanamido)-4-hydroxy-2-naphthoic acid (**8b**), and 6-(3-(2-(1*H*-indol-3-yl)ethyl)ureido)-4-

hydroxy-2-naphthoic acid (**9b**) were obtained from the corresponding esters **7a**, **8a**, and **9a**, respectively, following the same general procedure above described for **1b, 2b, 3b, 4b and 6b**.

7b:
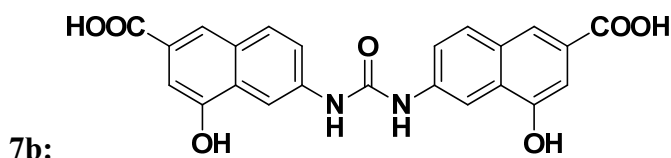
white solid (yield 90%); mp>290 °C; ^{1}H NMR (DMSO-d$_6$) δ 10.33 (s, 2H), 9.13 (s, 2H), 8.44 (d, J = 2 Hz, 2H), 8.00 (s, 2H), 7.96 (d, J = 9 Hz, 2H), 7.59 (dd, J_1 = 9 Hz, J_2 = 2 Hz, 2H), 7.35 (s, 2H); MS (ESI) m/z (%): 433 (M+H)$^+$; Anal. calcd for C$_{23}$H$_{16}$N$_2$O$_7$: C 63.89, H 3.73, N 6.48, found: C 63.95, H 3.73, N 6.47.

8b:
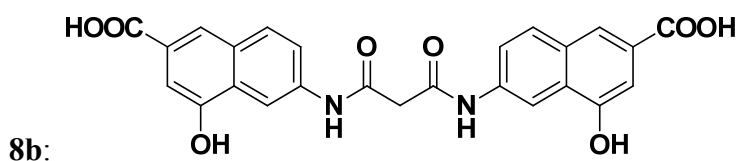
white solid (yield 85%); mp >290 °C; ^{1}H NMR (CD$_3$OD) δ 8.54 (d, J = 2 Hz, 2H), 8.09 (s, 2H), 7.91 (d, J = 9 Hz, 2H), 7.76 (dd, J_1 = 9 Hz, J_2 = 2 Hz, 2H), 7.39 (s, 2H), 3.51 (s, 2H); MS (ESI) m/z (%): 475 (M+H)$^+$; Anal. calcd for C$_{25}$H$_{18}$N$_2$O$_8$: C 63.29, H 3.82, N 5.90, found: C 63.38, H 3.81, N 5.89.

9b:
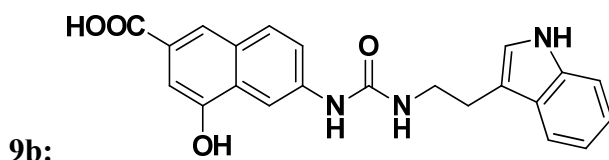
white solid (yield 98%); mp >290 °C; ^{1}H NMR (DMSO-d$_6$) δ 10.86 (s, 1H), 10.21 (s, 1H) 8.87 (s, 1H), 8.29 (d, J = 2 Hz, 1H), 7.94 (s, 1H), 7.86 (d, J = 9

Hz, 1H), 7.61 (d, *J* = 8 Hz), 7.53 (dd, *J$_1$* = 9 Hz, *J$_2$* = 2 Hz, 1H), 7.37 (d, *J* = 8 Hz, 1H), 7.30 (d, *J* = 1 Hz, 1H), 7.21 (d, *J* = 1 Hz, 1H), 7.09-7.05 (m, 1H), 7.00-6.95 (m, 1H), 6.24 (t, *J* = 7 Hz, 1H), 3.47-3.43 (m, 2H), 2.91 (t, *J* = 7 Hz); MS (ESI) *m/z* (%)*:* 390 (M+H)$^+$; Anal. calcd for C$_{22}$H$_{19}$N$_3$O$_4$: C 67.86, H 4.92, N 10.79, found: C 67.96, H 4.91, N 10.78.

Preparation of methyl 4-acetoxy-6-(3-ethoxy-3-oxopropanamido)-2-naphthoate (19)

Title compound was obtained starting from **18 (**1.0 g, 3.85 mmol) following the same procedure above described for the preparation of **13**, to yield a white solid (1.30 g, 90%); mp. 170.5-171.9 °C; ^{1}H NMR (DMSO-d$_6$) *δ* 10.66 (s, 1H), 8.52 (s, 1H), 8.32 (s, 1H), 8.20 (d, *J* = 9 Hz, 1H), 7.80-7.76 (m, 2H), 4.16 (q, *J* = 7 Hz, 2H), 3.93 (s, 3H), 3.56 (s, 2H), 2.47 (s, 3H), 1.22 (t, *J* = 7 Hz, 3H); MS (ESI) *m/z* (%)*:* 374 (M+H)$^+$.

Preparation of methyl 4-hydroxy-6-(3-(6-(methoxycarbonyl)-8-hydroxynaphthalen-2-ylamino)-3-oxopropanamido)-2-naphthoate (8a)
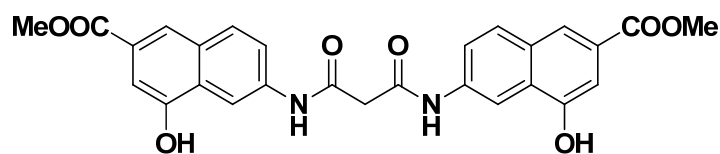
Compound **16** (0.762 g, 2.94mmol) was added to a solution of compound **18** (1,00 g, 2.68 mmol) in toluene (10 mL) and 1-methyl-2-pyrrolidinone (1 mL) and the mixture was irradiated (3 × 30 min) at 300 W, keeping temperature below 120 °C (air flow cooling). After solvent removal under reduced

pressure, the residual oil was taken up with ethyl acetate (150 mL), washed with 1N HCl (3 × 60 mL), dried, and evaporated under vacuum. The crude residue thus obtained was dissolved in ethanol (50 mL) and K_2CO_3 (0.407 g, 2.94 mmol) was added. The mixture was heated at 70 °C for 2h, then evaporated, taken up with 100 mL of ethyl acetate and washed with 3N HCl solution (3 × 70 mL). The organic phase was washed with brine, dried and evaporated. The mixture was then purified by column chromatography on silica gel (gradient, dichloromethane/methanol, 99:1 to 90:10) to give a white solid (0.673 g, 50%); mp. 287.8-288.8 °C. ^{1}H NMR (DMSO-d_6) δ 10.51 (s, 2H), 10.44 (s, 2H), 8.55 (d, $J = 2$ Hz, 2H), 8.01 (s, 2H), 7.98 (d, $J = 9$ Hz, 2H), 7.73 (dd, $J_1 = 9$ Hz, $J_2 = 2$ Hz, 2H), 7.32 (s, 2H), 3.86 (s, 6H), 3.60 (s, 2H); MS (ESI) *m/z* (%)*:* 503 (M+H)[+]; Anal. calcd for $C_{27}H_{22}N_2O_8$: C 64.54, H 4.41, N 5.58, found: C 64.61, H 4.40, N 5.57.

Preparation of methyl 4-acetoxy-6-(2,2,2-trichloroacetamido)-2-naphthoate (20a) and methyl 4-hydroxy-6-(2,2,2-trichloroacetamido)-2-naphthoate (20b)
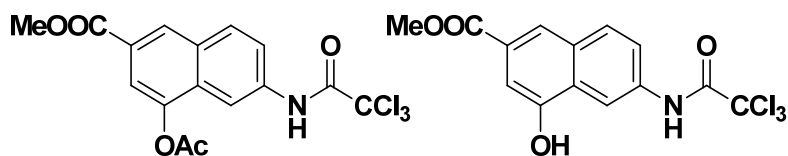
Title compounds were obtained as a mixture starting from the intermediate **198** (1.0 g, 3.85 mmol) following the same procedure above described for the preparation of **14**, to yield a crude white solid (1.14 g, 82%) that was directly used in the following step. For characterization purposes, analytical samples of **20a** and **20b** were obtained by column chromatography on silica gel (gradient, dichloromethane/methanol, 99:1 to 95:5); **20a**: mp 162-163 °C; ^{1}H NMR (DMSO-d_6) δ 11.25 (s, 1H), 8.56 (s, 1H), 8.32 (s, 1H), 8.27 (d, $J = 9$ Hz, 1H), 8.03 (d, $J = 9$ Hz, 1H), 7.80 (s, 1H), 3.93 (s, 3H), 2.51 (s, 3H); **20b**: mp 225-

226 °C; ^{1}H NMR (DMSO-d6) δ 11.13 (s, 1H), 10.63 (s, 1H), 8.55 (s, 1H), 8.07-8.05 (m, 2H), 7.85 (dd, J_1 = 9 Hz, J_2 = 2 Hz), 7.39 (s, 1H), 3.89 (s, 3H); MS (ESI) *m/z* (%): 362 + 404 (M+H)[+].

Preparation of methyl 6-(3-(2-(1*H*-indol-3-yl)ethyl)ureido)-4-hydroxy-2-naphthoate (9a)
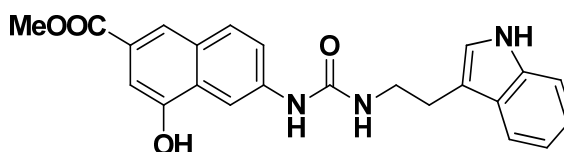
Compound **9a** was prepared starting from the crude mixture of **20a** and **20b** (1.0 g , 2.77 mmol) following the same procedure above described for the preparation of **4a**, to yield a white solid (0.704 g, 63%); mp 218.8-219.8 °C; ^{1}H NMR (DMSO-d6) δ 10.83 (s, 1H), 10.26 (s, 1H), 8.87 (s, 1H), 8.26 (d, *J* = 2 Hz, 1H), 7.95 (s, 1H), 7.86 (d, *J* = 9 Hz, 1H), 7.57 (d, *J* = 8 Hz, 1H), 7.51 (dd, J_1 = 9 Hz, J_2 = 2 Hz, 1H), 7.33 (d, *J* = 8 Hz, 1H), 7.27 (s, 1H), 7.17 (d, *J* = 2 Hz, 1H), 7.06-7.03 (m, 1H), 6.97-6.93 (m, 1H), 6.22 (t, *J* = 6 Hz, 1H), 3.84 (s, 3H), 3.44-3.40 (m, 2H), 2.87 (t, *J* = 7 Hz); MS (ESI) *m/z* (%): 404 (M+H)[+]; Anal. calcd for $C_{23}H_{21}N_3O_4$: C 68.47, H 5.25, N 10.42, found: C 68.58, H 5.24, N 10.41.

Synthesis of ethyl 5-amino-1H-indole-2-carboxylate (26):
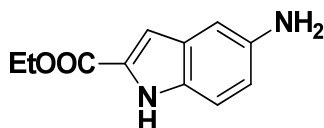
To a solution of ethyl 5-nitro-1H-indole-2-carboxylate (500 mg; 2.24 mmol) in ethanol (250 ml), 5% palladium on activated carbon (237 mg, 0.112 mmol) was added. The reaction was stirred under H_2 (1 atm) for 12h at room temperature. The colorless solution was filtrated and the solvent evaporated

under vacuum yielding 452 mg of a white solid (99%). ^{1}H NMR (DMSO-d$_6$) δ 11.39 (s, 1H); 7.16 (d, J = 9 Hz, 1H); 6.84 (s, 1H); 6.71 - 6.68 (m, 3H); 4.65 (s, 2H); 4.30 (q, J = 7 Hz, 2H); 1.32 (t, J = 7 Hz, 3H). ESI m/z: 205 [M + H]$^+$. Mp: 113 – 115 °C

Synthesis of methyl 5-amino-1H-indole-3-carboxylate (37):
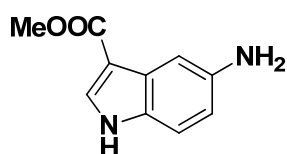
Compound **10** was prepared following the same procedure of **26** starting from methyl 5-nitro-1H-indole-3-carboxylate (500 mg; 2.27 mmol), yielding 427 mg of a white solid (99%).^{1}H NMR (DMSO-d$_6$) δ 11.49 (s, 1H), 7.82 (s, 1H), 7.17 (d, J= 2Hz, 1H), 7.13 (d, J= 9Hz, 1H), 6.55 (dd, J$_1$= 9Hz, J$_2$= 2Hz, 1H), 4.74 (brs, 2H), 3.75 (s, 3H). ESI m/z = 191 [M+H]$^+$. Mp: 144-146 °C

Synthesis of diethyl 5,5'-(carbonylbis(azanediyl))bis(1H-indole-2-carboxylate) (21a):
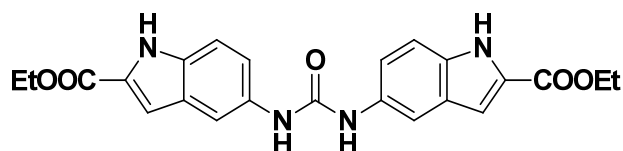
To a solution of **26** (437 mg; 2.14 mmol) in dry DCM (80 ml), triethylamine was added (446 µl, 3.21 mmol). A solution of trifosgene (254 mg; 0.856 mmol) in dry DCM (10 ml) was then added dropwise over 10 min. The reaction mixture was stirred for additional 30 min and then **1** (437 mg, 2.14 mmol) and triethylamine (446 µl, 3.21 mmol) in dry DCM (10 ml) was added dropwise. The reaction mixture was stirred at room temperature under N$_2$ for 12h. The solvent was evaporated and the resulting oil was first diluted in

AcOEt (180 ml) and then washed with 1N HCl (3 x 60 ml), with NaHCO$_3$ saturated solution (3 x 60 ml), brine and anhydrified over Na$_2$SO$_4$. After solvent evaporation, the resulting solid was recrystallized from acetonitrile yielding 650 mg of a white solid (70%). ^{1}H NMR (DMSO-d$_6$) δ 11.71 (s, 2H); 8.48 (s, 2H,); 7.83 (s, 2H); 7.35 (d, J = 9 Hz, 2H); 7.22 (dd, J$_1$ = 9 Hz, J$_2$ = 2 Hz, 2H); 7.06 (s, 2H); 4.31 (q, J = 7 Hz, 4H); 1.32 (t, J = 7 Hz, 6H). ESI m/z: 435 [M + H]$^+$ M.p.: 292.3 - 293 °C.

Synthesis of 5,5'-(carbonylbis(azanediyl))bis(1H-indole-2-carboxylic acid) (21b):
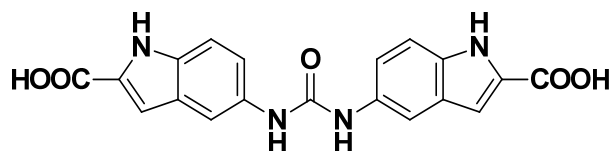
To a solution of **21a** (55 mg: 0.126 mmol) in THF/H$_2$O (10 ml), NaOH (101 mg; 2.53 mmol) and pyridine (20.μL; 0.253 mmol) were added and the resulting mixture was stirred at room temperature for 12h. The solvent was then evaporated and the resulting oil taken up with H$_2$O (20 ml). The water phase was washed with DCM (3 x 10 ml), acidified to pH 2 with HCl and extracted with AcOEt (3 x 10 ml). The organic phase was collected, washed with brine and anhydrified over Na$_2$SO$_4$, evaporated and purified by column chromatography (SiO$_2$, AcOEt/ACOH 99:1), yielding 39 mg of a white solid (82%). ^{1}H NMR (DMSO-d$_6$) δ 11.53 (s, 2H); 8.54 (s, 2H); 7.80 (s, 2H); 7.32 (d, J = 9 Hz, 2H); 7.21 (d, J = 9 Hz, 2H); 6.97 (s, 2H). ESI m/z: 379 [M + H]$^+$ M.p. : > 300 °C.

Synthesis of dimethyl 5,5'-(carbonylbis(azanediyl))bis(1H-indole-3-carboxylate) (38a):
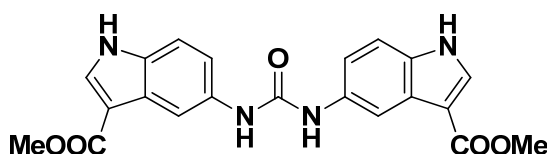
Compound **38a** was prepared following the same procedure of **21a** starting from **37**. Crystallization from ethanol yield 800 mg of a light brown solid (87%). ^{1}H NMR (DMSO-d_6) δ 11.81 (brs, 2H), 8.53 (s, 2H), 8.07 - 8.00 (m, 4H), 7.40 - 7.36 (m, 4H), 3.80 (s, 6H). ESI m/z = 407 [M+H$^+$] M.p: 250 °C d.

Synthesis of 5,5'-(carbonylbis(azanediyl))bis(1H-indole-3-carboxylic acid) (38b):
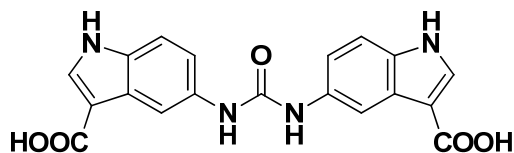
Compound **38b** was prepared following the same procedure of **21b** starting from **38a** (0.80 g; 0.197 mmol), yielding 23 mg a brown solid (30%).^{1}H NMR (DMSO-d_6) δ 11.57 (s, 2H), 8.47 (s, 2H), 8.13 (s, 2H), 7.92 (d, J=2 Hz, 2H), 7.34 (d, J= 8 Hz, 2H), 7.27 (d, J= 8 Hz, 2H). ESI m/z = 379 [M+H] $^+$, 401 [M+Na]$^+$ M.p: 250 °C d

Synthesis of diethyl 5,5'-(succinylbis(azanediyl))bis(1H-indole-2-carboxylate) (22a):
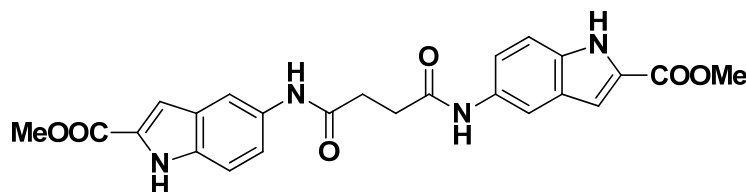
A solution of **26** (390 mg; 1.91 mmol) and triethylamine (531 µl; 3.28 mmol) in acetone (8 ml) was cooled at -78 °C, succinyl chloride (231 µl; 2.10 mmol) was added dropwise and the resulting mixture was stirred for 2h. Solvent was then evaporated and the resulting oil taken up with water (50 ml). Aqueous phase was extracted with AcOEt (3 x 15 ml); the organic phase were collected, washed with 3N HCl (3 x 15 ml), brine, anhydrified over Na$_2$SO$_4$, and evaporated under vacuum. The solid was purified by column chromatography (SiO$_2$, gradient, DCM/AcOEt, 8:2 to 1:1) yielding 400 mg of a white solid (70%). ^{1}H NMR (DMSO-d$_6$) δ 11.74 (s, 2H); 9.86 (s, 2H); 8.01 (s, 2H); 7.41 – 7.34 (m, 4H); 7.05 (s, 2H); 4.31 (q, J = 7 Hz, 4H); 2.64 (s, 4H); 1.31 (t, J = 7 Hz, 6H). ESI m/z: 491 [M + H]$^+$ M.p: > 300°C

Synthesis of 5,5'-(succinylbis(azanediyl))bis(1H-indole-2-carboxylic acid) (22b):
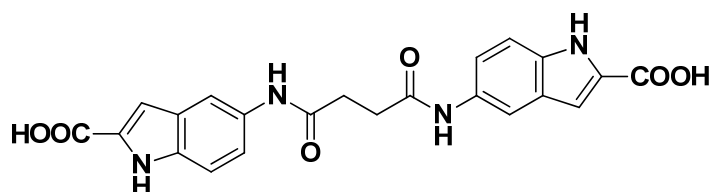
Compound **22b** was prepared following the same procedure of 21**b** starting from **22a** (0.040 g; 0.0815 mmol), yielding 35 mg of a white solid (98%). [1]H

NMR (DMSO-d$_6$) δ 11.62 (s, 2H); 9.86 (s, 2H); 8.00 (s, 2H); 7.43 − 732 (m, 4H); 6.99 (s, 2H); 2.64 (s, 4H). ESI m/z: 435 [M + H]$^+$M.p: 272 - 273°C

Synthesis of dimethyl 5,5'-(succinylbis(azanediyl))bis(1H-indole-3-carboxylate) (40a):
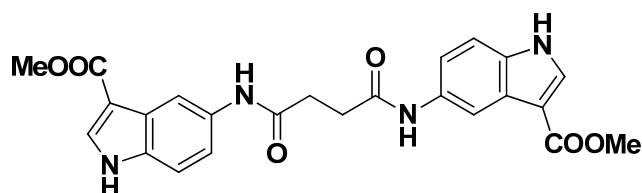
Compound **40a** was prepared following the same procedure of **22a** starting from **37** (800 mg; 4,20 mmol). Crystallization from acetonitrile yield 456 mg of white solid (47 %). ^{1}H NMR (DMSO-d$_6$) δ 11.84 (s, 2H), 9.94 (s, 2H), 8.26 (s, 2H), 8.01 (s, 2H), 7.47 (d, J= 9 Hz, 2H), 7.37 (d, J= 9 Hz, 2H), 3.78 (s, 6H), 2.67 (s, 4H).ESI m/z = 463 [M+H]$^+$ M.p: 269 - 271 °C

Synthesis of ethyl 5-(3-ethoxy-3-oxopropanamido)-1H-indole-2-carboxylate (27):
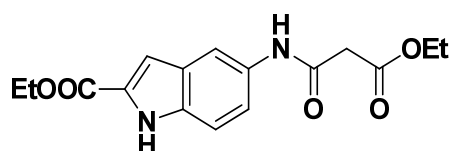
Compound **26** (610 mg; 2.99 mmol) and diethylmalonate (6 ml) were placed in a microwave vessel, and irradiated for 20 min at 300W keeping temperature below 100 °C using air flow. The reaction mixture was then diluted with AcOEt (100 ml), washed with 1N HCl (3 x 30ml), brine, anhydrified over Na$_2$SO$_4$, and evaporated under vacuum. The resulting oil was purified by column chromatography (SiO$_2$, gradient, DCM/AcOEt, 9:1 to 8:2) yielding 570 mg of a brown solid (60%).^{1}H NMR (DMSO-d$_6$) δ 11.81 (s, 1H); 10.06 (s, 1H); 7.99 (s, 1H); 7.38 (d, J = 9 Hz, 1H); 7.30 (d, J = 9 Hz, 1H); 7.09 (s, 1H);

4.31 (q, J =7 Hz, 2H); 4.11 (q, J = 7 Hz, 2H); 3.43 (s, 2H); 1.29 (t, J = 7, 3H); 1.19 (t, J = 7, 3H). ESI m/z: 319 [M + H]$^+$M.p.: 156 - 158 °C.

Synthesis of methyl 5-(3-ethoxy-3-oxopropanamido)-1H-indole-3-carboxylate (41):
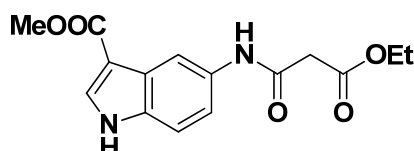
Compound **41** was prepared following the same procedure of **27** starting from **37** (431 mg; 2.27 mmol). Purification by column chromatography (SiO$_2$, gradient, DCM/MeOH, 95:5 to 90:10) yield a 400 mg of a brown solid (58%). ^{1}H NMR (DMSO-d$_6$) δ 11.87 (s, 1H) 10.12 (s, 1H), 8.22 (s, 1H), 8.04 (d, J= 2 Hz, 1H), 7.45 (d, J= 9 Hz, 1H), 7.40 (d, J= 9 Hz, 1H), 4.11 (q, J= 7 Hz, 2H), 3.79 (s, 3H), 3.45 (s, 2H), 1.21 (t, J= 7 Hz, 3H).ESI m/z = 305 [M+H]$^+$ M.p: 171 - 173 °C

Synthesis of diethyl 5,5'-(malonylbis(azanediyl))bis(1H-indole-2-carboxylate) (23a):
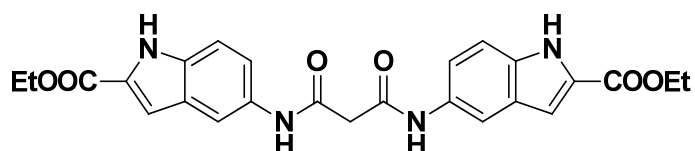
In a microwave vessel compound **26** (143 mg; 0.703 mmol) and **27** (146 mg; 0.457 mmol) were solubilized in toluene (5 ml) and N-methyl-pyrrolidinone (0.5 ml) and irradiated (3 x 40 min) at 300W keeping temperature below 120 °C. Solvent was evaporated, the resulting oil was taken up with HCl 4N (100 ml), the aqueous phase was extracted with AcOEt (3 x 50 ml). The organic phase was collected, washed with brine, anhydrified over Na$_2$SO$_4$, and

evaporated under vacuum. The resulting oil was purified by column chromatography (SiO$_2$, gradient, DCM/MeOH, 99:1 to 90:10) yielding 156 mg of a brown solid (65%).^{1}H NMR (DMSO-d$_6$) δ 11.81 (s, 2H); 10.10 (s, 2H); 8.04 (s, 2H); 7.42 – 7.35 (m, 4H); 7.10 (s, 2H); 4.31 (q, J = 7 Hz, 4H); 3.47 (s, 2H); 1.33 (t, J = 7 Hz, 6H). ESI m/z: 477 [M + H]$^+$ M.p.: 259 - 260 °C

Synthesis of dimethyl 5,5'-(malonylbis(azanediyl))bis(1H-indole-2-carboxylate) (39a):
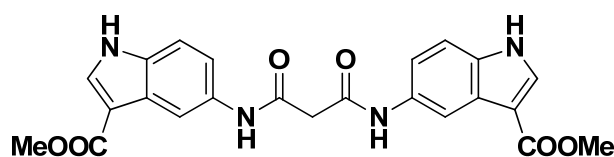
Compound **39a** was prepared following the same procedure of **23a** starting from **41** (400 mg; 1.32 mmol) and **37** (426 mg; 2.24 mmol). Crystallization from ethanol yield 291 mg of a white solid (49%).^{1}H NMR (DMSO-d$_6$) δ 11.97 (s, 2H), 10.15 (s, 2H), 8.29 (d, J= 2 Hz, 2H), 8.06 (s, 2H), 7.50 (dd, J$_1$= 9 Hz, J$_2$= 2 Hz, 2H), 7.43 (d, J= 9 Hz, 2H), 3.80 (s, 6H), 3.50 (s, 2H). ESI m/z = 449 [M+H]$^+$ M.p: 283 - 285 °C.

**Synthesis of 5,5'-(malonylbis(azanediyl))bis(1H-indole-2-carboxylic acid) (23b):**
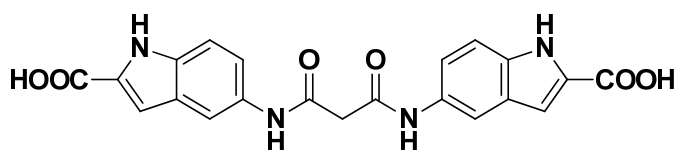
Compound **23b** was prepared following the same procedure of **21b** starting from **23a** (148 mg; 0.310 mmol), yielding 100 mg of a light brown solid (77%).^{1}H NMR (DMSO-d$_6$) δ 11.71 (s, 2H); 10.09 (s, 2H); 8.05 (s, 2H); 7.41

– 7.34 (m, 4H); 7.07 (d, J = 1.5 Hz, 2H); 3.49 (s, 2H). ESI m/z: 421 [M + H]$^+$ M.p.: 227.5 – 228.2 °C

**Synthesis of 5,5'-(malonylbis(azanediyl))bis(1H-indole-3-carboxylic acid) (39b):**
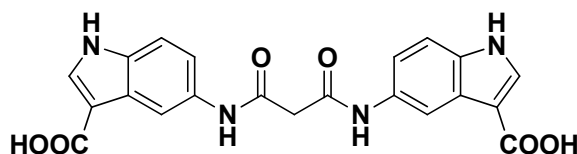
Compound **39b** was prepared following the same procedure of 2**1b** starting from **39a** (140 mg; 0.32 mmol), yielding 30 mg of a light brown solid (25%).^{1}H NMR (DMSO-d$_6$) δ 11.77 (s, 2H), 10.11 (s, 2H), 8.29 (s, 2H), 7.97 (d, J= 2 Hz, 2H), 7.51 (d, J= 9 Hz, 2H), 7.41 (d, J= 9 Hz, 2H), 3.50 (s, 2H). ESI m/z = 421 [M+H]$^+$ M.p: 211 - 213°C d.

Synthesis of ethyl 5-(2,2,2-trichloroacetamido)-1H-indole-2-carboxylate (28):
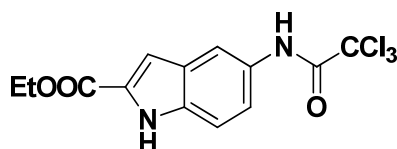
To a solution of **26** (436 mg; 2.13 mmol) and triethylamine (447 µL; 3.20 mmol) in dry DCM (10 ml), trichloroacetylchloride (357 µL; 3.20 mmol) was added dropwise. After 30 min at room temperature, solvent was evaporated and the resulting oil taken up with 100 ml of AcOEt. The organic phase was washed with NaHCO$_3$ saturated solution (3 x 30ml), 10% citric acid water solution (3 x 30ml), brine and anhydrified over Na$_2$SO$_4$. After solvent evaporation, the resulting solid was purified by column chromatography (SiO$_2$,

gradient, DCM/MeOH, 99:1 to 90:10) yielding 545 mg of yellow solid (73%). ¹H NMR (CDCl₃) δ 8.89 (s, 1H); 8.38 (s, 1H), 8.02 (s, 1H); 7.45 (d, J = 9 Hz, 1H); 7.39 (d, J = 9 Hz, 1H); 7.22 (s, 1H); 4.42 (q, J = 7 Hz, 2H); 1.43 (t, J = 7 Hz, 3H). ESI m/z: 349 (100%) [M + H]⁺; 351 (70%) [M + 2H]⁺; 353 (30%) [M + 4H]⁺ Mp: 196.9 – 197.8 °C

Synthesis of methyl 5-(2,2,2-trichloroacetamido)-1H-indole-3-carboxylate (42):
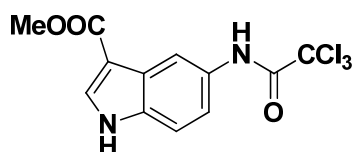
Compound **42** was prepared following the same procedure of **28** starting from **37** (427 mg; 2.25 mmol), yielding 698 mg of a white solid (92%). ¹H NMR (DMSO-d₆) δ 12.00 (s, 1H), 10.79 (s, 1H), 8.31 (s, 1H), 8.11 (s, 1H), 7.49 (d, J= 9 Hz, 1H), 7.44 (d, J= 9 Hz, 1H), 3.81 (s, 3H). ESI m/z = 335 (100%) [M+H⁺], 337 (70%) [M+2+H⁺], 339 (30%) [M+4+H]⁺. M.p: 202 - 204 °C

Synthesis of ethyl 5-(3-(2-(1H-indol-3-yl)ethyl)ureido)-1H-indole-2-carboxylate (30a):
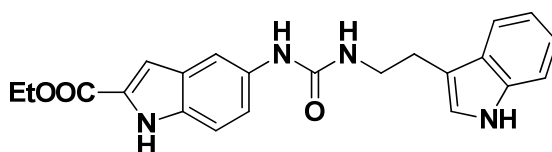
In a sealed vessel **28** (224 mg; 0.69 mmol), triptamine (176 mg; 1.10 mmol) and Na₂CO₃ (364 mg; 3.43 mmol) were suspended in dry DMF (15 ml). The reaction mixture was heated to 150 °C for 1h. The solvent was then evaporated, the resulting oil was diluted in NH₄Cl saturated solution (100 ml) and extracted with AcOEt (3 x 50 ml). The organic phase was collected,

washed with brine, anhydrified over Na_2SO_4 and evaporated under vacuum. The resulting brown solid was purified by column chromatography (SiO_2, AcOEt/DCM, 1:1) yielding 236 mg of white solid (88%). ^{1}H NMR (DMSO-d_6) δ 11.64 (s, 1H); 10.81 (s, 1H); 8.33 (s, 1H); 7.75 (s, 1H); 7.56 (d, J = 9, 1H); 7.34 (d, J = 9 Hz, 1H); 7.31 (d, J = 9 Hz, 1H); 7.16 (d, J = 2 Hz, 1H); 7.05 – 6.96 (m, 4H); 6.03 (t, J = 6 Hz, 1H); 4.30 (q, J = 7 Hz, 2H); 3.45 - 3.39 (m, 2H); 2.84 (t, J = 7 Hz, 2H); 1.32 (t, J = 7 Hz, 3H). ESI m/z: 391 $[M + H]^+$ Mp: 232.2 - 232.7 °C

Synthesis of methyl 5-(3-(2-(1H-indol-3-yl)ethyl)ureido)-1H-indole-3-carboxylate (43a):
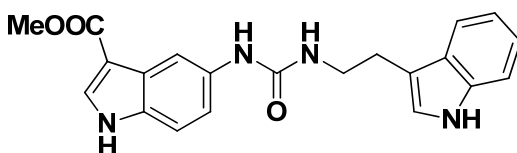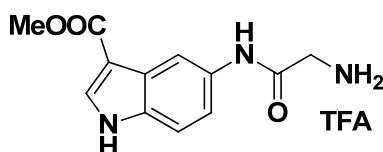

Compound **43a** was prepared following the same procedure of **30a** starting from **42** (400 mg; 1.18 mmol), yielding 335 mg of a white solid (75%). ^{1}H NMR (DMSO-d_6) δ 11.76 (s, 1H), 10.83 (s, 1H), 8.44 (s, 1H), 8.00 - 7.97 (m, 2H), 7.60 (d, J= 8 Hz, 1H), 7.36 (d, J= 8 Hz, 1H), 7.34-7.32 (m, 2H), 7.18 (d, J= 2 Hz, 1H), 7.11-7.06 (m, 1H), 7.00-6.96 (m, 1H), 6.03 (t, J= 6 Hz, 1H), 3.79 (s, 3H), 3.44-3.40 (m, 2H), 2.87 (t, J= 7 Hz, 2H). ESI m/z = 377 $[M+H]^+$ M.p: 225 - 227°C d.

Synthesis of 5-(3-(2-(1H-indol-3-yl)ethyl)ureido)-1H-indole-2-carboxylic acid (30b):
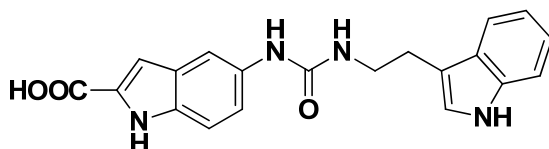
Compound **30b** was prepared following the same procedure of **20b** starting from **30a** (124 mg; 0.32 mmol), yielding 72 mg of a light brown solid (62%). ^{1}H NMR (DMSO-d_6) δ 11.44 (s, 1H); 10.81 (s, 1H); 8.27 (s, 1H); 7.71 (s, 1H); 7.56 (d, J = 9 Hz, 1H); 7.33 (d, J = 9 Hz, 1H); 7.26 (d, J = 9 H, 1H); 7.16 (d, J = 2 Hz, 1H); 7.12 – 7. 03 (m, 2H, scambiabile con D$_2$O); 6.99 – 6.94 (m, 1H); 6.91 (s, 1H); 6.03 (t, J = 6 Hz, 1H); 2.84 (t, J = 7 Hz, 2H) ESI m/z: 363 [M + H]$^+$ M.p.: 249 - 250 °C

**Synthesis of 5-(3-(2-(1H-indol-3-yl)ethyl)ureido)-1H-indole-3-carboxylic acid (43b):**
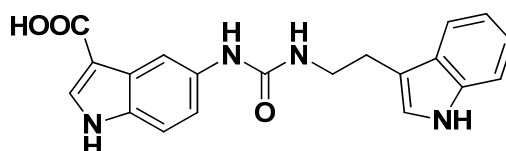
Compound **43b** was prepared following the same procedure of **21b** starting from **43a** (140 mg; 0.37 mmol), yielding 50 mg of a white solid (36%).^{1}H NMR (DMSO-d_6) δ 11.61 (s, 1H), 10.82 (s, 1H), 8.39 (s, 1H), 8.00 (s, 1H); 7.89 (s, 1H), 7.58 (d, J= 8 Hz, 1H), 7.34 (d, J= 8 Hz, 1H), 7.28 - 7.23 (m, 2H), 7.18 (s, 1H), 7.09-7.04 (m, 1H), 7.00-6.95 (m, 1H) 5.98 (t,J= 6 Hz, 1H), 4.60 - 4.56 (m, 2H), 2.87 (t, J= 7 Hz, 2H). ESI m/z = 363 [M+H$^+$] 385 [M+Na$^+$] M.p: 223-224 °C d.

Synthesis of ethyl 5-(2-((tert-butoxycarbonyl)amino)acetamido)-1H-indole-2-carboxylate (29a):
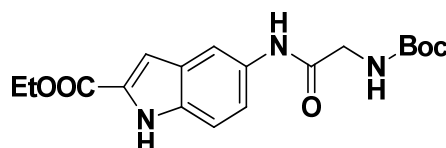
A solution of HOBt (347 mg; 2.57 mmol), HBtU (925 mg; 2.57 mmol), Boc-Gly-OH (375 mg, 2.14 mmol) and DIEA (918 µl; 5.14 mmol) in 9 ml of dry THF/DMF (7/2) was added to a solution of **26** (500 mg; 2.14 mmol) in THF (3 ml). After 12h, the solvent was evaporated and the resulting oil was taken up with AcOEt (100 ml). The organic phase was washed with NaHCO$_3$ saturated solution (3 x 30 ml), 5% citric acid water solution (3 x 30ml), brine and anhydrified over Na$_2$SO$_4$. After solvent evaporation, the resulting solid was purified by column chromatography (SiO$_2$, AcOEt/HEX 7:3) yielding 629 mg of white solid (81%). ^{1}H NMR (DMSO-d$_6$) δ 11.78 (s, 1H); 9.78 (s, 1H); 7.98 (s, 1H); 7.38 – 7.33 (m, 2H); 7.08 (d, J = 2 Hz, 1H); 6.99 (t, J = 6 Hz 1H); 4.31 (q, J = 7 Hz, 2H); 3.70 (d, J = 6 Hz, 2H); 1.38 (s, 9H); 1.32 (t, J = 7 Hz, 3H). ESI m/z: 362 [M + H]$^+$ M.p: 193.0 – 193.9 °C

Synthesis of methyl 5-(2-((tert-butoxycarbonyl)amino)acetamido)-1H-indole-3-carboxylate (44a):
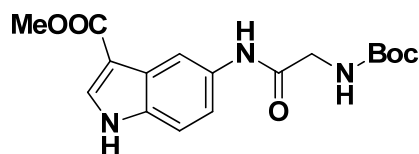
Compound **16** was prepared following the same procedure of **29a** starting from **37** (442 mg; 1.90 mmol), yielding 680 mg of a white solid (70%).^{1}H NMR (DMSO-d$_6$) δ 11.85 (s, 1H), 9.85 (s, 1H), 8.22 (s, 1H), 8.03 (d, J= 2 Hz, 1H), 7.46 (dd, J$_1$= 9 Hz, J$_2$= 2 Hz, 1H), 7.39 (d, J= 9 Hz, 1H), 7.01 (t, J= 6 Hz, 1H), 3.79 (s, 3H), 3.73 (d, J= 6 Hz, 2H), 1.41 (s, 9H). ESI m/z = 348 [M+H]$^+$ M.p: 214.7 – 216.0 °C

Synthesis of 2-((2-(ethoxycarbonyl)-1H-indol-5-yl)amino)-2-oxoethanaminium 2,2,2-trifluoroacetate (29b):
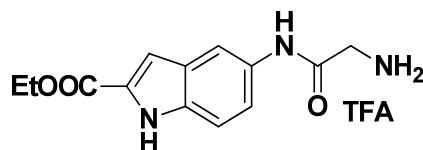
To a suspension of **29a** (500 mg, 1.38 mmol) in DCM (4 ml), TFA (4 ml) was added and the resulting solution was stirred at room temperature for 30 min. The solution was than evaporated yielding 520 mg of a white solid (99.9%). ^{1}H NMR (DMSO-d_6) δ 11.88 (s, 1H); 10.30 (s, 1H); 8.08 (brs, 2H); 7.99 (s, 1H); 7.43 (d, J = 9 Hz, 1H); 7.34 (d, J = 9 Hz, 1H); 7.14 (s, 1H); 4.33 (q, J = 7 Hz, 2H); 3.77 (s, 2H); 1.34 (t, J = 7 Hz, 3H).ESI m/z: 262 [M + H]$^+$ M.p: 225.4 – 226.3 °C

Synthesis of 2-((3-(methoxycarbonyl)-1H-indol-5-yl)amino)-2-oxoethanaminium 2,2,2-trifluoroacetate (44b):

Compound **44b** was prepared following the same procedure of **29b** starting from **44a** (500 mg; 1.38 mmol), yielding 520 mg of a white solid (99.9%).^{1}H NMR (DMSO-d_6) δ 11.93 (s, 1H), 10.31 (s, 1H), 8.26 (s, 1H), 8.06 (d, J= 2 Hz, 1H), 7.96 - 7.70 (m, 2H), 7.47 - 7.41(m, 2H), 3.79 (s, 3H), 3.75 - 3.70 (m, 2H). ESI m/z = 248 [M+H]$^+$ M.p: 229.0 – 230.0 °C

General procedure for the synthesis of compounds 31a-36a and 45a-50a:
To a solution of the proper arylisocianate (1.20 mol eq) in dry THF (8 ml), a dry THF solution (20 ml) of indole derivative (1 mol eq) and triethylamine (3 mol eq) was added dropwise. The resulting mixture was stirred at room for 12 h. The solid formed was recovered by filtration, washed with water (3 x 20 ml) and diethyl ether (3 x 20 ml), yielding pure compound **31a-36a**.

Ethyl 5-(2-(3-(4-nitrophenyl)ureido)acetamido)-1H-indole-2-carboxylate (31a)
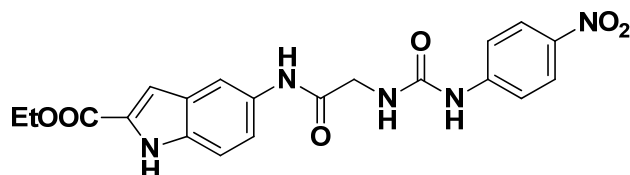
white solid (70%). ^{1}H NMR (DMSO-d$_6$) δ 11.84 (s, 1H); 9.99 (s, 1H); 9.74 (s, 1H); 8.18 (d, J = 9 Hz, 2H); 8.02 (s, 1H); 7.67 (d, J = 9 Hz, 2H); 7.43 – 7.36 (m, 2H); 7.12 (s, 1H); 6.85- 6.84 (m, 1H); 4.35 (q, J = 7 Hz, 2H); 3.99 (d, J = 5 Hz, 2H); 1.35 (t, J = 7 Hz, 3H). ESI m/z: 426 [M + H]$^+$ M.p: 288.9 – 289.7 °C

ethyl 5-(2-(3-phenylureido)acetamido)-1H-indole-2-carboxylate (32a)
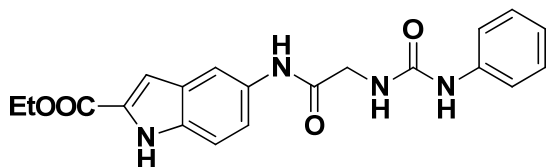
white solid (75%). ^{1}H NMR (DMSO-d$_6$) δ 11.81 (s, 1H); 9.94(s, 1H); 8.82 (s, 1H); 7.99 (s, 1H); 7.41-7.38 (m, 4H); 7.25-7.20(m, 2H); 7.10 (s, 1H); 6.92-6.87 (m, 1H) 6.43 (t, J=5Hz, 1H); 4.36 (q, J=7 Hz, 2H); 3.94 (d, J=5Hz, 2H); 1.35 (t, J = 7 Hz, 3H). ESI m/z: 381 [M + H] $^+$, 403 [M + Na] $^+$ M.p:263,3-265,4 d

ethyl 5-(2-(3-(p-tolyl)ureido)acetamido)-1H-indole-2-carboxylate (33a)
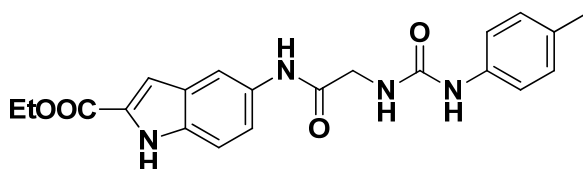
white solid (84%) ^{1}H NMR (DMSO-d$_6$) δ 11.80 (s, 1H); 9.92(s, 1H); 8.70 (s, 1H); 7.99 (s, 1H); 7.40-7.33 (m, 2H); 7.28 (d, J=8Hz, 2H); 7.09 (s, 1H); 7.02 (d, J= 8Hz, 2H); 6.37 (t, J= 5Hz, 1H); 4.36 (q, J=7Hz, 2H); 3.93 (d, J=5Hz, 2H); 2.21 (s,3H); 1.35(t, J = 7 Hz, 3H). ESI m/z: 395 [M + H]$^+$ 417 [M + Na]$^+$ M.p:271,9-273,3 d

ethyl 5-(2-(3-(4-methoxyphenyl)ureido)acetamido)-1H-indole-2-carboxylate (34a)
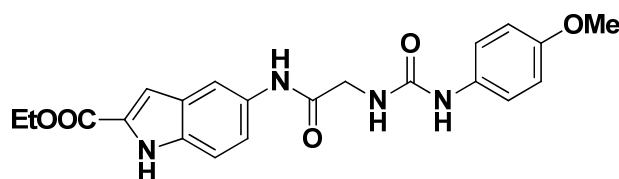
white solid (77%) ^{1}H NMR (DMSO-d$_6$) δ 11.80 (s, 1H); 9.91(s, 1H); 8.61 (s, 1H); 7.99 (s, 1H); 7.40-7.37 (m, 2H); 7.30 (d, J=8Hz, 2H); 7.10 (s, 1H); 6.81 (d, J=8Hz, 2H); 6.31 (t, J= 5Hz, 1H); 4.36 (q, J=7Hz, 2H); 3.93 (d, J=5Hz, 2H); 3.69 (s,3H); 1.35(t, J = 7 Hz, 3H). ESI m/z: 411[M + H]$^+$ M.p: 257,9-260,3 d

ethyl 5-(2-(3-(4-cyanophenyl)ureido)acetamido)-1H-indole-2-carboxylate (35a)
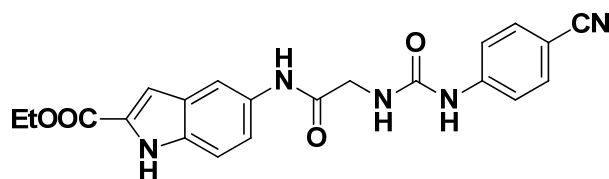
white solid (72%) ^{1}H NMR (DMSO-d$_6$) δ 11.80 (s, 1H); 9.95(s, 1H); 9.38 (s, 1H); 7.99 (s, 1H); 7.67 (d, J=8Hz, 2H); 6.58 (d, J=8Hz, 2H); 7.38-7.37 (m, 2H) 7.10 (s,1H) 6.64 (t, J= 5Hz, 1H); 4.36 (q, J=7Hz, 2H); 3.97 (d, J=5Hz, 2H); 1.35(t, J = 7 Hz, 3H). ESI m/z: 406 [M + H]$^+$ M.p:280-282 d

ethyl 5-(2-(3-(4-(dimethylamino)phenyl)ureido)acetamido)-1H-indole-2-carboxylate (36a)
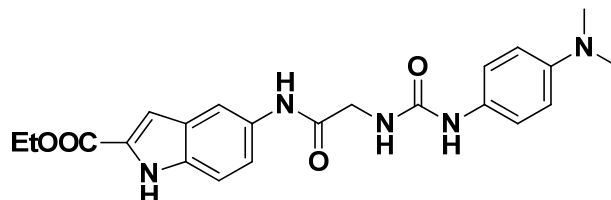
white solid (71%) ^{1}H NMR (DMSO-d$_6$) δ 11.70 (s, 1H); 9.90 (s, 1H); 8.45 (s, 1H); 7.99 (s, 1H); 7.43-7.33 (m, 2H); 7.22 (d, J= 9Hz, 2H); 7.09 (s, 1H); 6.66 (d, J= 9Hz, 2H); 6.29 (t, J= 5Hz, 1H); 4.32 (q, J= 7Hz, 2H); 3.90 (d, J=5Hz, 2H); 2.80 (s, 6H); 1.33 (t, J= 7Hz, 3H). ESI m/z: 424 [M + H] $^+$ M.p:250-252 d

methyl 5-(2-(3-(4-nitrophenyl)ureido)acetamido)-1H-indole-3-carboxylate (45a)
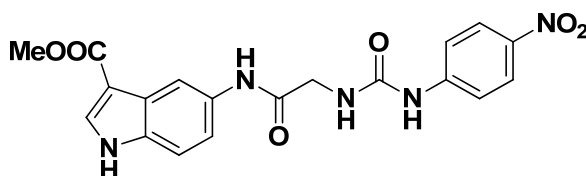
white solid (69%) ^{1}H NMR (DMSO-d$_6$) δ 11.87 (s, 1H), 10.04 (s, 1H), 9.66 (s, 1H), 8.27 (s, 1H), 8.16 (d, J= 9 Hz, 2H), 8.06 (d, J= 2 Hz, 1H), 7.65 (d, J= 9 Hz, 2H), 7.47 - 7.44 (m, 2H), 6.73 (t, J= 4 Hz, 1H), 3.99 (d, J= 4 Hz, 2H), 3.79 (s, 3H). ESI m/z = 412 [M+H]$^+$ M.p: 289 – 290 °C d

methyl 5-(2-(3-phenylureido)acetamido)-1H-indole-3-carboxylate (46a)
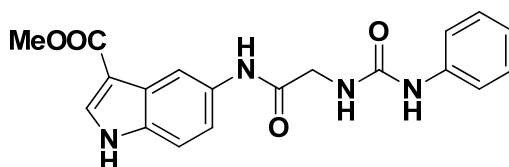
white solid (63%) ^{1}H NMR (DMSO-d$_6$) δ 11.87 (s, 1H), 9.99 (s, 1H), 8.82 (s, 1H), 8.25 (s, 1H), 8.04 (s, 1H), 7.47-7.39 (m, 4H), 7.25-7.20 (m, 2H), 6.90 (t, J=7 Hz, 1H), 6.42 (t, J=5Hz, 1H), 3.95 (d, J= 5Hz, 2H), 3.79 (s, 3H). ESI m/z = 367 [M+H]$^+$, 389 [M+Na]$^+$ M.p: 260-262 °C d

methyl 5-(2-(3-(p-tolyl)ureido)acetamido)-1H-indole-3-carboxylate (47a)
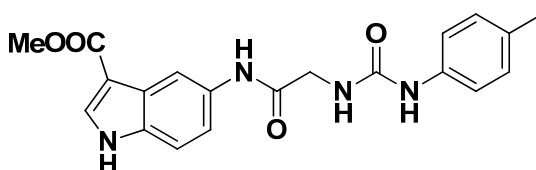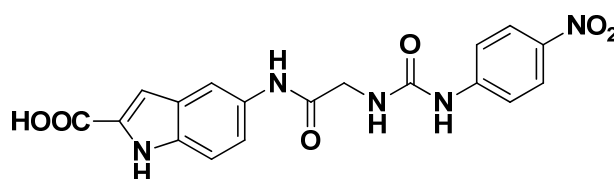

white solid (83%) ^{1}H NMR (DMSO-d$_6$) δ 11.86 (s, 1H), 9.98 (s, 1H), 8.70 (s, 1H), 8.25 (s, 1H), 8.03 (d, J= 2Hz, 1H), 7.45-7.38 (m, 2H), 7.29 (d, J= 9Hz, 2H), 7.03 (d, J= 9Hz, 2H), 6.38 (t, J= 5Hz, 1H), 3.94 (d, J= 5Hz, 2H), 3.79 (s, 3H), 2.21 (s, 3H). ESI m/z= 381 [M+H]$^+$, 403 [M+Na]$^+$ M.p: 271-273 °C d

methyl   5-(2-(3-(4-methoxyphenyl)ureido)acetamido)-1H-indole-3-carboxylate (48a)
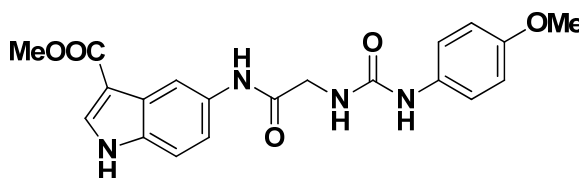
white solid (81%) ^{1}H NMR (DMSO-d$_6$) δ 11.85 (s, 1H), 9.96 (s, 1H), 8.61 (s, 1H), 8.25 (s, 1H), 8.03 (d, J= 2Hz, 1H), 7.45 (d, J= 9Hz, 1H), 7.40 (d, J= 9Hz, 1H), 7.30 (d, J= 8Hz, 2H), 6.82 (d, J= 8Hz, 2H), 6.32 (t, J= 5Hz, 1H), 3.93 (d, J= 5Hz, 2H), 3.70 (s, 3H), 3.70 (s, 3H). ESI m/z = 397 [M+H]$^+$, 419 [M+Na]$^+$ M.p: 249-250 °C d

methyl 5-(2-(3-(4-cyanophenyl)ureido)acetamido)-1H-indole-3-carboxylate (49a)
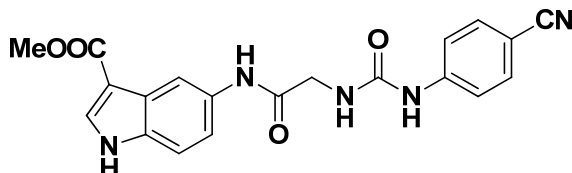
white solid (79%) ^{1}H NMR (DMSO-d$_6$) δ 11.86 (s, 1H), 10.01 (s, 1H), 9.39 (s, 1H), 8.25 (s, 1H), 8.03 (d, J= 2Hz, 1H), 7.68 (d, J= 9Hz, 2H), 7.59 (d. J= 9Hz, 2H), 7.45 (dd, J$_1$= 9Hz, J$_2$= 2Hz, 1H), 7.40 (d, J= 9Hz, 1H), 6.65 (t, J= 5Hz, 1H), 3.97 (d, J= 5Hz, 2H), 3.79 (s, 3H). ESI m/z = 392 [M+H]$^+$, 411 [M+Na]$^+$ M.p: 268-271 °C d

methyl 5-(2-(3-(4-(dimethylamino)phenyl)ureido)acetamido)-1H-indole-3-carboxylate (50a)
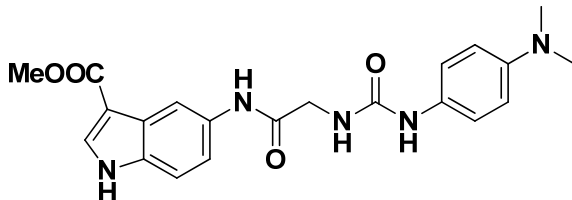
white solid (65%) ^{1}H NMR (DMSO-d$_6$) δ 11.85 (s, 1H), 9.94 (s, 1H), 8.41 (s, 1H), 8.25 (s, 1H), 8.03 (d, J= 2Hz, 1H), 7.46 (dd, J$_1$= 9Hz, J$_2$= 2Hz, 1H), 7.40 (d, J= 9Hz, 1H), 7.21 (d, J= 9Hz, 2H), 6.66 (d, J= 9Hz, 2H), 6.25 (t, J= 5Hz, 1H), 3.92 (d, J= 5Hz, 2H), 3.79 (s, 3H), 2.80 (s, 6H). ESI m/z = 432 [M+Na]$^+$ M.p: 244.5-246.8 °C d

General procedure for the synthesis of compounds 31b-36b: Compound **31a-36a** (1.00 mol eq) dissolved in a mixture 4/1 of THF/H$_2$0 (20 ml), NaOH (10.00 mol eq) and pyridine (0.20 mol eq) added and the resulting mixture was stirred at room temperature for 12h. The solvent was then evaporated and the

resulting oil taken up with H_2O (20 ml). The water phase was washed with DCM (3 x 10 ml), acidified to pH 2 with concentrated HCl. The resulting solid was recovered by filtration, washed with water yielding pure **31b-36b**

5-(2-(3-(4-nitrophenyl)ureido)acetamido)-1H-indole-2-carboxylic   acid (31b)

white solid (90%) ^{1}H NMR (DMSO-d_6) δ 11.71 (s, 1H); 9.98 (s, 1H); 9.67(s, 1H); 8.18 (d, J = 9 Hz, 2H); 8.00 (s, 1H); 7.67 (d, J = 9 Hz, 2H); 7.40 – 7.33 (m, 2H); 7.06 (s, 1H); 6.74 – 6.73 (m, 1H); 4.00 (d, J = 5 Hz, 2H).). ESI m/z = 383 [M+H]$^+$ M.p: 283.5 – 283.9 °C

5-(2-(3-phenylureido)acetamido)-1H-indole-2-carboxylic acid (32b)
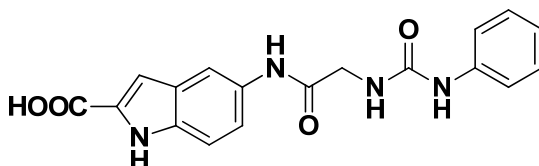
 white solid (93[1]H NMR (DMSO-d_6) δ 11.68 (s, 1H); 9.93(s, 1H); 8.84 (s, 1H); 7.98 (s, 1H); 7.41-7.35 (m, 4H); 7.25-7.20(m, 2H); 7.04 (s, 1H); 6.92-6.87 (m, 1H) 6.45 (s, 1H); 3.94 (s, J=5Hz, 2H). ESI m/z = 353 [M+H]$^+$ M.p: 252-254 °C

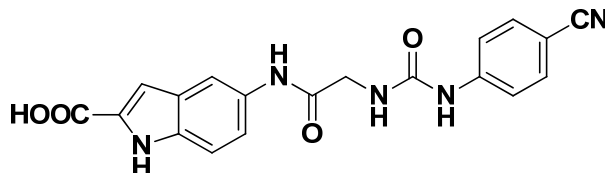**5-(2-(3-(p-tolyl)ureido)acetamido)-1H-indole-2-carboxylic acid (32b)**

white solid (96%) ^{1}H NMR (DMSO-d_6) δ 11.80 (s, 1H); 9.92(s, 1H); 8.70 (s, 1H); 7.99 (s, 1H); 7.40-7.33 (m, 2H); 7.28 (d, J=8Hz, 2H); 7.04-7.01 (m, 3H); 6.37 (t, J= 5Hz, 1H); 3.93 (d, J=5Hz, 2H); 2.21 (s,3H). ESI m/z = 367 [M+H]$^+$, 389 [M+Na]$^+$ M.p: 242-244 °C d

**5-(2-(3-(4-methoxyphenyl)ureido)acetamido)-1H-indole-2-carboxylic acid (33b)**
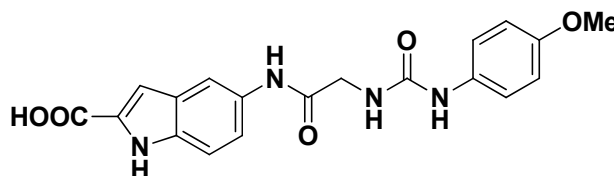
white solid (89%) ^{1}H NMR (DMSO-d_6) δ 11.67 (s, 1H); 9.89(s, 1H); 8.61 (s, 1H); 7.98 (s, 1H); 7.38-7.35 (m, 2H); 7.30 (d, J=8Hz, 2H); 7.03 (s, 1H); 6.81 (d, J=8Hz, 2H); 6.32 (t, J= 5Hz, 1H); 3.93 (d, J=5Hz, 2H); 3.69 (s, 3H). ESI m/z = 383 [M+H]$^+$ M.p: 260-261 °C d

5-(2-(3-(4-cyanophenyl)ureido)acetamido)-1H-indole-2-carboxylic acid (34b)

white solid (93%) ^{1}H NMR (DMSO-d$_6$) δ 11.68 (s, 1H); 9.94(s, 1H); 9.39 (s, 1H); 7.97 (s, 1H); 7.67 (d, J=8Hz, 2H); 6.58 (d, J=8Hz, 2H); 7.38-7.31 (m, 2H) 7.04 (s,1H) 6.64 (t, J= 5Hz, 1H); 3.97 (d, J=5Hz, 2H). ESI m/z = 378 [M+H]$^+$ M.p: 269-270 °C d

5-(2-(3-(4-(dimethylamino)phenyl)ureido)acetamido)-1H-indole-2-carboxylic acid (35b)
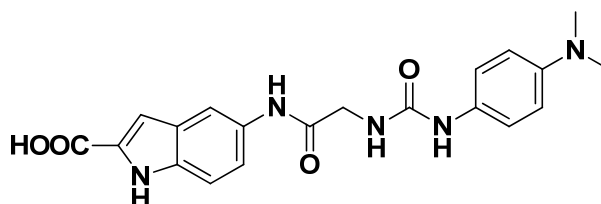
white solid (81%) ^{1}H NMR (DMSO-d$_6$) δ 11.69 (s, 1H); 9.95 (s, 1H); 9.15 (s, 1H); 7.99 (s, 1H); 7.55-7.45 (m, 4H); 7.39-7.32 (m, 2H); 7.03 (s, 1H); 6.54(s, 1H); 3.94(s, 2H); 3.07 (s, 6H). ESI m/z = 396 [M+H]$^+$ M.p: 241-243 °C d

Synthesis of tert-butyl 5-nitro-1H-indole-3-carboxylate:
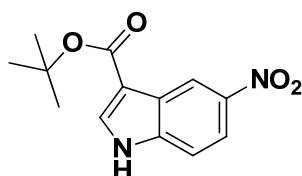
5-nitro-1H-indole-3-carboxylic acid (500 mg; 2.42 mmol) was poured in a sealed vessel and dissolved with dry DMF (5 ml). TEA (1.01 ml; 7.26 mmol), tert-Butanol (3.40 ml; 36.30 mmol) and DCC (1.50 g; 7.26 mmol) were then added and the resulting mixture was heated at 120 °C for 3h. Solvent was then evaporated and the resulting oil was taken up with AcOEt (100 ml), washed with NaHCO$_3$ (3 x 60 ml) and brine (60 ml). Organic phase was anhydrified over sodium sulphate, filtered, concentrated under vacuum and purified by

column chromatography (SiO$_2$, DCM/AcOEt 9:1) yielding 585 mg of light brown solid (92%). ^{1}H NMR (DMSO-d$_6$) δ 9.11 (s, 1H), 8.86 (s, 1H), 8.18 (dd, J$_1$= 9 Hz, J$_2$= 2 Hz, 1H), 8.01 (d, J= 2 Hz, 1H), 7.46 (d, J= 9 Hz, 1H), 1.67 (s, 9 H). ESI m/z = 261 [M+H]$^+$ M.p: 212-214 °C

Synthesis of tert-butyl 5-amino-1H-indole-3-carboxylate (51):
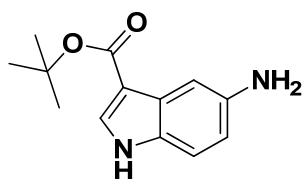
To a solution of **31** (500 mg; 1.90 mmol) in ethanol (150 ml), 5% palladium on activated carbon (237 mg, 0.112 mmol) was added. The reaction was stirred under H$_2$ (1 atm) for 12h at room temperature. The colorless solution was filtrated and the solvent evaporated under vacuum yielding 420 mg of a white solid (95%). ^{1}H NMR (DMSO-d$_6$) δ 11.62 (s, 1H), 8.32 (s, 1H), 7.90 (d, J= 2 Hz, 1H), 7.62 (brs, 2H), 7.36 (d, J= 9 Hz, 1H), 6.90 (d, J= 9 Hz, 1H), 1.56 (s, 9H). ESI m/z: 233 [M + H]$^+$. Mp: 60 – 63 °C

Synthesis of tert-butyl 5-(2-((((9H-fluoren-9-yl)methoxy)carbonyl)amino)acetamido)-1H-indole-3-carboxylate (52a):
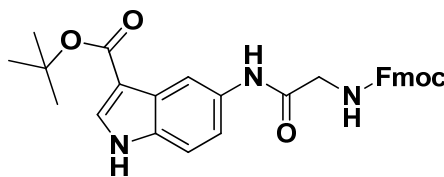
a solution of HOBt (349 mg; 2.28 mmol), HBtU (865 mg; 2.28 mmol), Fmoc-Gly-OH (558 mg, 1.90 mmol) and DIEA (400 µl; 2.28 mmol) in 18 ml of dry THF/DMF (7/2) was added to a solution of **51** (442 mg; 1.90 mmol) in dry THF (3 ml). After 12h, the solvent was evaporated and the resulting oil was
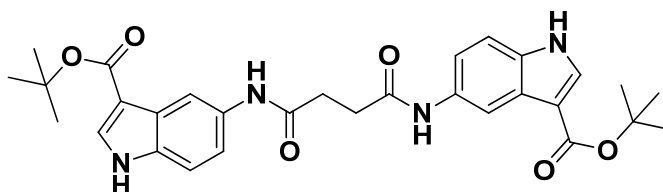
taken up with AcOEt (100 ml). The organic phase was washed with NaHCO$_3$ saturated solution (3 x 30 ml), 5% citric acid water solution (3 x 30ml), brine and anhydrified over Na$_2$SO$_4$. After solvent evaporation, the resulting solid was purified by column chromatography (SiO$_2$, DCM/AcOEt 7:3) yielding 680 mg of white solid (70%). ^{1}H NMR (DMSO-d$_6$) δ 11.75 (s, 1H), 9.85 (s, 1H), 8.32 (s, 1H), 7.91 - 7.7.88 (m, 3H), 7.74 (d, J= 8 Hz, 2H), 7.66 - 7.62 (m, 1H), 7.45 - 7.31 (m, 6H), 4.32 - 4.26 (m, 3H), 3.81 (d, J= 6 Hz, 2H), 1.59 (s, 9H). ESI m/z: 534 [M + Na]$^+$, 550 [M + K]$^+$. Mp: 95 – 97 °C

Synthesis of tert-butyl 5-(2-aminoacetamido)-1H-indole-3-carboxylate (52b):
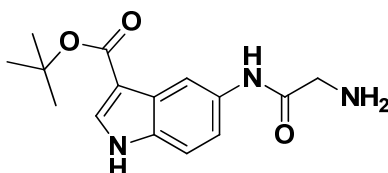
To a suspension of **52a** (400 mg; 0.78 mmol) in DCM (8 ml), piperidine (2 ml) was added and the resulting mixture was stirred at RT for 30 min. The solvent was then evaporated and the resulting solid was washed with hexane (3 x 30 ml) yielding 225 mg of a white solid (99%). ^{1}H NMR (DMSO-d$_6$) δ 11.75 (s, 1H), 9.85 (s, 1H), 8.35 (s, 1H), 7.90 (s, 1H), 7.38 - 7.34 (m, 2H), 7.25 - 7.16 (m, 2H), 2.79 - 2.75 (m, 2H), 1.56 (s, 9H). ESI m/z: 312 [M + Na]$^+$. Mp: 89 – 91 °C

**Synthesis of di-tert-butyl 5,5'-(succinylbis(azanediyl))bis(1H-indole-3-carboxylate) (53):**

To a solution of **51** (500 mg; 2.14 mmol) in acetone (10ml), TEA was added (598 µl; 4.28 mmol) and the reaction mixture was cooled to -78°C. Succinyl chloride (188 µl; 1.71 mmol) was then added dropwise and the reaction was slowly warmed to RT and stirred for 12h. Solvent was then evaporated and the resulting oil was taken up with $NaHCO_3$ saturated solution (100ml) and extracted with AcOEt (3 x 30 ml). The organic phase was collected, washed with 10% citric acid water solution (3 x 30 ml), brine (50 ml), anhydrified over Na_2SO_4 and evaporated under vacuum. Purification by column chromatography (SiO_2, DCM/AcOEt 6:4) yield 200 mg of brown solid (36%).^{1}H NMR (DMSO-d_6) δ 11.69 (s, 2H), 9.87 (s, 2H), 8.30 (s, 2H), 7.87 (s, 2H), 7.41 - 7.32 (m, 4H), 2.66 (s, 4H), 1.54 (s, 18H). ESI m/z: 547 $[M + H]^+$, 569 $[M + Na]^+$. Mp: 223 – 225 °C d

General procedure for the synthesis of compounds 55-60:

To a solution of the proper arylisocianate (1.20 mol eq) in dry THF (8 ml), a dry THF solution (20 ml) of **52b** (1 mol eq) and triethylamine (3 mol eq) was added dropwise. The resulting mixture was stirred at room for 12 h. The solid formed was recovered by filtration, washed with water (3 x 20 ml) and diethyl ether (3 x 20 ml), yielding compound **55-60**.
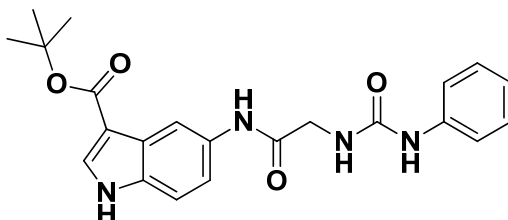
tert-butyl 5-(2-(3-(4-nitrophenyl)ureido)acetamido)-1H-indole-3-carboxylate (55):
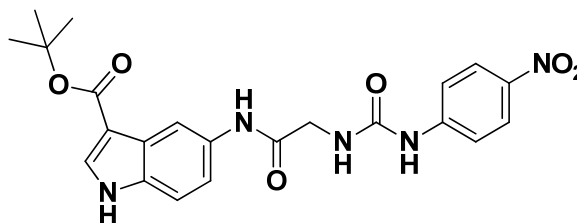
yellow solid (71%) ^{1}H NMR (DMSO-d_6) δ 11.76 (s, 1H), 9.98 (s, 1H), 9.65 (s, 1H), 8.32 (s, 1H), 8.15 (d, J= 9 Hz, 2H), 7.91 (d, J= 2 Hz, 1H), 7.65 (d, J= 9
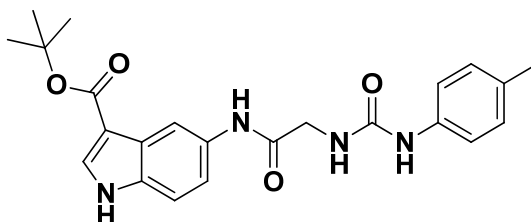
Hz, 2H), 7.40 - 7.37 (m, 2H), 6.72 (t, J= 5 Hz, 1H), 4.00 (d, J= 5 Hz, 2H), 1.57 (s, 9H). ESI m/z: 476 [M + Na]$^+$. Mp: 237-239 °C d

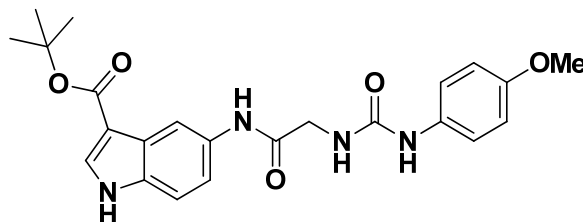**tert-butyl 5-(2-(3-phenylureido)acetamido)-1H-indole-3-carboxylate (56):**

.white solid (65%) ^{1}H NMR (DMSO-d$_6$) δ 11.76 (s, 1H), 9.94 (s, 1H), 8.82 (s, 1H), 8.32 (s, 1H), 7.91 (d, J= 2Hz, 1H), 7.42-7.37 (m, 5H), 7.25-7.20 (m, 2H), 6.89 (t, J= 5Hz, 1H), 3.95 (d, J= 5Hz, 2H), 1.57 (s, 9H). ESI m/z: 409 [M + H]$^+$. Mp: 238-239 °C d

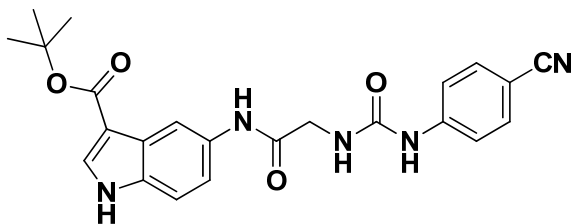**tert-butyl 5-(2-(3-(p-tolyl)ureido)acetamido)-1H-indole-3-carboxylate (57):**

white solid (80%) ^{1}H NMR (DMSO-d$_6$) δ 11.75 (s, 1H), 9.93 (s, 1H), 8.72 (s, 1H), 8.32 (s, 1H), 7.91 (s, 1H), 7.38-7.35 (m, 2H), 7.29 (d, J= 8Hz, 2H), 7.03 (d, J= 8Hz, 2H), 6.38 (t, J= 5Hz, 1H), 3.94 (d, J= 5Hz, 2H), 2.21 (s, 3H), 1.57 (s, 9H). ESI m/z: 423 [M + H]$^+$, 445 [M + Na]$^+$. Mp: 242-245 °C d

tert-butyl 5-(2-(3-(4-methoxyphenyl)ureido)acetamido)-1H-indole-3-carboxylate (58):


white solid (67%) ^{1}H NMR (DMSO-d$_6$) δ 11.75 (s, 1H), 9.92 (s, 1H), 8.62 (s, 1H), 8.32 (s, 1H), 7.91 (s, 1H), 7.39-7.36 (m, 2H), 7.32 (d, J= 9Hz, 2H), 6.82 (d, J= 9Hz, 2H), 6.33 (t, J= 5hz, 1H), 3.94 (d, J= 5Hz, 2H), 3.69 (s, 3H), 1.57 (s, 9H). ESI m/z: 439 [M + H]$^+$, 461 [M + Na]$^+$. Mp: 238-240 °C d

tert-butyl 5-(2-(3-(4-cyanophenyl)ureido)acetamido)-1H-indole-3-carboxylate (59):

white solid (75%) ^{1}H NMR (DMSO-d$_6$) δ 11.76 (s, 1H), 9.96 (s, 1H), 9.44 (s, 1H), 8.31 (s, 1H), 7.91 (s, 1H), 7.97 (d, J= 9Hz, 2H), 7.59 (d, J= 9Hz, 2H), 7.39-7.35 (m, 2H), 6.88 (t, J= 5Hz, 1H), 3.97 (d, J= 5Hz, 2H), 1.56 (s, 9H). ESI m/z: 456 [M + Na]$^+$. Mp: 228-230 °C d

tert-butyl   5-(2-(3-(4-(dimethylamino)phenyl)ureido)acetamido)-1H-indole-3-carboxylate (60):
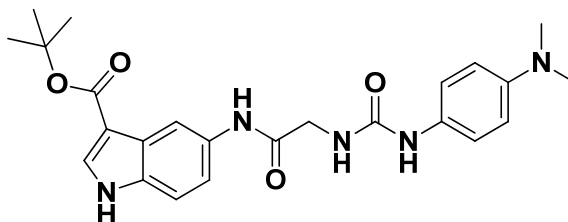
white solid (71%) ^{1}H NMR (DMSO-d$_6$) δ 11.78 (s, 1H), 9.92 (s, 1H), 8.50 (s, 1H), 8.32 (s, 1H), 7.90 (d, J= 2Hz, 1H), 7.38-7.35 (m, 2H), 7.21 (d, J= 9Hz, 2H), 6.67 (d, J= 9Hz, 2H), 6.30-6.32 (m, 1H) 3.92 (d, J= 5Hz, 2H), 2.80 (s, 6H), 1.57 (s, 9H). ESI m/z: 452 [M + H]$^+$, 474 [M + Na]$^+$. Mp: 225-227 °C d

General procedure for the synthesis of compounds 40b, 45b-50b: To a suspension of tert-butyl ester derivatives **53-60** (1.20 mol eq) in DCM (10 ml), TFA (3 ml) was added. The resulting mixture was stirred at RT for 1 h. Solvent was then evaporated yielding pure **40b,45b-60b**

5,5'-(succinylbis(azanediyl))bis(1H-indole-3-carboxylic acid) (40b):
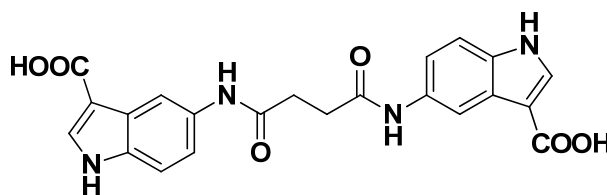
white solid (99%) ^{1}H NMR (DMSO-d$_6$) δ 11.69 (s, 2H), 9.89 (s, 2H), 8.25 (s, 2H), 7.92 (s, 2H), 7.48 (d, J= 9 Hz, 2H); 7.33 (d, J= 9 Hz, 2H), 2.66 (s, 4H). ESI m/z: 435 [M + H]$^+$ Mp: 230-232 °C d

5-(2-(3-(4-nitrophenyl)ureido)acetamido)-1H-indole-3-carboxylic   acid (45b):
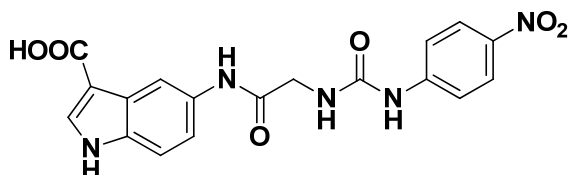
 yellow solid (99%) ^{1}H NMR (DMSO-d_6) δ 11.89 (s, 1H), 11.75 (s, 1H), 10.00 (s, 1H), 9.63 (s, 1H), 8.16 (d, J= 9Hz, 2H), 7.95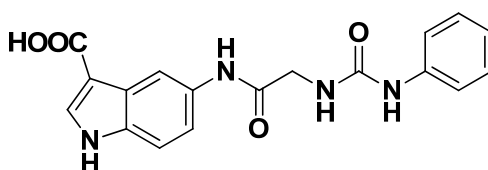 (d, J=2Hz, 1H), 7.65 (d, J= 9Hz, 2H), 7.47 (d, J= 8 Hz, 1H), 7.39 (d, J= 8 Hz, 1H), 6.72 (t, J= 5Hz, 1H), 3.98 (d, J= 5Hz, 2H). ESI m/z: 398 [M + H]$^+$. Mp: 283-285 °C d

5-(2-(3-phenylureido)acetamido)-1H-indole-3-carboxylic acid (46b):

white solid (99%) ^{1}H NMR (DMSO-d_6) δ 11.74 (s, 1H), 9.96 (s, 1H), 8.81 (s, 1H), 8.24 (s, 1H), 7.95 (d, J= 2Hz, 1H), 7.48-7.37 (m, 4H), 7.25-7.20 (m, 2H), 6.92-6.97 (m, 1H), 6.42 (t, J= 5Hz, 1H), 3.94 (J= 5Hz 2H). ESI m/z: 353 [M + H]$^+$, 357 [M + Na]$^+$. Mp: 249-250 °C d

5-(2-(3-(p-tolyl)ureido)acetamido)-1H-indole-3-carboxylic acid (47b):

white solid (99%) ^{1}H NMR (DMSO-d_6) δ 11.86 (s, 1H), 9.95 (s, 1H), 8.70 (s, 1H), 8.24 (s, 1H), 7.96 (d, J= 2Hz, 1H), 7.46 (d, J= 8Hz, 1H), 7.38 (d, J= 8Hz,

1H), 7.28 (d, J= 9Hz, 2H), 7.03 (d, J= 9Hz, 2H), 6.38 (t, J= 5Hz, 1H), 3.94 (d, J= 5Hz, 2H), 2.21 (s, 3H). ESI m/z: 367 [M + H]$^+$, 389 [M + Na]$^+$. Mp: 271-273 °C d

5-(2-(3-(4-methoxyphenyl)ureido)acetamido)-1H-indole-3-carboxylic   acid (48b):

white solid (99%) ^{1}H NMR (DMSO-d$_6$) δ 11.74 (s, 1H), 9.95 (s, 1H), 8.61 (s, 1H), 8.22 (s, 1H), 7.94 (d, J=2Hz, 1H), 7.45 (d, J= 8Hz, 1H), 7.36 (d, J= 8Hz, 1H), 7.28 (d, J= 9Hz, 2H), 6.80 (d, J= 9Hz, 2H), 6.33 (t, J= 5Hz, 1H), 3.93 (d, J= 5Hz, 2H), 3.69 (s, 3H). ESI m/z: 381 [M + H]$^+$. Mp: 238-240 °C d

5-(2-(3-(4-cyanophenyl)ureido)acetamido)-1H-indole-3-carboxylic   acid (49b):
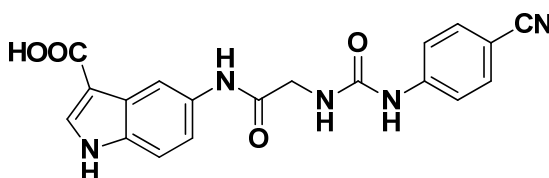
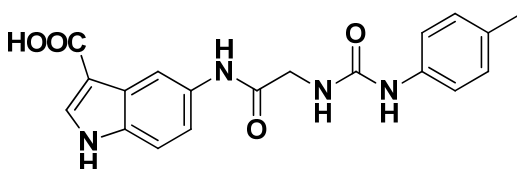white solid (99%) ^{1}H NMR (DMSO-d$_6$) δ 11.75 (s, 1H), 9.99 (s, 1H), 9.40 (s, 1H), 8.23 (s, 1H), 7.95 (d, J= 2Hz, 1H), 7.68 (d, J= 9Hz, 2H), 7.58 (d, J= 9Hz, 2H), 7.46 (d, J= 8Hz, 1H), 7.38 (d, J= 8Hz, 1H), 6.65 (brs, 1H), 3.95 (d, J= 5Hz, 2H). ESI m/z: 376 [M + H]$^+$. Mp: 228-230 °C d
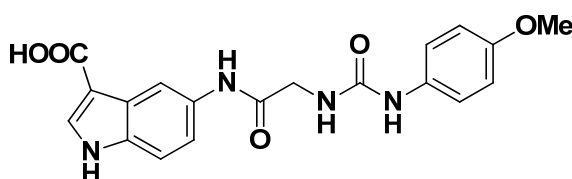
5-(2-(3-(4-(dimethylamino)phenyl)ureido)acetamido)-1H-indole-3-carboxylic acid (50b):
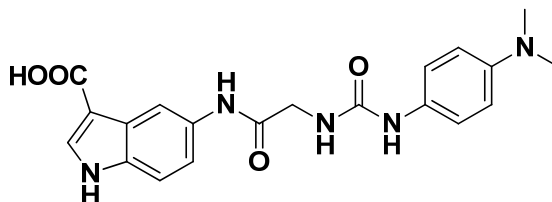
white solid (99%) ^{1}H NMR (DMSO-d$_6$) δ 11.88 (s, 1H), 10.02 (s, 1H), 9.33 (s, 1H) 8.26 (s, 1H), 7.94 (s, 1H), 7.47-7.36(m,6H), 6.67 (s, 1H,), 3.93 (s, 2H), 2.37 (s, 6H). ESI m/z: 396 [M + H]$^+$. Mp: 201-204 °C d

7.2 Oxindole derivatives

General Experimental

Tetrahydrofuran, hexanes, diethyl ether, and ethyl acetate (Fisher ACS grade) were used as received. Column chromatography was performed using EM Science 230-400-mesh silica gel. ^{1}H NMR, ^{13}C NMR spectra were recorded on 400 MHz, ^{1}H (100 MHz, ^{13}C), 500 MHz, ^{1}H (126 MHz, ^{13}C) spectrometers. Spectra were referenced to residual chloroform (δ 7.26 ppm, ^{1}H; δ 77.00 ppm, ^{13}C). Chemical shifts are reported in ppm (δ); multiplicities are indicated by s (singlet), d (doublet), t (triplet), q (quartet), quint (pentet), m (multiplet), and br (broad). Coupling constants, *J*, are reported in Hertz.

Mass spectroscopy was performed by the Scripps Research Institute Mass Spectrometer Center. Electron impact (EI) was obtained using methane as the carrier gas. Analytical thin-layer chromatography was performed on Merck silica gel plates with QF-254 indicator. Visualization was accomplished with anisaldehyde or KMnO4.

High performance liquid chromatography (HPLC) was performed on Hatachi detectors (λ = 254 nm) using Daicel Chiralpak IC, OD-H, AD-H, and OJ-H columns. Retention times (*t*R) and peak areas for HPLC were obtained from reporting integrators. Oxindole starting materials were prepared according to published procedures.

General Procedure for *α*-Aminations of Aryl Oxindoles
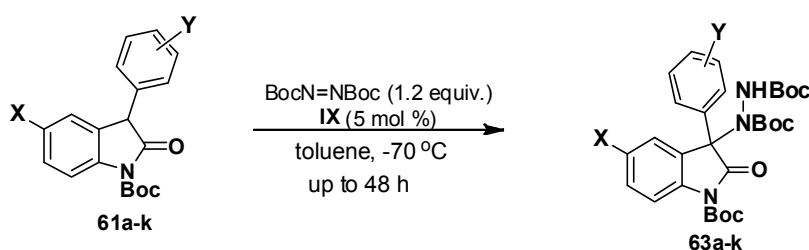
Di-tert-butyl azodicarboxylate (22 mg, 0.095 mmol, 1.2 equiv) was added to a solution of oxindole (27 mg, 0.079 mmol, 1 equiv.) and dimeric catalyst (2.9 mg, 0.05 equiv.) in toluene (0.8 mL) at -70 ^{0}C. The resulting solution was stirred at -70 ^{0}C for up to 48 h. The reaction mixture was then quenched with a saturated aqueous ammonium chloride solution. The aqueous layer was separated and extracted with ethylacetate (3x). The combined organic layers were dried over MgSO$_4$, filtered, and concentrated in vacuo. The crude material was purified by flash column chromatography (hexanes/ethyl acetate; 4:1) to afford the 3-aryl-3-amine-2-oxindole derivative.

Compound 63a: Di-*tert*-butyl1-(1-(*tert*-butoxycarbonyl)-2-oxo-3-phenylindolin-3-yl)hydrazine-1,2-dicarboxylate.
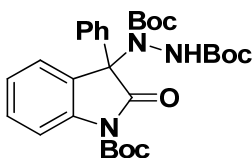
white solid, yield 93 %; ^{1}H NMR (500 MHz, CDCl$_3$) δ 8.25 (d, J = 7.3 Hz, 1H), 7.80 (d, J = 8.0 Hz, 1H), 7.58 – 7.51 (m, 2H), 7.38 – 7.32 (m, 1H), 7.32 – 7.21 (m, 4H), 6.32 (s, 1H), 1.60 (s, 9H), 1.29 (s, 9H), 1.19 (s, 9H); ^{13}C NMR (125 MHz, CDCl$_3$) δ 174.22, 154.90, 153.21, 149.23, 138.89, 133.07, 129.80, 128.92, 128.36, 126.59, 124.54, 114.89, 84.33, 83.19, 81.02, 72.61, 28.19, 28.10, 27.80.

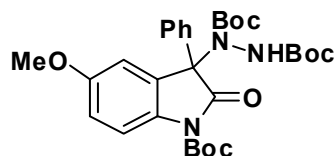HRMS (*m/z*): [M+H]$^+$ calcd for C$_{29}$H$_{37}$N$_3$O$_7^+$ 540.270, found 540.272. Enantiomeric excess: 98%, determined by HPLC (Chiralpak AD-H, hexane/*i*-PrOH = 90: 10, flow rate 1.00 mL/min, λ = 220 nm, rt): t_R (major) = 17.5 min, t_R (minor) = 12.2 min.

Compound 63b: Di-*tert*-butyl 1-(1-(*tert*-butoxycarbonyl)-5-methoxy-2-oxo-3-phenylindolin-3-yl)hydrazine-1,2-dicarboxylate.

white solid, yield 96%; ^{1}H NMR (500 MHz, CDCl$_3$) δ 7.92 (d, J = 2.4 Hz, 1H), 7.71 (d, J = 8.9 Hz, 1H), 7.54 (d, J = 3.7 Hz, 2H), 7.30-7.28 (m, 3H), 6.88 (dd, J = 8.9 and 2.7 Hz, 1H), 6.27 (s, 1H), 3.88 (s, 3H), 1.59 (s, 3H), 1.29 (s, 3H), 1.22 (s, 3H). ^{13}C NMR (125 MHz, CDCl$_3$) δ 174.12, 156.93, 154.78, 153.28, 149.29, 133.29, 132.32, 130.57, 129.68, 128.88, 128.36, 115.82, 114.12, 112.68, 84.12, 83.21, 80.96, 72.89, 55.86, 28.20, 28.08, 27.85. HRMS (*m/z*): [M+H]$^+$ calcd for C$_{30}$H$_{39}$N$_3$O$_8^+$ 570.281, found 570.2804. Enantiomeric excess: 96%, determined by HPLC (Chiralpak OD-H, hexane/*i*-PrOH = 99: 1, flow rate 1.00 mL/min, λ = 220 nm, rt): t_R (major) = 20.4 min, t_R (minor) = 13.0 min.

Compound 63c: Di-*tert*-butyl 1-(1-(*tert*-butoxycarbonyl)-2-oxo-3-(*p*-tolyl)indolin-3-yl)hydrazine-1,2-dicarboxylate.
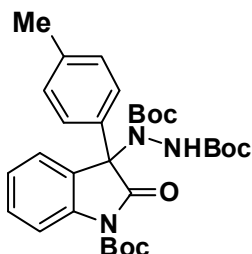
white solid, yield 71%; ^{1}H NMR (500 MHz, CDCl$_3$) δ 8.31 (d, J = 7.2 Hz, 1H), 7.86 (d, J = 7.9 Hz, 1H), 7.49 (d, J = 7.9 Hz, 1H), 7.43-7.36 (m, 2H), 7.18 (d, J = 8.1 Hz, 1H), 6.37 (s, 1H), 2.38 (s, 3H), 1.68 (s, 9H), 1.38 (s, 9H), 1.27 (s, 9H). ^{13}C NMR (125 MHz, CDCl$_3$) δ 174.2, 154.8, 153.1, 149.1, 138.8, 138.7, 129.9, 129.6, 129.5, 128.9, 128.7, 126.4, 124.4, 114.7, 84.1, 83.0, 80.8, 72.3, 28.1, 28.0, 27.7, 21.0. HRMS (*m/z*): [M+H]$^+$ calcd for C$_{30}$H$_{39}$N$_3$O$_7$$^+$ 554.2861, found 554.2862. Enantiomeric excess: 96%, determined by HPLC (Chiralpak AD-H, hexane/*i*-PrOH = 90: 10, flow rate 1.00 mL/min, λ = 220 nm, rt): t$_R$ (major) = 26.6 min, t$_R$ (minor) = 13.2 min.

Compound 63d: Di-*tert*-butyl 1-(1-(*tert*-butoxycarbonyl)-3-(3-methoxyphenyl)-2-oxoindolin-3-yl)hydrazine-1,2-dicarboxylate.
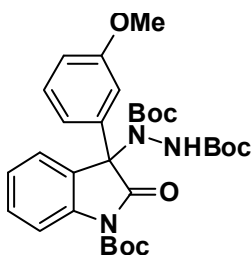

white solid, yield 95%; ^{1}H NMR (500 MHz, CDCl$_3$) δ 8.22 (d, J = 7.20 Hz, 1H), 7.78 (d, J = 8.0 Hz, 1H), 7.33 (t, J = 7.9 Hz, 1H), 7.29-7.24 (m, 1H), 7.21 (t, J = 7.9 Hz, 1H), 7.14-7.11 (m, 2H), 6.83 (d, J = 8.0 Hz, 1H), 6.30 (s, 1H),

3.74 (s, 3H), 1.60 (s, 9H), 1.32 (s, 9H), 1.19 (s, 9H). ^{13}C NMR (125 MHz, CDCl$_3$) δ 173.99, 159.45, 154.93, 153.12, 149.13, 138.79, 134.55, 129.22, 128.89, 126.38, 124.47, 121.96, 115.40, 114.80, 114.59, 84.25, 83.09, 80.96, 72.53, 60.41, 55.22, 28.12, 28.05, 27.74.. HRMS (*m/z*): [M+H]$^+$ calcd for C$_{30}$H$_{39}$N$_3$O$_8$$^+$ 570.281, found 570.2809. Enantiomeric excess: 97.4%, determined by HPLC (Chiralpak AD-H, hexane/*i*-PrOH = 97:3, flow rate 1.00 mL/min, λ = 220 nm, rt): t$_R$ (major) = 64.7 min, t$_R$ (minor) = 46.8 min.

Compound 63e: Di-tert-butyl 1-(1-(tert-butoxycarbonyl)-3-(4-(tert-butyl)phenyl)-2-oxoindolin-3-yl)hydrazine-1,2-dicarboxylate.
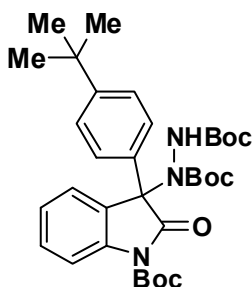
white solid, yield 76%; ^{1}H NMR (500 MHz, CDCl$_3$) δ 8.27 (d, *J* = 7.2 Hz, 1H), 7.77 (d, *J* = 7.8 Hz, 1H), 7.47 (d, *J* = 8.2 Hz, 2H), 7.34-7.28 (m, 4H), 6.27 (s, 3H), 1.60 (s, 9H), 1.27 (s, 9H), 1.26 (s, 9H), 1.17 (s, 9H). ^{13}C NMR (125 MHz, CDCl$_3$) δ 174.7, 155.1, 153.5, 152.3, 149.6, 139.1, 130.0, 129.9, 129.1, 126.8, 125.6, 124.7, 115.1, 84.6, 83.4, 81.1, 72.7, 34.9, 31.6, 28.5, 28.4, 28.1. HRMS (*m/z*): [M+H]$^+$ calcd for C$_{33}$H$_{45}$N$_3$O$_7$$^+$ 596.333, found 596.3321. Enantiomeric excess: 96%, determined by HPLC (Chiralpak AD-H, hexane/*i*-PrOH = 90: 10, flow rate 1.00 mL/min, λ = 220 nm, rt): t$_R$ (major) = 13.4 min, t$_R$ (minor) = 6.7 min.

Compound 63f: Di-tert-butyl 1-(1-(tert-butoxycarbonyl)-3-(4-fluorophenyl)-2-oxoindolin-3-yl)hydrazine-1,2-dicarboxylate.

colorless oil, yield 87%; ^{1}H NMR (500 MHz, CDCl$_3$) δ. 8.24 (d, J = 7.3 Hz, 1H), 7.80 (d, J = 8.0 Hz, 1H), 7.57 – 7.50 (m, 2H), 7.39 – 7.33 (m, 1H), 7.32 – 7.28 (m, 1H), 7.02 – 6.96 (m, 2H), 6.30 (s, 1H), 1.61 (s, 9H), 1.32 (s, 9H), 1.19 (s, 9H). ^{13}C NMR (100 MHz, CDCl$_3$) δ 174.24, 164.02, 162.04, 155.02, 153.13, 149.19, 138.91, 131.97, 131.91, 129.34, 129.16, 126.51, 124.72, 115.34, 115.17, 115.02, 84.56, 83.39, 81.29, 71.96, 28.22, 28.13, 27.83. HRMS (*m/z*): [M+H]$^+$ calcd for C$_{29}$H$_{36}$FN$_3$O$_7^+$ 558.271, found 558.271. Enantiomeric excess: 96%, determined by HPLC (Chiralpak AD-H, hexane/*i*-PrOH = 90: 10, flow rate 1.00 mL/min, λ = 220 nm, rt): t$_R$ (major) = 32.4 min, t$_R$ (minor) = 13.0 min.

Compound 63g: Di-*tert*-butyl 1-(1-(tert-butoxycarbonyl)-5-methoxy-2-oxo-3-(p-tolyl)indolin-3-yl)hydrazine-1,2-dicarboxylate.

white solid, yield 94%; ^{1}H NMR (500 MHz, CDCl$_3$) δ 7.90 (d, J = 2.0 Hz, 1H), 7.70 (d, J = 8.8 Hz, 1H), 7.40 (d, J = 7.8 Hz, 2H), 7.09 (d, J = 8.3 Hz,

2H), 6.86 (dd, *J* = 8.9 and 2.7 Hz, 1H), 6.26 (s, 1H), 3.87 (s, 3H9, 2.29 (s, 3H), 1.58 (s, 9H), 1.29 (s, 9H), 1.21 (s, 9H). ^{13}C NMR (100 MHz, CDCl$_3$) δ 174.25, 156.92, 154.84, 153.32, 149.35, 138.87, 132.29, 130.81, 130.25, 129.63, 129.11, 115.81, 114.03, 112.61, 84.07, 83.17, 80.94, 72.73, 55.89, 28.24, 28.13, 27.88, 21.15. HRMS (*m/z*): [M+H]$^+$ calcd for C$_{31}$H$_{41}$N$_3$O$_8$$^+$ 584.2966, found 584.2969. Enantiomeric excess: 98%, determined by HPLC (Chiralpak OD-H, hexane/*i*-PrOH = 99: 1, flow rate 1.00 mL/min, λ = 220 nm, rt): t$_R$ (major) = 11.9 min, t$_R$ (minor) = 8.7 min.
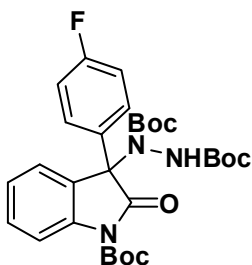
Compound 63h: Di-tert-butyl 1-(1-(tert-butoxycarbonyl)-5-methoxy-3-(3-methoxyphenyl)-2-oxoindolin-3-yl)hydrazine-1,2-dicarboxylate.
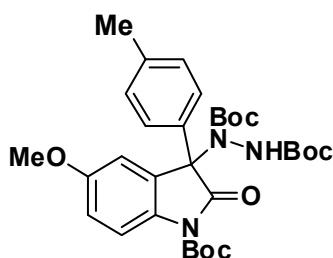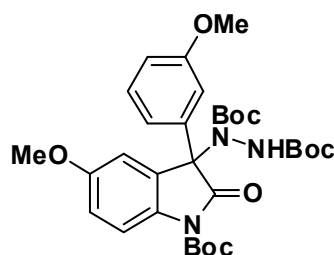

 white solid, yield 92%; ^{1}H NMR (500 MHz, CDCl$_3$) δ 7.89 (d, *J* = 2.4 Hz, 1H), 7.70 (d, *J* = 8.8 Hz, 1H), 7.23-7.19 (m, 1H), 7.12 (bs, 2H), 6.87 (dd, *J* = 8.9 and 2.7 Hz, 1H), 6.84 (d, *J* = 7.95 Hz, 1H), 6.28 (s, 1H), 3.87 (s, 3H), 3.75 (s, 3H), 1.59 (s, 9H), 1.31 (s, 9H), 1.22 (s, 9H). ^{13}C NMR (125 MHz, CDCl$_3$) δ 174.3, 159.8, 157.2, 155.2, 153.6, 149.5, 135.2, 132.6, 130.9, 129.6, 122.2, 116.1, 115.6, 114.9, 114.6, 112.7, 84.4, 83.5, 81.3, 73.2, 56.2, 55.6, 28.5, 28.4, 28.1. HRMS (*m/z*): [M+H]$^+$ calcd for C$_{31}$H$_{41}$N$_3$O$_9$$^+$ 600.2915, found 600.2909. Enantiomeric excess: 97%, determined by HPLC (Chiralpak OD-H, hexane/*i*-PrOH = 99:1, flow rate 1.00 mL/min, λ = 220 nm, rt): t$_R$ (major) = 18.1 min, t$_R$ (minor) = 10.7 min.

Compound 63i: Di-tert-butyl 1-(1-(tert-butoxycarbonyl)-3-(4-fluorophenyl)-5-methoxy-2-oxoindolin-3-yl)hydrazine-1,2-dicarboxylate.

colorless oil, yield 91%; ^{1}H NMR (500 MHz, CDCl$_3$) δ. 7.92 (d, *J* = 2.2 Hz, 1H), 7.73 (d, *J* = 8.9 Hz, 1H), 7.57 – 7.51 (m, 2H), 7.03 – 6.98 (m, 2H), 6.89 (dd, *J* = 8.9, 2.7 Hz, 1H), 6.29 (s, 1H), 3.88 (s, 3H), 1.60 (s, 9H), 1.31 (s, 9H), 1.22 (s, 9H). ^{13}C NMR (100 MHz, CDCl$_3$) δ 174.11, 171.19, 163.93, 162.02, 157.05, 154.88, 153.19, 149.24, 132.31, 131.85, 131.78, 115.96, 115.33, 115.16, 114.22, 112.66, 84.32, 83.37, 81.20, 72.23, 55.90, 28.22, 28.10, 27.87. HRMS (*m/z*): [M+H]$^+$ calcd for C$_{30}$H$_{38}$FN$_3$O$_8$$^+$ 588.2716, found 588.2711. Enantiomeric excess: 73%, determined by HPLC (Chiralpak AD-H, hexane/*i*-PrOH = 90: 10, flow rate 1.00 mL/min, λ = 220 nm, rt): t$_R$ (major) = 48.5 min, t$_R$ (minor) = 22.9 min
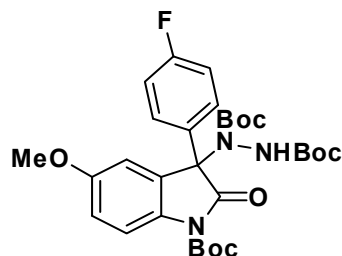
Compound 63j: Di-tert-butyl-1-(1-(tert-butoxycarbonyl)-3-(3-methoxyphenyl)-2-oxo-5-(trifluoromethoxy) indolin-3-yl)hydrazine-1,2-dicarboxylate.

colorless oil, yield 93%; ^{1}H NMR (500 MHz, CDCl$_3$) δ 8.26 (s, 1H), 7.85 (d, *J* = 8.9 Hz, 1H), 7.26 – 7.20 (m, 2H), 7.11 (d, *J* = 7.5 Hz, 1H), 7.04 (s, 1H), 6.87 (dd, *J* = 8.2, 2.5 Hz, 1H), 6.28 (s, 1H), 3.73 (s, 1H), 1.60 (s, 9H), 1.32 (s, 9H), 1.23 (s, 9H). ^{13}C NMR (100 MHz, CDCl$_3$) δ 173.54, 159.76, 154.98, 153.21, 149.12, 146.04, 137.52, 133.92, 129.62, 121.86, 121.83, 120.05, 116.06, 115.51, 114.96, 84.91, 83.59, 81.38, 72.57, 55.34, 28.28, 28.19, 27.93. HRMS (*m/z*): [M+H]$^+$ calcd for C$_{30}$H$_{38}$F$_3$N$_3$O$_9^+$ 654.2633, found 654.2633 . Enantiomeric excess: 93%, determined by HPLC (Chiralpak AD-H, hexane/*i*-PrOH = 98: 2, flow rate 1.00 mL/min, λ = 220 nm, rt): t$_R$ (major) = 50.7 min, t$_R$ (minor) = 38.9 min.

Compound 63k: Di-tert-butyl 1-(1-(tert-butoxycarbonyl)-5-fluoro-3-(3-methoxyphenyl)-2-oxoindolin-3-yl) hydrazine-1,2-dicarboxylate.
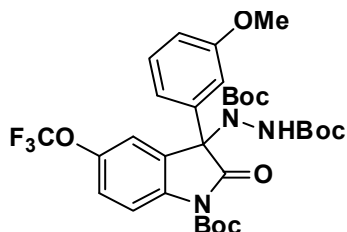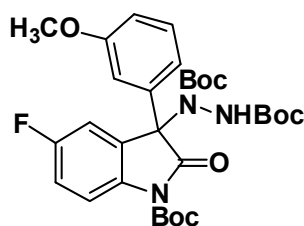

colorless oil, yield 87%; ^{1}H NMR (500 MHz, CDCl$_3$) δ 8.07 (d, *J* = 5.8 Hz, 1H), 7.78 (dd, *J* = 8.9, 4.5 Hz, 1H), 7.25-7.21 (m, 1H), 7.12-7.08 (m, 2H), 7.06-7.02 (m, 1H), 6.86 (dd, *J* = 8.2, 2.4 Hz, 1H), 3.76 (s, 3H), 1.60 (s, 9H), 1.32 (s, 9H), 1.24 (s, 9H) . ^{13}C NMR (100 MHz, CDCl$_3$) δ 173.68, 160.98, 159.64, 159.05, 154.98, 153.13, 149.16, 134.90, 134.11, 129.45, 121.96, 116.20, 115.42, 114.78, 114.25, 114.04, 84.57, 83.49, 81.29, 77.41, 77.16, 76.91, 72.58, 55.40, 28.22, 28.13, 27.90. HRMS (*m/z*): [M+H]$^+$ calcd for C$_{30}$H$_{38}$FN$_3$O$_8^+$ 588.2716, found 588.2707 . Enantiomeric excess: 87%, determined by HPLC (Chiralpak OD-H, hexane/*i*-PrOH = 99: 1, flow rate 1.00 mL/min, λ = 220 nm, rt): t$_R$ (major) = 10.2 min, t$_R$ (minor) = 7.4 min.

Compound IX[3]: **(1S)-(6-(3-((4-((S)-hydroxy((2S,4R,8S)-8-vinylquinuclidin -2-yl)methyl)quinolin-6-yloxy)methyl)benzyloxy)quinolin-4-yl)(8-vinyl quinuclidin-2-yl)methanol**
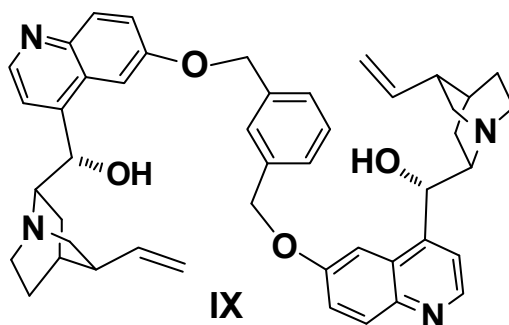
^{1}H NMR (500 MHz, CDCl$_3$): δ 8.61 (d, *J* = 4.5, 1H), 7.96 (d, *J* = 9.2, 1H), 7.50 (s, 1H), 7.48 (d, *J* = 4.5, 1H), 7.38 (dd, *J* = 9.2, 2.6, 1H), 7.31 (s, 2H), 7.48 (d, *J* = 2.5, 1H), 6.02-5.95 (m, 1H), 5.45 (d, *J* = 3.9, 1H), 5.27 (d, *J* = 13.0, 1H), 5.15 (d, *J* = 13.0, 1H). 5.02 (br, 1H), 4.99 (d, *J* = 4.3, 1H). 3.24-3.20 (m, 1H), 2.91-2.87 (m, 1H), 2.67-2.62 (m, 1H), 2.53 (t, *J* = 10.6, 1H), 2.39-2.35 (m, 1H), 2.11 (q, *J* = 6.3, 1H), 1.92 (t, *J* = 10.9, 1H), 1.66 (br, 1H), 1.38-1.33 (m, 2H), 1.07-1.02 (m, 1H). ^{13}C NMR (125 MHz, CDCl$_3$): δ 156.45, 147.92, 147.77, 144.10, 140.52, 137.30, 131.59, 128.88, 126.56, 126.43, 126.06, 121.79, 118.56, 114.53, 103.05, 71.42, 69.90, 59.58, 49.77, 49.36, 39.85, 28.05, 26.17, 21.37. HRMS: calcd for C$_{46}$H$_{50}$N$_4$O$_4$ (MH$^+$) 723.3905, found 723.3901.

Compound XI: (S)-(6-(3-((quinolin-6-yloxy)methyl)benzyloxy)quinolin-4-yl)((2R,4S,8R)-8-vinylquinuclidin-2-yl)methanol.
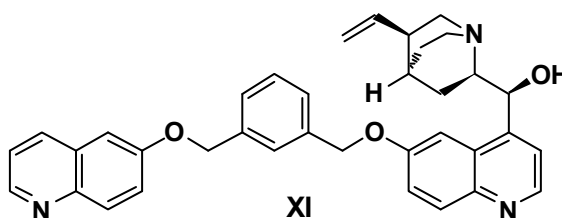
white solid, ^{1}H NMR (500 MHz, CDCl$_3$) δ 8.73 (dd, *J* = 4.3, 1.6 Hz, 1H), 8.54 (d, *J* = 4.5 Hz, 1H), 8.02 – 7.94 (m, 2H), 7.76 (d, *J* = 9.2 Hz, 1H), 7.60 – 7.58 (m, 2H), 7.47 – 7.40 (m, 4H), 7.31 – 7.27 (m, 2H), 7.15 – 7.12 (m, 2H), 6.98 (d, *J* = 2.4 Hz, 1H), 6.42 (s, 1H), 6.02 (ddd, *J* = 17.5, 10.0, 7.5 Hz, 1H), 5.24 – 5.13 (m, 4H), 5.08 (d, *J* = 13.3 Hz, 1H), 4.90 (d, *J* = 13.3 Hz, 1H), 4.30 – 4.25 (m, 1H), 3.26 – 3.20 (m, 1H), 3.10 – 3.05 (m, 1H), 3.03 – 2.82 (m, 2H), 2.47 – 2.41 (m, 1H), 2.33 – 2.25 (m, 1H), 1.76 – 1.64 (m, 1H), 1.47 – 1.38 (m, 1H), 0.91 – 0.82 (m, 2H); ^{13}C NMR (100 MHz, CDCl$_3$) δ 157.15, 148.44, 147.68, 144.80, 144.26, 138.00, 137.28, 136.98, 135.35, 131.93, 131.27, 129.67, 129.11, 127.21, 126.96, 126.57, 125.72, 123.09, 122.82, 121.81, 118.97, 117.76, 107.03, 101.20, 70.67, 70.12, 60.82, 60.42, 49.66, 48.98, 38.29, 28.01, 24.10, 21.46, 18.49, 14.61; HRMS (*m/z*): [M+H]$^+$ calcd for C$_{36}$H$_{35}$N$_3$O$_3$$^+$ 558.275 found 558.276**.**

Compound XII: (S)-(6-(3-(phenoxymethyl)benzyloxy)quinolin-4-yl)((2R,4S,8R)-8-vinyl quinuclidin-2-yl) methanol.
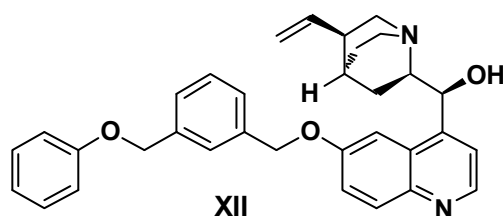
yellow solid, ^{1}H NMR (500 MHz, CDCl$_3$) δ 8.53 (d, *J* = 4.5 Hz, 1H), 7.98 (s, 1H), 7.74 (d, *J* = 9.2 Hz, 1H), 7.59 (d, *J* = 4.4 Hz, 1H), 7.54 (s, 1H), 7.47 – 7.41 (m, 1H), 7.39 – 7.33 (m, 2H), 7.31 – 7.22 (m, 2H), 7.11 (dd, *J* = 9.2, 2.3 Hz, 1H), 7.02 – 6.89 (m, 4H), 6.44 (s, 1H), 6.04 (ddd, *J* = 17.5, 10.0, 7.5 Hz, 1H), 5.25 – 5.16 (m, 2H), 5.15 – 5.03 (m, 3H), 4.90 (d, *J* = 13.2 Hz, 1H), 4.35 – 4.23 (m, 1H), 3.33 – 3.19 (m, 1H), 3.15 – 3.05 (m, 1H), 3.03 – 2.89 (m,1H), 2.53 – 2.41 (m, 1H), 2.37 – 2.27 (m, 1H), 1.92 – 1.82 (m, 1H), 1.78 – 1.66 (m, 1H), 1.55 – 1.41 (m, 1H), 0.95 – 0.81 (m, 2H); ^{13}C NMR (100 MHz, CDCl$_3$) δ

161.83, 158.00, 155.97, 146.42, 144.00, 142.97, 136.69, 136.34, 136.14, 130.63, 128.71, 127.79, 125.86, 125.76, 125.37, 121.66, 120.15, 117.80, 116.57, 114.11, 100.05, 69.13, 69.02, 66.19, 59.26, 48.48, 47.79, 37.08, 35.71, 30.66, 26.86, 22.88, 17.25; HRMS (*m/z*): [M+H]$^+$ calcd for $C_{33}H_{34}N_2O_3^+$ 507.2642 found 507.2638

III. Synthetic route to 3-amino aryl oxindoles (compound 3l)[4]
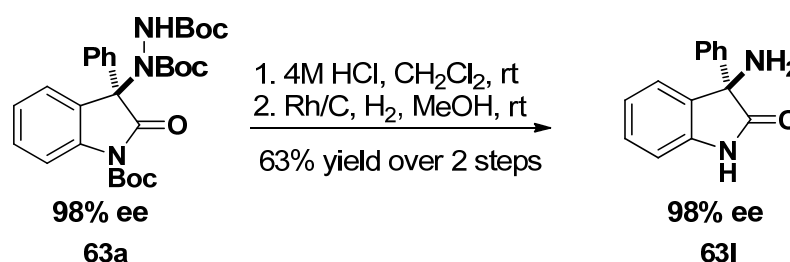
Compound 3l: To a 4 M HCl solution in 1,4-dioxane (1.5 mL) at room temperature was added compound **3a** (100 mg, 0.18 mmol). The reaction mixture was stirred for 2 h at room temperature. The reaction mixture was evaporated to give the crude material, which was used for the next step without purification. To a round bottom flask with this crude material was added MeOH (1.5 mL) and Rh/C (50 mg). The reaction was stirred for 12 h at rt under H_2 (1 atm), then was filtered through a filter paper and washed with MeOH. The filtrate was concentrated under reduced pressure to give a pale yellow solid. The residue was purified by silica gel flash column chromatography (30% DCM in AcOEt) to afford **3l** (25.5 mg, 0.11 mmol, 63% yield) as a colorless oil. ^{1}H NMR (500 MHz, CDCl$_3$) δ 7.93 (brs, 1H), 7.49 – 7.44 (m, 2H), 7.36 – 7.30 (m, 2H), 7.29 – 7.27 (m, 1H), 7.26 – 7.24 (m, 2H), 7.07 – 7.02 (m, 1H), 6.94 (d, *J* = 7.4 Hz, 1H), 2.16 (brs, 2H). ^{13}C NMR (100 MHz, CDCl$_3$) δ 182.16, 141.10, 140.44, 129.55, 129.04, 128.31, 126.06,

125.54, 123.72, 110.55, 64.66. HRMS (*m/z*): [M+H]$^+$ calcd for $C_{14}H_{12}N_2ONa^+$ 247.0842, found 247.0841. Enantiomeric excess: 98%, determined by HPLC (Chiralpak AD-H, hexane/*i*-PrOH = 90: 10, flow rate 1.00 mL/min, λ = 220 nm, rt): t_R (major) = 18.2 min, t_R (minor) = 25.6 min.

IV. Determination of the absolute configuration[5]:

Diethyl 1-(1-(tert-butoxycarbonyl)-2-oxo-3-phenylindolin-3-yl)hydrazine-1,2-dicarboxylate

Compound 3m: Diethyldiazocarboxylate (15 µL, 0.096 mmol, 1.2 equiv) was added to a solution of oxindole **61a** (25 mg, 0.08 mmol, 1 equiv.) and catalyst **IX** (2.9 mg, 0.05 equiv.) in toluene (0.8 mL) at -70 ^{0}C. The resulting solution was stirred at -70 ^{0}C for 24 h. The reaction mixture was then quenched with a saturated aqueous ammonium chloride solution. The aqueous layer was separated and extracted with ethylacetate (3x). The combined organic layers were dried over MgSO$_4$, filtered, and concentrated in vacuo. The crude material was purified by flash column chromatography (hexanes/ethyl acetate; 4:1) to afford compound **63m** in 88% yield; ^{1}H NMR (500 MHz, CDCl$_3$) δ 8.16 (d, *J* = 7.4 Hz, 1H), 7.83 (d, *J* = 8.1 Hz, 1H), 7.54 (bs, 2H), 7.36 (t, *J* = 7.8 Hz, 1H), 7.34-7.30 (m, 4H), 6.63 (s, 1H), 4.04-3.99 (m, 4H), 1.59 (s, 9H), 1.09 (t, *J* = 7.0 Hz, 3H), 1.04 (t, *J* = 7.0 Hz, 3H). ^{13}C NMR (125 MHz, CDCl$_3$) δ 174.08, 156.2, 154.8, 149.4, 139.5, 132.9, 130.1, 129.6, 129.5, 128.8, 128.6, 128.5, 126.9, 124.8, 115.3, 84.7, 73.0, 63.5, 62.4,

28.5, 14.7, 14.3. Enantiomeric excess: 80%, determined by HPLC (Chiralpak AD-H, hexane/*i*-PrOH = 90: 10, flow rate 1.00 mL/min, λ = 220 nm, rt): t_R (major) = 29.2 min, t_R (minor) = 14.2 min.

Compound 63n: Dichloromethane (75 µL) and TFA (75 µL) were added to the flask containing compound **63m** (30 mg, 0.062 mmol). The resulting mixture was stirring for 1 h at room temperature. The reaction mixture was then quenched with a saturated aqueous $NaHCO_3$ solution. The aqueous layer was separated and extracted with dichloromethane (3x). The combined organic layers were dried over $MgSO_4$, filtered, and concentrated in vacuo. The crude material was purified by flash column chromatography (hexanes/ethyl acetate; 1:1) to afford compound **63n** in 84% yield (20 mg). H NMR (500 MHz, $CDCl_3$) δ8.06 (d, J = 7.4 Hz, 1H), 7.63-7.61 (m, 2H), 7.30 (s, 4H), 7.14 (t, J = 7.4 Hz, 1H), 6.82 (d, J = 7.7 Hz, 1H), 6.67 (bs, 1H), 4.06-4.00 (m, 4H), 1.69 (bs, 1H), 1.10 (t, J = 7.0 Hz, 3H), 1.05-1.04 (m, 3H); HRMS (*m/z*): [M+H]$^+$ calcd for $C_{20}H_{21}N_3O_5^+$ 384.2078, found 384.1558. $[\alpha]_D^{20}$ = -101.3 (*c* = 0.92; $CHCl_3$, 80% *ee*). Literature value -99.27 (*c* = 0.55 in $CHCl_3$, 93% *ee*).

ACKNOWLEDGMENTS

Foremost, I would like to express my sincere gratitude to my tutor Prof. Gianluca Sbardella for the continuous support of my Ph.D study and research, for his patience, motivation, enthusiasm, and knowledge. His guidance helped me in all the time of research and writing of this thesis.

A really special thanks goes to Prof. Sabrina Castellano, she provided encouragement, sound advice (a lot), good teaching, good company, and thousands of good ideas.

I would like to show my gratitude to Prof. Carlos Barbas, III of the SCRIPPS research institute for hosting me in his research lab and for all the helpful discussion. Special thanks goes to Tommy Bui, Masanobu Nagano, Nuno Candeias and all the other postdoc of the Barbas lab.

Last but not least, I thank my fellow labmates Monica Viviano, Marisabella Santoriello and all the other EMCL lab former members for the stimulating discussions, for all the time we were working together and for all the fun we have had in the last three years.

REFERENCES

1. Bird, A., Perceptions of epigenetics. *Nature* **2007,** *447* (7143), 396-398.

2. Luger, K.; Mader, A. W.; Richmond, R. K.; Sargent, D. F.; Richmond, T. J., Crystal structure of the nucleosome core particle at 2.8[thinsp]A resolution. *Nature* **1997,** *389* (6648), 251-260.

3. (a) Margueron, R.; Trojer, P.; Reinberg, D., The key to development: interpreting the histone code? *Current Opinion in Genetics & Development* **2005,** *15* (2), 163-176; (b) Nightingale, K. P.; O'Neill, L. P.; Turner, B. M., Histone modifications: signalling receptors and potential elements of a heritable epigenetic code. *Current Opinion in Genetics & Development* **2006,** *16* (2), 125-136.

4. Hazzalin, C. A.; Mahadevan, L. C., Dynamic Acetylation of All Lysine 4–Methylated Histone H3 in the Mouse Nucleus: Analysis at *c-fos* and *c-jun>. PLoS Biol* **2005,** *3* (12), e393.

5. Kouzarides, T., Chromatin Modifications and Their Function. *Cell* **2007,** *128* (4), 693-705.

6. Fischle, W.; Tseng, B. S.; Dormann, H. L.; Ueberheide, B. M.; Garcia, B. A.; Shabanowitz, J.; Hunt, D. F.; Funabiki, H.; Allis, C. D., Regulation of HP1-chromatin binding by histone H3 methylation and phosphorylation. *Nature* **2005,** *438* (7071), 1116-1122.

7. Nelson, C. J.; Santos-Rosa, H.; Kouzarides, T., Proline Isomerization of Histone H3 Regulates Lysine Methylation and Gene Expression. *Cell* **2006,** *126* (5), 905-916.

8. Clements, A.; Poux, A. N.; Lo, W.-S.; Pillus, L.; Berger, S. L.; Marmorstein, R., Structural Basis for Histone and Phosphohistone Binding by the GCN5 Histone Acetyltransferase. *Molecular cell* **2003,** *12* (2), 461-473.

9. Zhang, Y.; Reinberg, D., Transcription regulation by histone methylation: interplay between different covalent modifications of the core histone tails. *Genes & Development* **2001,** *15* (18), 2343-2360.

10. Lee, D. Y.; Teyssier, C.; Strahl, B. D.; Stallcup, M. R., Role of Protein Methylation in Regulation of Transcription. *Endocr Rev* **2005,** *26* (2), 147-170.

11. (a) Bedford, M. T., Arginine methylation at a glance. *J Cell Sci* **2007,** *120* (24), 4243-4246; (b) Bedford, M. T.; Clarke, S. G., Protein Arginine Methylation in Mammals: Who, What, and Why. *Mol. Cell* **2009,** *33* (1), 1-13; (c) Lake, A. N.; Bedford, M. T., Protein methylation and DNA repair. *Mutation Research/Fundamental and Molecular Mechanisms of Mutagenesis* **2007,** *618* (1-2), 91-101; (d) Smith, B. C.; Denu, J. M., Chemical mechanisms of histone lysine and arginine modifications. *Biochimica et Biophysica Acta (BBA) - Gene Regulatory Mechanisms* **2009,** *1789* (1), 45-57.

12. Bedford, M. T.; Richard, S., Arginine Methylation: An Emerging Regulatorof Protein Function. *Molecular cell* **2005,** *18* (3), 263-272.

13.   (a) Bachand, F., Protein Arginine Methyltransferases: from Unicellular Eukaryotes to Humans. *Eukaryotic Cell* **2007,** *6* (6), 889-898; (b) Pahlich, S.; Zakaryan, R. P.; Gehring, H., Protein arginine methylation: Cellular functions and methods of analysis. *Biochim. Biophys. Acta, Proteins Proteomics* **2006,** *1764* (12), 1890-1903.

14.   Zobel-Thropp, P.; Gary, J. D.; Clarke, S., δ-N-Methylarginine Is a Novel Posttranslational Modification of Arginine Residues in Yeast Proteins. *Journal of Biological Chemistry* **1998,** *273* (45), 29283-29286.

15.   (a) Trojer, P.; Dangl, M.; Bauer, I.; Graessle, S.; Loidl, P.; Brosch, G., Histone Methyltransferases in Aspergillus nidulans: Evidence for a Novel Enzyme with a Unique Substrate Specificity†. *Biochemistry* **2004,** *43* (33), 10834-10843; (b) Krause, C. D.; Yang, Z.-H.; Kim, Y.-S.; Lee, J.-H.; Cook, J. R.; Pestka, S., Protein arginine methyltransferases: Evolution and assessment of their pharmacological and therapeutic potential. *Pharmacol. Ther.* **2007,** *113* (1), 50-87.

16.   Chang, B.; Chen, Y.; Zhao, Y.; Bruick, R. K., JMJD6 Is a Histone Arginine Demethylase. *Science* **2007,** *318* (5849), 444-447.

17.   Lin, W.-J.; Gary, J. D.; Yang, M. C.; Clarke, S.; Herschman, H. R., The Mammalian Immediate-early TIS21 Protein and the Leukemia-associated BTG1 Protein Interact with a Protein-arginine N-Methyltransferase. *Journal of Biological Chemistry* **1996,** *271* (25), 15034-15044.

18.   Tang, J.; Frankel, A.; Cook, R. J.; Kim, S.; Paik, W. K.; Williams, K. R.; Clarke, S.; Herschman, H. R., PRMT1 Is the Predominant Type I Protein Arginine Methyltransferase in Mammalian Cells. *Journal of Biological Chemistry* **2000,** *275* (11), 7723-7730.

19.   Kwak, Y. T.; Guo, J.; Prajapati, S.; Park, K.-J.; Surabhi, R. M.; Miller, B.; Gehrig, P.; Gaynor, R. B., Methylation of SPT5 Regulates Its Interaction with RNA Polymerase II and Transcriptional Elongation Properties. *Molecular cell* **2003,** *11* (4), 1055-1066.

20.   (a) Boisvert, F.-M.; Déry, U.; Masson, J.-Y.; Richard, S., Arginine methylation of MRE11 by PRMT1 is required for DNA damage checkpoint control. *Genes & Development* **2005,** *19* (6), 671-676; (b) Smith, J. J.; Rücknagel, K. P.; Schierhorn, A.; Tang, J.; Nemeth, A.; Linder, M.; Herschman, H. R.; Wahle, E., Unusual Sites of Arginine Methylation in Poly(A)-binding Protein II and in Vitro Methylation by Protein Arginine Methyltransferases PRMT1 and PRMT3. *Journal of Biological Chemistry* **1999,** *274* (19), 13229-13234.

21.   Bedford, M. T.; Frankel, A.; Yaffe, M. B.; Clarke, S.; Leder, P.; Richard, S., Arginine Methylation Inhibits the Binding of Proline-rich Ligands to Src Homology 3, but Not WW, Domains. *Journal of Biological Chemistry* **2000,** *275* (21), 16030-16036.

22.   Tang, J.; Gary, J. D.; Clarke, S.; Herschman, H. R., PRMT 3, a Type I Protein Arginine N-Methyltransferase That Differs from PRMT1 in Its Oligomerization, Subcellular Localization, Substrate Specificity, and Regulation. *Journal of Biological Chemistry* **1998,** *273* (27), 16935-16945.

23.   Singh, V.; Miranda, T. B.; Jiang, W.; Frankel, A.; Roemer, M. E.; Robb, V. A.; Gutmann, D. H.; Herschman, H. R.; Clarke, S.; Newsham, I. F., DAL-1//4.1B tumor suppressor interacts with protein arginine N-methyltransferase 3 (PRMT3) and

inhibits its ability to methylate substrates in vitro and in vivo. *Oncogene* **2004,** *23* (47), 7761-7771.

24.   Chen, D.; Ma, H.; Hong, H.; Koh, S. S.; Huang, S.-M.; Schurter, B. T.; Aswad, D. W.; Stallcup, M. R., Regulation of Transcription by a Protein Methyltransferase. *Science* **1999,** *284* (5423), 2174-2177.

25.   Chen, D.; Huang, S.-M.; Stallcup, M. R., Synergistic, p160 Coactivator-dependent Enhancement of Estrogen Receptor Function by CARM1 and p300. *Journal of Biological Chemistry* **2000,** *275* (52), 40810-40816.

26.   Feng, Q.; Yi, P.; Wong, J.; O'Malley, B. W., Signaling within a Coactivator Complex: Methylation of SRC-3/AIB1 Is a Molecular Switch for Complex Disassembly. *Mol. Cell. Biol.* **2006,** *26* (21), 7846-7857.

27.   Chen, S. L.; Loffler, K. A.; Chen, D.; Stallcup, M. R.; Muscat, G. E. O., The Coactivator-associated Arginine Methyltransferase Is Necessary for Muscle Differentiation. *Journal of Biological Chemistry* **2002,** *277* (6), 4324-4333.

28.   Yadav, N.; Lee, J.; Kim, J.; Shen, J.; Hu, M. C.-T.; Aldaz, C. M.; Bedford, M. T., Specific protein methylation defects and gene expression perturbations in coactivator-associated arginine methyltransferase 1-deficient mice. *Proceedings of the National Academy of Sciences of the United States of America* **2003,** *100* (11), 6464-6468.

29.   Yadav, N.; Cheng, D.; Richard, S.; Morel, M.; Iyer, V. R.; Aldaz, C. M.; Bedford, M. T., CARM1 promotes adipocyte differentiation by coactivating PPAR[gamma]. *EMBO Rep* **2008,** *9* (2), 193-198.

30.   Hassa, P. O.; Covic, M.; Bedford, M. T.; Hottiger, M. O., Protein Arginine Methyltransferase 1 Coactivates NF-[kappa]B-Dependent Gene Expression Synergistically with CARM1 and PARP1. *Journal of Molecular Biology* **2008,** *377* (3), 668-678.

31.   Pollack, B. P.; Kotenko, S. V.; He, W.; Izotova, L. S.; Barnoski, B. L.; Pestka, S., The Human Homologue of the Yeast Proteins Skb1 and Hsl7p Interacts with Jak Kinases and Contains Protein Methyltransferase Activity. *Journal of Biological Chemistry* **1999,** *274* (44), 31531-31542.

32.   Jansson, M.; Durant, S. T.; Cho, E.-C.; Sheahan, S.; Edelmann, M.; Kessler, B.; La Thangue, N. B., Arginine methylation regulates the p53 response. *Nat. Cell Biol.* **2008,** *10* (12), 1431-1439.

33.   Boulanger, M.-C.; Liang, C.; Russell, R. S.; Lin, R.; Bedford, M. T.; Wainberg, M. A.; Richard, S., Methylation of Tat by PRMT6 Regulates Human Immunodeficiency Virus Type 1 Gene Expression. *J. Virol.* **2005,** *79* (1), 124-131.

34.   Lee, J.; Sayegh, J.; Daniel, J.; Clarke, S.; Bedford, M. T., PRMT8, a New Membrane-bound Tissue-specific Member of the Protein Arginine Methyltransferase Family. *Journal of Biological Chemistry* **2005,** *280* (38), 32890-32896.

35.   Wolf, S., The protein arginine methyltransferase family: an update about function, new perspectives and the physiological role in humans. *Cellular and Molecular Life Sciences* **2009,** *66* (13), 2109-2121.

36.   (a) Zhang, X.; Zhou, L.; Cheng, X., Crystal structure of the conserved core of protein arginine methyltransferase PRMT3. *EMBO J.* **2000,** *19* (14), 3509-3519; (b)

Troffer-Charlier, N.; Cura, V.; Hassenboehler, P.; Moras, D.; Cavarelli, J., Expression, purification, crystallization and preliminary crystallographic study of isolated modules of the mouse coactivator-associated arginine methyltransferase 1. *Acta Crystallogr Sect F Struct Biol Cryst Commun* **2007,** *63* (Pt 4), 330-3.

37.   Cheng, D.; Yadav, N.; King, R. W.; Swanson, M. S.; Weinstein, E. J.; Bedford, M. T., Small molecule regulators of protein arginine methyltransferases. *J. Biol. Chem.* **2004,** *279* (23), 23892-23899.

38.   Spannhoff, A.; Heinke, R.; Bauer, I.; Trojer, P.; Metzger, E.; Gust, R.; Schule, R.; Brosch, G.; Sippl, W.; Jung, M., Target-Based Approach to Inhibitors of Histone Arginine Methyltransferases. *J. Med. Chem.* **2007,** *50* (10), 2319-2325.

39.   Spannhoff, A.; Machmur, R.; Heinke, R.; Trojer, P.; Bauer, I.; Brosch, G.; Schüle, R.; Hanefeld, W.; Sippl, W.; Jung, M., A novel arginine methyltransferase inhibitor with cellular activity. *Bioorg. Med. Chem. Lett.* **2007,** *17* (15), 4150-4153.

40.   Heinke, R.; Spannhoff, A.; Meier, R.; Trojer, P.; Bauer, I.; Jung, M.; Sippl, W., Virtual Screening and Biological Characterization of Novel Histone Arginine Methyltransferase PRMT1 Inhibitors. *ChemMedChem* **2009,** *4* (1), 69-77.

41.   Selvi, B. R.; Batta, K.; Kishore, A. H.; Mantelingu, K.; Varier, R. A.; Balasubramanyam, K.; Pradhan, S. K.; Dasgupta, D.; Sriram, S.; Agrawal, S.; Kundu, T. K., Identification of a Novel Inhibitor of Coactivator-associated Arginine Methyltransferase 1 (CARM1)-mediated Methylation of Histone H3 Arg-17. *J. Biol. Chem.* **2010,** *285* (10), 7143-7152.

42.   Feng, Y.; Li, M.; Wang, B.; Zheng, Y. G., Discovery and Mechanistic Study of a Class of Protein Arginine Methylation Inhibitors. *J. Med. Chem.* **2010,** *53* (16), 6028-6039.

43.   Purandare, A. V.; Chen, Z.; Huynh, T.; Pang, S.; Geng, J.; Vaccaro, W.; Poss, M. A.; Oconnell, J.; Nowak, K.; Jayaraman, L., Pyrazole inhibitors of coactivator associated arginine methyltransferase 1 (CARM1). *Bioorg. Med. Chem. Lett.* **2008,** *18* (15), 4438-4441.

44.   Wan, H.; Huynh, T.; Pang, S.; Geng, J.; Vaccaro, W.; Poss, M. A.; Trainor, G. L.; Lorenzi, M. V.; Gottardis, M.; Jayaraman, L.; Purandare, A. V., Benzo[d]imidazole inhibitors of Coactivator Associated Arginine Methyltransferase 1 (CARM1)--Hit to Lead studies. *Bioorg. Med. Chem. Lett.* **2009,** *19* (17), 5063-5066.

45.   Dowden, J.; Hong, W.; Parry, R. V.; Pike, R. A.; Ward, S. G., Toward the development of potent and selective bisubstrate inhibitors of protein arginine methyltransferases. *Bioorg. Med. Chem. Lett.* **2010,** *20* (7), 2103-2105.

46.   (a) Sbardella, G.; Castellano, S.; Vicidomini, C.; Rotili, D.; Nebbioso, A.; Miceli, M.; Altucci, L.; Mai, A., Identification of long chain alkylidenemalonates as novel small molecule modulators of histone acetyltransferases. *Bioorg. Med. Chem. Lett.* **2008,** *18* (9), 2788-2792; (b) Mai, A.; Cheng, D.; Bedford, M. T.; Valente, S.; Nebbioso, A.; Perrone, A.; Brosch, G.; Sbardella, G.; De Bellis, F.; Miceli, M.; Altucci, L., Epigenetic Multiple Ligands: Mixed Histone/Protein Methyltransferase, Acetyltransferase, and Class III Deacetylase (Sirtuin) Inhibitors. *J. Med. Chem.* **2008,** *51* (7), 2279-2290; (c) Castellano, S.; Kuck, D.; Sala, M.; Novellino, E.; Lyko, F.; Sbardella, G., Constrained Analogues of Procaine as Novel Small Molecule Inhibitors

of DNA Methyltransferase-1. *J. Med. Chem.* **2008,** *51* (7), 2321-2325; (d) Mai, A.; Rotili, D.; Tarantino, D.; Ornaghi, P.; Tosi, F.; Vicidomini, C.; Sbardella, G.; Nebbioso, A.; Miceli, M.; Altucci, L.; Filetici, P., Small-Molecule Inhibitors of Histone Acetyltransferase Activity: Identification and Biological Properties. *J. Med. Chem.* **2006,** *49* (23), 6897-6907.

47.   Ragno, R.; Simeoni, S.; Castellano, S.; Vicidomini, C.; Mai, A.; Caroli, A.; Tramontano, A.; Bonaccini, C.; Trojer, P.; Bauer, I.; Brosch, G.; Sbardella, G., Small Molecule Inhibitors of Histone Arginine Methyltransferases: Homology Modeling, Molecular Docking, Binding Mode Analysis, and Biological Evaluations. *J. Med. Chem.* **2007,** *50* (6), 1241-1253.

48.   (a) Zhang, Y.-L.; Keng, Y.-F.; Zhao, Y.; Wu, L.; Zhang, Z.-Y., Suramin Is an Active Site-directed, Reversible, and Tight-binding Inhibitor of Protein-tyrosine Phosphatases. *J. Biol. Chem.* **1998,** *273* (20), 12281-12287; (b) McGeary, R. P.; Bennett, A. J.; Tran, Q. B.; Cosgrove, K. L.; Ross, B. P., Suramin: clinical uses and structure-activity relationships. *Mini-Rev. Med. Chem.* **2008,** *8* (13), 1384-1394; (c) Chen, F.; Fulton, D. J. R., An Inhibitor of Protein Arginine Methyltransferases, 7,7 - Carbonylbis(azanediyl)bis(4-hydroxynaphthalene-2-sulfonic acid (AMI-1), Is a Potent Scavenger of NADPH-Oxidase–Derived Superoxide. *Mol. Pharmacol.* **2010,** *77* (2), 280-287.

49.   Beech, W. F.; Legg, N., 198. Aminohydroxynaphthoic acids. Part II. Attempted synthesis of 7-amino-4-hydroxy-2-naphthoic acid ("carboxy j-acid") from 3-amino-2-naphthoic acid. *Journal of the Chemical Society (Resumed)* **1950**, 961-966.

50.   Doulut, S.; Dubuc, I.; Rodriguez, M.; Vecchini, F.; Fulcrand, H.; Barelli, H.; Checler, F.; Bourdel, E.; Aumelas, A., Synthesis and analgesic effects of N-[3-[(hydroxyamino)carbonyl]-1-oxo-2(R)-benzylpropyl]-L-isoleucyl-L-leucine, a new potent inhibitor of multiple neurotensin/neuromedin N degrading enzymes. *J. Med. Chem.* **1993,** *36* (10), 1369-1379.

51.   Serra, S.; Fuganti, C., A New Preparative Route to Substituted Dibenzofurans by Benzannulation Reaction. An Application to the Synthesis of Cannabifuran. *Synlett* **2003,** *2003* (13), 2005-2008.

52.   Awad, W. I.; Kandile, N. G.; Wassef, W. N.; Mohamed, M. I., Synthesis of Some Itaconates via Wittig reaction. *J. Prakt .Chem.* **1989,** *331* (3), 405-410.

53.   Castellano, S.; Milite, C.; Campiglia, P.; Sbardella, G., Highly efficient synthesis and chemical separation of 5-amino- and 7-amino-4-hydroxy-2-naphthoic acids. *Tetrahedron Lett.* **2007,** *48* (27), 4653-4655.

54.   Narayana, B.; Ashalatha, B. V.; Vijaya Raj, K. K.; Fernandes, J.; Sarojini, B. K., Synthesis of some new biologically active 1,3,4-oxadiazolyl nitroindoles and a modified Fischer indole synthesis of ethyl nitro indole-2-carboxylates. *Bioorganic & Medicinal Chemistry* **2005,** *13* (15), 4638-4644.

55.   Bui, T.; Candeias, N. R.; Barbas, C. F., *J. Am. Chem. Soc.* **2010,** *132* (null), 5574.

56.   (a) Rottmann, M.; McNamara, C.; Yeung, B. K. S.; Lee, M. C. S.; Zou, B.; Russell, B.; Seitz, P.; Plouffe, D. M.; Dharia, N. V.; Tan, J.; Cohen, S. B.; Spencer, K. R.; González-Páez, G. E.; Lakshminarayana, S. B.; Goh, A.; Suwanarusk, R.; Jegla, T.;

Schmitt, E. K.; Beck, H. P.; Brun, R.; Nosten, F.; Renia, L.; Dartois, V.; Keller, T. H.; Fidock, D. A.; Winzeler, E. A.; Diagana, T. T., *Science* **2010,** *329* (null), 1175; (b) Griebel, G.; Simiand, J.; Gal, C. S. L.; Wagnon, J.; Pascal, M.; Scatton, B.; Maffrand, J. P.; Soubrie, P., *Proc. Natl. Acad. Sci.* **2002,** *99* (null), 6370; (c) Zhou, F.; Liu, Y. L.; Zhou, J., *Adv. Synth. Catal.* **2010,** *352* (null), 1381; (d) Peddibhotla, S., *Curr. Bioact. Compd.* **2009,** *5* (null), 20; (e) Dounay, A. B.; Overman, L. E., *Chem. Rev.* **2003,** *103* (null), 2945; (f) Marti, C.; Carreira, E. M., *Eur. J. Org. Chem.* **2003,** *null* (null), 2209.

57.   (a) Bui, T.; Borregan, M.; Barbas Iii, C. F., *J. Org. Chem.* **2009,** *74* (null), 8935; (b) Cheng, L.; Liu, L.; Wang, D.; Chen, Y. J., *Org. Lett.* **2009,** *11* (null), 3874; (c) Qian, Z. Q.; Zhou, F.; Du, T. P.; Wang, B. L.; Zhou, J., *Chem. Commun.* **2009,** *null* (null), 6753.

58.   Bui, T.; Hernández-Torres, G.; Milite, C.; Barbas, C. F., Highly Enantioselective Organocatalytic α-Amination Reactions of Aryl Oxindoles: Developing Designer Multifunctional Alkaloid Catalysts. *Organic Letters* **2010,** *12* (24), 5696-5699.

59.   McBride, A. E.; Cook, J. T.; Stemmler, E. A.; Rutledge, K. L.; McGrath, K. A.; Rubens, J. A., Arginine Methylation of Yeast mRNA-binding Protein Npl3 Directly Affects Its Function, Nuclear Export, and Intranuclear Protein Interactions. *J. Biol. Chem.* **2005,** *280* (35), 30888-30898.

60.   Zorn, J.; Wells, J., Turning enzymes ON with small molecules. *Nature Chemical Biology* **2010,** *6* (3), 179-188.

61.   Goodsell, D. S.; Morris, G. M.; Olson, A. J., Automated docking of flexible ligands: applications of AutoDock. *J. Mol. Recognit.* **1996,** *9* (1), 1-5.

62.   Wang, R.; Lai, L.; Wang, S., Further development and validation of empirical scoring functions for structure-based binding affinity prediction. *J Comput Aided Mol Des* **2002,** *16* (1), 11-26.

63.   Shilatifard, A., Chromatin Modifications by Methylation and Ubiquitination: Implications in the Regulation of Gene Expression. *Annu. Rev. Biochem.* **2006,** *75* (1), 243-269.